Electronic Supporting Information

Aromatic aldehydes as tuneable and ppm potent promoters for zeolite catalysed methanol dehydration to DME

Zhiqiang Yang,[a] Benjamin J. Dennis-Smither,*[b] Corneliu Buda,[c] Fiona Jackson,[b] Amie Easey,[b] Gregory A. Price,[b] Neil Sainty,[b] Xingzhi Tan,[a] Zhuoran Xu,[c] and Glenn J. Sunley*[b]

[a] *Applied Sciences, bp Innovation & Engineering, Energy Innovation Laboratory, BP Office (Dalian Institute of Chemical Physics), BP plc, Dalian, China.*
[b] *Applied Sciences, bp Innovation & Engineering, BP plc, Saltend, Hull, HU12 8DS, United Kingdom. * E-mail: glennsunley@yahoo.co.uk and benjamin.dennis-smither@uk.bp.com.*
[c] *Applied Sciences, bp Innovation and Engineering, BP plc, 30 South Wacker Drive, Chicago, IL 60606, United States of America.*

This version replaces the originally published version where two numbers on page 20 relating to IR spectra in the main text were incorrectly quoted.

CONTENTS

1. REAGENTS

Zeolite catalysts NH_4-SSZ-13 SAR 24 (Product code ZD08028), NH_4-ZSM-5 SAR 23 (Product code CBV2314), NH_4-ZSM-5 SAR 80 (Product code CBV8014), NH_4-ZSM-5 SAR 280 (Product code CBV28014), NH_4-beta SAR 25 (Product code CP814E) and H-Y SAR 30 (Product code CBV720) were all obtained from Zeolyst

International. We thank Zeolyst International for supplying the H-SSZ-13 sample and a sample of silicalite-1 (Product code ZD08026) for research purposes. Zeolite catalyst NH_4-ZSM-11 SAR 50 (Product code MZ110012) was obtained from ACS Material. MCM-41 SAR 79 (Product code 643653) was obtained from Sigma-Aldrich. The zeolite and MCM-41 catalysts were calcined in air at 500 °C before testing, see procedure below. Silicotungstic acid (STA) was obtained from Nipon Organic Chemicals. Carborundum (Product code C/3091/53, 80 grit) was obtained from Fisher Scientific. Silica (Davicat SP550-10013, G57) was obtained from Grace. Helium (CP grade, 99.999%) and nitrogen (oxygen free, 99.998%) gases were obtained from BOC. Table S 1 below provides details of the organic chemicals used in the experiments.

Table S 1. Organic reagents.

Chemical	**Supplier**	**Product Number**
Methanol	Honeywell	34860
Benzaldehyde	Sigma-Aldrich	418099
Toluene	Fischer Scientific	T/2250/PB17
Benzaldehyde dimethyl acetal	Sigma-Aldrich	226076
4-Trifluoromethyl benzaldehyde	Sigma-Aldrich	224944
4-Methyl benzaldehyde	Sigma-Aldrich	T35602
3-Methyl benzaldehyde	Sigma-Aldrich	T35505
2-Methyl benzaldehyde	Sigma-Aldrich	117552
4-Ethyl benzaldehyde	Sigma-Aldrich	233633
4-n-Propyl benzaldehyde	Sigma-Aldrich	562882
4-n-Butyl benzaldehyde	Sigma-Aldrich	518042
4-n-Pentyl benzaldehyde	Sigma-Aldrich	PH015542
4-Methoxy benzaldehyde	Sigma-Aldrich	A0519
3-Methoxy benzaldehyde	Sigma-Aldrich	129658
Methyl 4-formylbenzoate	Sigma-Aldrich	244740
4-Fluorobenzaldehyde	Sigma-Aldrich	128376
4-Chlorobenzaldehyde	Sigma-Aldrich	112216
4-Bromobenzaldehyde	Sigma-Aldrich	B57400
3-Fluorobenzaldehyde	Sigma-Aldrich	F5005
3-Chlorobenzaldehyde	Sigma-Aldrich	124974
3-Bromobenzaldehyde	Sigma-Aldrich	B57206
2-Methylbenzaldehyde	Sigma-Aldrich	117552
2-MeO-benzaldehyde	Sigma Aldrich	102233978
2-F-benzaldehyde	Sigma Aldrich	F4807
2-Cl-benzaldehyde	Sigma Aldrich	124974
2-Br-benzaldehyde	Sigma Aldrich	B57001

The aldehydes were used as received and stored in a fridge before use. A fresh bottle used for each experiment. The methanol was analysed for organic nitrogen-containing impurities by gas chromatography using nitrogen chemiluminescence detection and the organic nitrogen content was found to be < 50 ppb (mass) as nitrogen. The purity of the aldehydes tested was generally checked by GC and was at or above the specification quoted by the supplier. Some samples of the 4-alkylbenzaldehydes were occasionally found to contain elevated levels of organic nitrogen containing impurities, up to 600 ppm, which may explain some of the very slow deactivation seen when occasionally when testing these promoters.

2. CATALYST PREPARATION

2.1 **Silicotungstic acid supported on silica**

30.1g of silica was added to a solution of 14.30g silicotungstic acid (STA) in 39.9g water. The silica/silicotungstic acid solution was left to stand for 30 minutes before being oven dried at a temperature of 120 °C for a period of 16 hours. The dried catalyst material was then cooled to 50 °C, with 40.93g of dried catalyst being recovered.

2.2 **Catalyst calcination**

The ammonium-form zeolites were converted into their H-form by calcination under air at 500 °C by placing a shallow bed (< 1 cm depth) of the catalyst, typically 5 to 10 g, in a ceramic dish in a furnace (Carbolite, AAF 11/18). The furnace was heated using the following temperature programme:

- Room temperature to 90 °C over 20 minutes then hold for 120 minutes.
- 90 °C to 110 °C over 20 minutes then hold for 120 minutes.
- 110 °C to 500 °C over 80 minutes then hold for 240 minutes.
- Cool to < 90 °C, after which the sample was transferred to a sealed vial.

The MCM-41 and H-Y catalysts were also calcined using the above procedure.

2.3 **Catalyst preparation for testing**

Prior to testing the calcined zeolite, MCM-41 and STA/silica powders were pressed, crushed and sieved to the required size range (100 to 200 µm). A sample of the powder, typically 0.5 to 1.5 g, was compacted at 12 tonnes in a 32 mm die set using a pneumatic press. The sample was then gently ground using a pestle and mortar and sieved to a particle size fraction of 100 to 200 µm diameter.

3. CATALYST AND PROMOTER TESTING

The methanol dehydration reactions were carried out using a 16-channel parallel fixed-bed reactor Flowrence™ system from Avantium NV, using stainless steel reactors of 2 mm internal diameter with a length of 300 mm. The liquid feed was introduced by a HPLC pump into a heated zone (220 ^{o}C) along with inert gas feeds before feeding to the reactors. In a typical experiment fifteen of the reactors were packed with 25 ±0.5 mg of catalyst, having a particle size fraction of 100 to 200 µm diameter. The catalyst was loaded on top of a 6cm deep bed of an inert material, carborundum (silicon-carbide). The reactor volume above the catalyst was also packed with

carborundum. The sixteenth reactor was packed with carborundum only. After a gas distribution test each reactor was heated, under a flow of inert gas (nitrogen mixed with helium at a volumetric ratio of 10:1 at 2.68 normal litres per hour per reactor), to a reaction temperature of 150 °C at a total pressure of 1100 kPa. After 1 hour at 150 °C a gaseous feed comprising 10 mol% methanol and inert gas (nitrogen mixed with helium as an internal standard, with a volumetric ratio of 10:1) was then introduced into each reactor for a period of 24 hours. The total volumetric feed rate of the gases and vaporised liquid feed was 2.98 normal litres per hour per reactor. After 24 hours an additional organic component (e.g. benzaldehyde or a benzaldehyde derivative) was added to the methanol feed to achieve a gaseous feed comprising 10 mol% methanol and typically 0.01 to 1 mol% organic additive (relative to methanol), with the nitrogen flow being reduced to keep the total volumetric feed rate of the gases and vaporised liquid feed at 2.98 normal litres per hour per reactor. Dew point calculations were performed to ensure that all the aldehyde promoters were tested at partial pressures such that they remained in the vapour phase at the reactor inlet. Thermodynamic equilibrium calculations were performed using a commercial simulator (AspenPlus v8.8) to predict the effect of promoters (benzaldehyde and its derivatives) on the mixture dew point of the reactor inlet. Pure component parameters were drawn from appropriate databases, while those missing were estimated with the use of appropriate group contribution methods.

The effluent stream from each reactor was diluted with inert gas (nitrogen) and was periodically analysed by online gas chromatography to determine the yield of dimethyl ether (DME) product. Space time yields (STY) in grammes per kilogramme of catalyst per hour (g kg^{-1} h^{-1}) for making DME from methanol were determined between 18 and 24 hours after introducing the methanol only feed. Space time yields for making DME from methanol in the presence of an additional organic component were typically determined between 1 and 24 hours after introducing the organic additive, with the maximum DME STY being reported for this period to take account of the few instances where some deactivation did occur during the organic additive testing period. In the 24-hour benzaldehyde promoter testing period for the wide pore zeolites tested in Figure 1 the DME STY for H-beta SAR 25 declined from 508 to 191 g kg^{-1} h^{-1} and for H-Y SAR 30 declined from 274 to 35 g kg^{-1} h^{-1}. The deactivation of the wide pore zeolites may be the result of undesirable side reactions occurring in the larger zeolite pores. An alternative possibility is the poor hydrolytic stability of the wide pore zeolites, especially at the SAR of the materials tested here, which is further exacerbated by the elevated amounts of water produced in the promoted methanol dehydration to DME (M2D) reaction. DME STY data collected for the more stable medium pore 3-dimensional zeolites H-ZSM-5 SAR 80 and H-ZSM-11 SAR 50 are given in Table S 2 and Table S 3.

In some instances, data for the impact of more than one organic co-feed was collected in the same experiment by flushing the reactors with methanol only for 24 hours after the first organic co-feed was tested. This was reliant on the methanol flush being able to return the catalyst being tested to the performance originally observed at the end of the first period when it was tested with methanol only. Figure S 1 shows the reversibility of promotion of DME formation by 0.1 mol % benzaldehyde tested with H-ZSM-5 SAR 80 and H-ZSM-5 SAR 280 and at 150 °C. The same sort of reversibility was observed with H-ZSM-5 SAR 23 (see Figure 2 in the main paper) and H-ZSM-11 SAR 50 when tested with 0.1 mol % benzaldehyde at these conditions.

Table S 2. DME space time yield data for zeolite catalysed methanol dehydration in the absence and presence of benzaldehyde and 3- and 4-substituted benzaldehyde derivatives.[a]

Catalyst	H-ZSM-5 SAR 80		H-ZSM-11 SAR 50
	DME STY / g kg^{-1} h^{-1}		**DME STY / g kg^{-1} h^{-1}**
Promoter	@ 110 °C	@ 150 °C	@ 150 °C
None	16[b]	388[b]	453[b]
Benzaldehyde	45	1274	1390
4-Methylbenzaldehyde	210	2709	3261
4-Ethylbenzaldehyde	280	3225	3744
4-n-Propylbenzaldehyde	557	6272	7628
4-n-Butylbenzaldehyde	609[c]	6548	7499
4-n-Pentylbenzaldehyde	946[d]	7815	9217
4-MeO-benzaldehyde	655	5651	6156
4-CF_3-benzaldehyde	16	576	705
4-F-benzaldehyde	n/a	1522	1863
4-Cl-benzaldehyde	53	1292	1463
4-Br-benzaldehyde	59	1656	1980
4-CO_2Me-benzaldehyde	n/a	2360	2603
3-MeO-benzaldehyde	190	2715	2296
3-Methylbenzaldehyde	110	1965	1633
3-F-benzaldehyde	19	703	751
3-Cl-benzaldehyde	27	972	918
3-Br-benzaldehyde	38	1381	1104

a) Conditions: temperature 110 or 150 °C, methanol WHSV 17.1 h^{-1}, methanol partial pressure 110 kPa, promoter partial pressure 0.011 kPa b) average of multiple experiments c) average from 3 repeat experiments d) average from 4 repeat experiments.

Table S 3. DME space time yield data for zeolite catalysed methanol dehydration in the presence of 2-substituted benzaldehyde derivatives.[a]

Catalyst	H-ZSM-5 SAR 80		H-ZSM-11 SAR 50
	DME STY / g kg^{-1} h^{-1}		**DME STY / g kg^{-1} h^{-1}**
Promoter	@ 110 °C	@ 150 °C	@ 150 °C
2-Methylbenzaldehyde	30	841	927
2-MeO-benzaldehyde	247	2423	2286
2-F-benzaldehyde	28	785	851
2-Cl-benzaldehyde	17	548	636
2-Br-benzaldehyde	16	505	565

a) Conditions: temperature 110 or 150 °C, methanol WHSV 17.1 h^{-1}, methanol partial pressure 110 kPa, promoter partial pressure 0.011 kPa

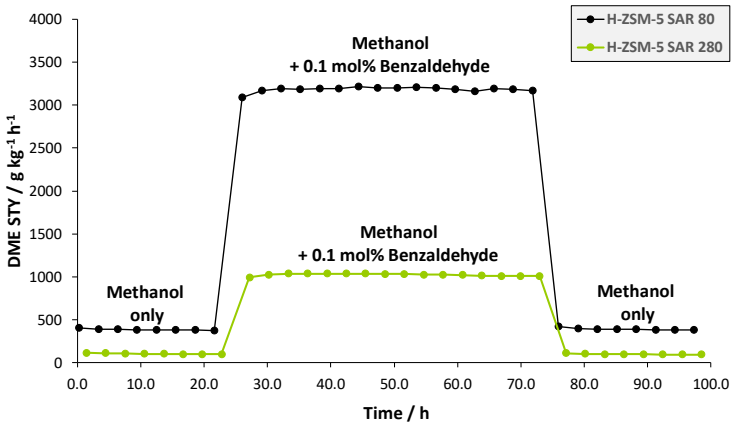

Figure S 1. Impact of co-feeding benzaldehyde on DME STY for H-ZSM-5 SAR 80 and H-ZSM-5 SAR 280. Conditions: 150 °C, methanol WHSV 17.1 h^{-1}, methanol partial pressure 110 kPa and benzaldehyde partial pressure 0.11 kPa.

3.1 **Note on reproducibility**

Some of the promoters tested in this work are very potent and promote methanol dehydration to DME at concentrations as low as 0.0001 mol % (1 ppm) relative to methanol fed. It is therefore important to flush the process lines with clean methanol for at least 24 hours at the end of each experiment to remove any traces of the promoter from the testing equipment. In addition, the standard testing protocol used fresh and clean methanol at the start of each experiment, to ensure that the baseline conditions had been returned to before subsequently testing a promoter diluted in methanol. For the first batch of H-ZSM-5 SAR 80 prepared this was tested over many years with methanol only as a control and gave a DME STY of 388 ± 20 g kg^{-1} h^{-1}, averaged over 82 separate experiments at 150 °C. A second batch of H-ZSM-5 SAR 80 prepared 3 years later than the first batch gave an DME STY of 404 g kg^{-1} h^{-1} at 150 °C. The H-ZSM-11 SAR 50 catalyst gave a DME STY of 453 ± 19 g kg^{-1} h^{-1}, averaged over 26 separate experiments at 150 °C. The 2 batches of H-ZSM-5 SAR 80 were also tested in 19 separate experiments with methanol only at 110 °C, giving an average DME STY of 16 ± 1.6 g kg^{-1} h^{-1}. The most potent promoter, 4-n-pentylbenzaldehyde, was tested in 4 separate experiments with H-ZSM-5 SAR 80 at 110 °C at a) 0.01 mol % of promoter, giving an average DME STY of 946 ± 17 g kg^{-1} h^{-1} b) 0.02 mol % of promoter, giving an average DME STY of 990 ± 41 g kg^{-1} h^{-1}.

As noted above, some samples of the 4-alkylbenzaldehydes were occasionally found to contain elevated levels of organic nitrogen containing impurities, up to 600 ppm, which may explain some of the very slow deactivation seen when occasionally testing these promoters. Slow deactivation or possibly inhibition was occasionally seen when some of the more potent promoters were tested at conditions approaching saturation kinetics; this was not explored further in this work. In both these circumstances the maximum DME STY observed was recorded, and the experiment terminated, with the HTE testing equipment being flushed with fresh and clean methanol.

3.2 **Reaction selectivity**

All the H-ZSM-5 and H-ZSM-11 catalysed methanol dehydration reactions conducted were observed to form DME with high selectivity, > 99%, with negligible formation of hydrocarbons. A representative GC trace is shown in Figure S 2 of the reactor effluent for a reaction which used 1 mol % benzaldehyde as a promoter with H-ZSM-5 SAR 80 as the zeolite catalyst at 150 °C. The benzaldehyde passed over the catalyst largely unconverted (>

99%), with trace amounts of benzaldehyde dimethyl acetal being formed, the formation of which was more apparent when the benzaldehyde promoter was tested at lower reaction temperatures, for example at 120 °C, as shown in Figure S 3. The only other significant by-product observed was trace amounts of dimethoxymethane. When 1 mol % benzaldehyde dimethyl acetal was tested as a promoter at 150 °C this gave a very similar DME STY, 6860 g kg^{-1} h^{-1}, to 1 mol % benzaldehyde, 6590 g kg^{-1} h^{-1}. The benzaldehyde dimethyl acetal largely (> 99%) converted to benzaldehyde under these conditions. At 120 °C the effluent composition from a reaction promoted by 1 mol% benzaldehyde dimethyl acetal was the same as that observed when using 1 mol% benzaldehyde as the promoter, as shown in Figure S 3. This indicates facile interconversion of the acetal and aldehyde under the methanol dehydration reaction conditions tested.

The most potent promoter found 4-n-pentylbenzaldehyde was tested with H-ZSM-5 SAR 80 at 0.01 mol %, 150 °C and a methanol WHSV of 4.3 h^{-1}. Under these conditions the 4-n-pentylbenzaldehyde increased the methanol conversion from 12% for the unpromoted reaction to 88% for the promoted reaction. Inspection of the GC traces showed that the reaction remained highly selective to DME, > 99%, with negligible amounts of by-products being formed. This experiment shows that the promoters are effective over a wide range of methanol conversion, even when considerable amounts of water are being produced by the methanol dehydration reaction.

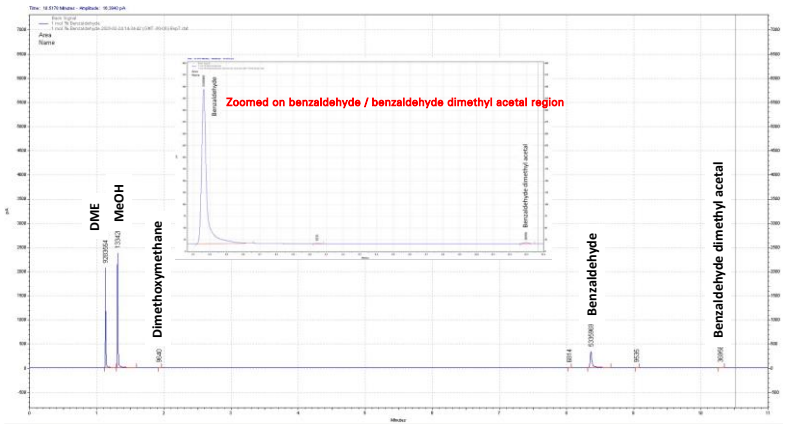

Figure S 2. GC chromatogram of products and by-products formed with H-ZSM-5 SAR 80 tested for methanol dehydration to DME with 1 mol% benzaldehyde as a promoter. Conditions: 150 °C, methanol WHSV 17.1 h^{-1}, methanol partial pressure 110 kPa and benzaldehyde partial pressure 1.1 kPa.

a) Benzaldehyde b) Benzaldehyde dimethyl acetal

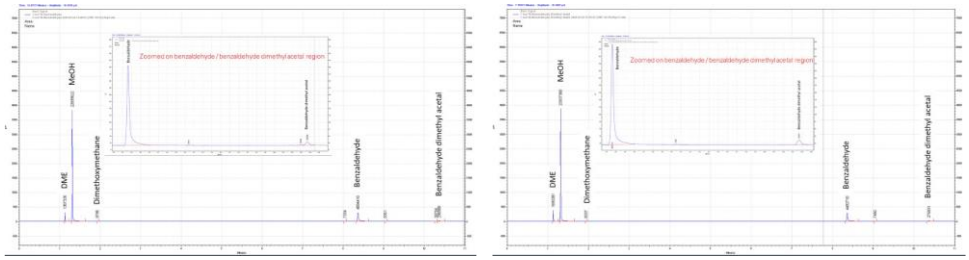

Figure S 3. GC chromatograms of products and by-products formed with H-ZSM-5 SAR 80 tested for methanol dehydration to DME with a) 1 mol% benzaldehyde and b) 1 mol% benzaldehyde dimethyl acetal as promoters. Conditions: 120 °C, methanol WHSV 17.1 h^{-1}, methanol partial pressure 110 kPa and promoter partial pressure 1.1 kPa.

3.3 **Testing of silicalite-1 and H-ZSM-5 catalysts with different SAR**

The impact of silica to alumina (SAR) on promoter potency was examined by testing 0.1 mol % benzaldehyde as a promoter at 150 °C with H-ZSM-5 with a SAR of 23, 80 and 280, see Figure S 4. All the catalysts showed a significant increase in DME STY when benzaldehyde was added to the methanol feed, with the higher SAR catalysts being more strongly promoted than the SAR 23 catalyst. Indeed, under these conditions the H-ZSM-5 SAR 80 catalyst gave a higher DME STY, of 3215 g kg^{-1} h^{-1}, than the H-ZSM-5 SAR 23 catalyst, which gave a DME STY of 3000 g kg^{-1} h^{-1}. This is the converse of what is seen when the catalysts were tested with methanol only, with the lowest SAR catalyst giving the highest DME STY. On average the BA sites in the higher SAR catalysts were found to be turning over to make DME at a significantly faster rate than those in the H-ZSM-5 SAR 23 catalyst, see Figure S 5. The H-ZSM-5 SAR 80 catalyst, which gave the highest DME STY and BA site turnover frequency was thus selected for further testing at 150 °C with benzaldehyde and its derivatives, but at a concentration of 0.01 mol % of aldehyde, to give plenty of headroom for promoter ranking by keeping the methanol conversion for the benzaldehyde promoted reference reaction below 5 %.

A sample of silicalite-1 (MFI) was tested at 140 °C for methanol dehydration to DME in the presence of 2 mol % benzaldehyde at a methanol WHSV of 17.1 h^{-1}. This material made negligible amounts of DME, whereas the H-ZSM-5 (MFI) SAR 80 catalyst made significant amounts of DME under these conditions, giving a DME STY of 4317 g kg^{-1} h^{-1} at 140 °C. The silicalite-1 sample also made negligible amounts of DME when tested with methanol only and methanol plus 2 mol % benzaldehyde at 110 °C. This illustrates that the silanol groups, on their own, in MFI are not strong enough to catalyse the dehydration of methanol to DME in the presence of benzaldehyde as a promoter.

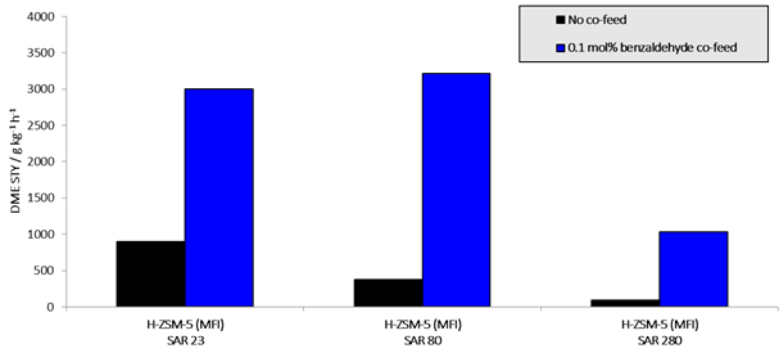

Figure S 4. Impact of co-feeding benzaldehyde on DME STY for H-ZSM-5 of SAR 23, SAR 80 and SAR 280. Conditions: 150 °C, methanol WHSV 17.1 h^{-1}, methanol partial pressure 110 kPa and benzaldehyde partial pressure 0.11 kPa. Black bar methanol only data.

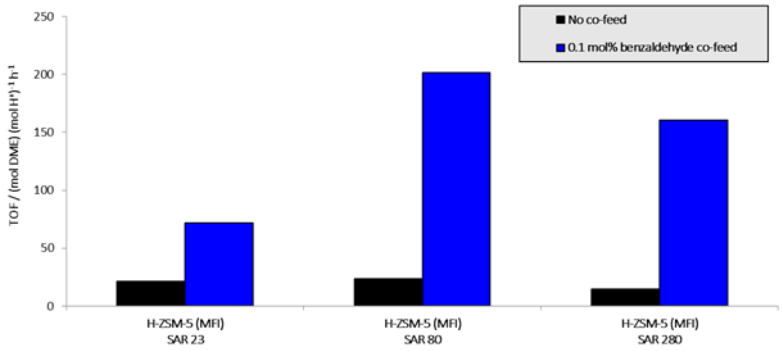

Figure S 5. Impact of co-feeding benzaldehyde on Brønsted acid site turnover frequency to DME for H-ZSM-5 of SAR 23, SAR 80 and SAR 280. Conditions: 150 °C, methanol WHSV 17.1 h^{-1}, methanol partial pressure 110 kPa and benzaldehyde partial pressure 0.11 kPa. Black bar methanol only data.

3.4 Kinetic experiments – effect of temperature, promoter concentration and partial pressure, methanol partial pressure and water addition for H-ZSM-5 SAR 80

The effect of promoter concentration on DME STY at 110 °C was explored for H-ZSM-5 SAR 80 with benzaldehyde and two promoters tested at opposite ends of the Hammett constant scale, 4-methoxybenzaldehyde, with a strongly donating -OMe group, and 4-trifluoromethylbenzaldehyde, with a strongly electron withdrawing -CF_3 group. In terms of the maximum DME STY observed (numbers in parentheses, in g kg^{-1} h^{-1}) this followed the trend 4-methoxybenzaldehyde (925) > benzaldehyde (557) > 4-trifluoromethylbenzaldehyde (66), Figure S 6. This demonstrates that electron-donating groups strongly favour DME formation at conditions indicative of Brønsted acid (BA) active site saturation, whereas electron-withdrawing groups disfavour (versus benzaldehyde) DME formation at BA active site saturation conditions. The two substituted benzaldehydes approached active site saturation at 0.1 % (4-methoxybenzaldehyde) and 1 mol % (4-trifluoromethylbenzaldehyde) of promoter, whereas benzaldehyde required a significantly higher concentration of promoter, 5 mol %, to approach active site saturation. Similar behaviour was seen for 4-methylbenzaldehyde and 4-chlorobenzaldehyde, with moderately electron-donating Me- and electron-withdrawing Cl- groups, Figure S 7. These promoters both approached active site saturation at 0.5 mol %, again significantly lower than that observed for benzaldehyde. In terms of the maximum DME STY observed these two promoters followed the trend 4-methylbenzaldehyde (728) > benzaldehyde (557) > 4-chorobenzaldehyde (305), consistent with the trend seen above for promoters with more strongly electron-withdrawing and electron-donating groups. As shown in Figure 6 in the main paper 4-n-pentyl benzaldehyde, the most potent promoter tested, approached active site saturation at 0.02 mol %, despite the fact it only contained a moderately electron-donating n-pentyl group. This promoter also gave the highest DME STY (990) of the promoters tested in the concentration studies at 110 °C. The 4-n-pentylbenzaldehyde was so potent that even 0.0001 mol % (1 ppm) could increase the DME STY 10-fold from 16 to 165 g kg^{-1} h^{-1} at 110 °C, once steady-state conditions had been reached, Figure S 8. The promoter concentration studies indicate that more than one factor is in play in determining promoter efficacy. Whilst the electron-withdrawing and electron-donating properties of substituents on the benzaldehyde aromatic ring play an important role, the shape and size of the promoter also plays a significant role. This illustrates the importance

of the zeolite confinement effect on promoter potency, in terms of its well-known solvent like effect of stabilizing reaction intermediates and lowering the energy of transition states.

The impact of benzaldehyde concentration on DME STY for H-ZSM-5 SAR 80 was also studied at 150 ^{o}C at a methanol GHSV of 17.1 h^{-1}. At 150 ^{o}C similar behaviour to that seen at lower temperature (110 ^{o}C) in Figure S 6 was observed; benzaldehyde concentrations of zero, 0.01, 0.1, 1.0 and 2.0 mol % gave DME STY's of 388, 1274, 3215, 6590 and 7660 g kg^{-1} h^{-1} respectively at the higher temperature. This indicates that the benzaldehyde concentration of 0.01 mol % chosen for testing in Figures 4 and 5 in the paper main is significantly away from saturation kinetics. The significant increase in DME STY to 1274 g kg^{-1} h^{-1} with 0.01 mol % benzaldehyde however suggests a reasonable degree of coverage of the active sites at this concentration.

The apparent activation energy was determined for H-ZSM-5 SAR 80 with methanol plus 0.02 mol % 4-n-pentylbenzaldehyde using 10 mg of catalyst diluted with 20 mg of carborundum. The data was collected in a temperature range (100 to 125 ^{o}C) such that the methanol conversion was kept below 10%. An Arrhenius plot of the data collected is shown in Figure S 9. The apparent activation energy for the methanol only reaction was previously determined to be 109 kJ mol^{-1},[1] whilst in the presence of 0.02 mol % 4-n-pentylbenzaldehyde it was found to be lowered to 76 kJ mol^{-1}. The apparent activation energy was also measured at a WHSV of 17.1 h^{-1}, over the narrow temperature range (100 to 115 ^{o}C), with a maximum methanol conversion of 11%. This gave a slightly higher apparent activation energy of 79 kJ mol^{-1}. Given the strong impact that the water co-product has on the promoted M2D reaction, see below and Figure S 10, it is likely that the apparent activation energy is very sensitive to conversion, even when measured below the 10 % methanol conversion,[2] which is often the conventional approach applied to measuring apparent activation energies.

The effect of co-feeding water, 5 mol % relative to methanol, on DME STY was explored at 110 ^{o}C for H-ZSM-5 SAR 80 with benzaldehyde and 4-n-pentylbenzaldehyde, tested at 5 mol % and 0.01 mol % respectively. The addition of water to the feed was found to markedly reduce the DME STY obtained for both the promoters, Figure S 10. However even with this amount of added water to the feed, equivalent to that formed at 10 % methanol conversion, there were still very significant increases in the DME STY with both promoters over the methanol only reaction. This is consistent with the promoters being effective over a wide range of methanol conversion, as also noted in Section 3.2.

The effect of methanol partial pressure on DME STY was explored at 110 ^{o}C for H-ZSM-5 SAR 80 with 4-n-pentylbenzaldehyde used as the promoter, at two aldehyde partial pressures, 0.00055 and 0.011 kPa, see Figure S 11. The methanol partial pressure was varied by changing the methanol WHSV, whilst the aldehyde partial pressure was kept constant at either 0.00055 or 0.011 kPa by varying its concentration in the methanol fed. An inverse dependence of DME STY on methanol partial is seen at the lower aldehyde partial pressure of 0.00055 kPa. At the higher partial of aldehyde, 0.011 kPa, reducing the methanol partial had much less impact on the DME STY, with only small variations (small increase, followed by a small decrease) seen in reducing the methanol

partial pressure from 110 to 55 and 27.5 kPa. The latter observation is consistent with the zeolite catalyst active sites being close to saturation with both promoter and methanol under these conditions.

The effect of methanol partial pressure on DME STY was also explored at 110 °C for H-ZSM-5 SAR 80 with benzaldehyde used as the promoter. The methanol partial pressure was varied by changing the methanol WHSV, whilst the benzaldehyde partial pressure was kept constant at 0.11 kPa by varying its concentration in the methanol fed. The nitrogen flow was correspondingly varied to keep the total volumetric feed rate of the gases and vaporised liquid feed at 2.98 normal litres per hour per reactor. The benzaldehyde partial pressure selected for this study was well away from that required for saturation kinetics when tested with 110 kPa of methanol i.e., where the DME STY was still increasing with benzaldehyde concentration, as indicated in Figure S 6. An inverse dependence of DME STY on methanol partial pressure was observed under these conditions, see Figure S 12, consistent with a reaction mechanism involving competitive adsorption between methanol and the aldehyde promoter on a Brønsted acid active site.

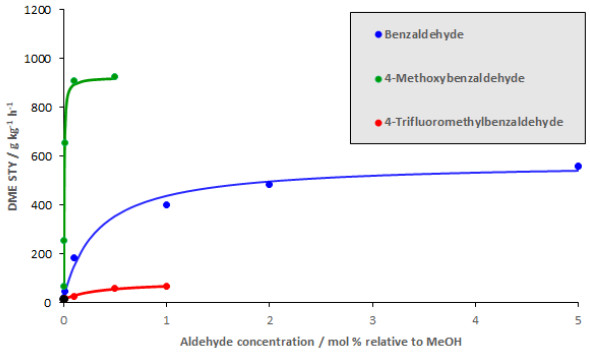

Figure S 6. Impact of co-feeding different concentrations of various aldehydes on DME STY for H-ZSM-5 SAR 80. Conditions: 110 °C, methanol WHSV 17.1 h^{-1} and methanol partial pressure 110 kPa. Black dot methanol only. Red, blue and green lines added to guide the eye.

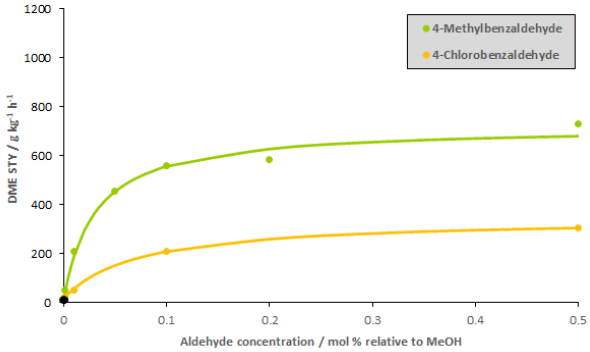

Figure S 7. Impact of co-feeding different concentrations of 4-methyl benzaldehyde and 4-chlorobenzaldehyde on DME STY for H-ZSM-5 SAR 80. Conditions: 110 °C, methanol WHSV 17.1 h^{-1} and methanol partial pressure 110 kPa. Black dot methanol only. Orange and light green lines added to guide the eye.

This version replaces the originally published version where two numbers on pg. 20 regardingwere incorrectly quoted.

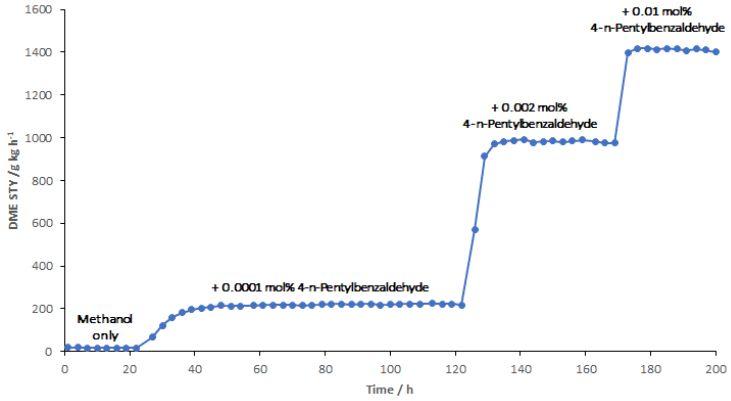

Figure S 8. Impact of co-feeding different concentrations of 4-n-pentylbenzaldehyde on DME STY for H-ZSM-5 SAR 80. Conditions: 110 °C, methanol WHSV 17.1 h^{-1} and methanol partial pressure 110 kPa.

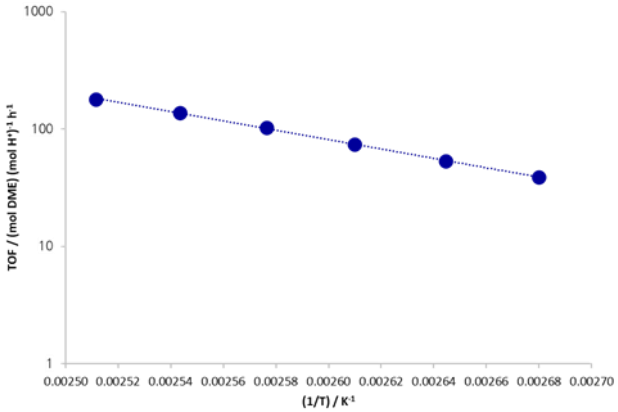

Figure S 9. Arrhenius plot for H-ZSM-5 SAR 80 tested for methanol dehydration to DME promoted by 4-n-pentylbenzaldehyde. Conditions: 100 to 125 °C, methanol WHSV 42.6 h-1, methanol partial pressure 110 kPa and 4-n-pentylbenzaldehyde partial pressure 0.022 kPa.

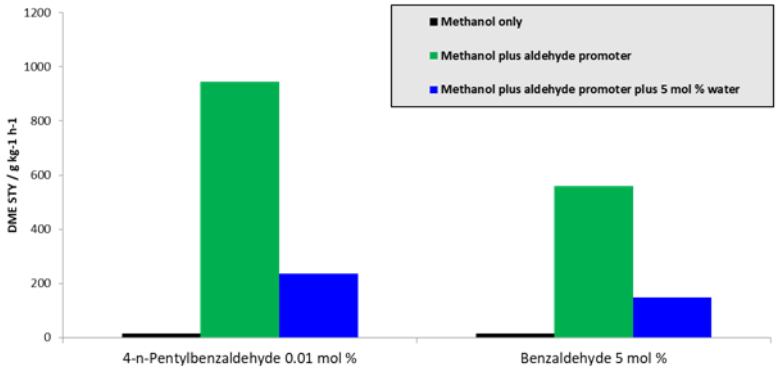

Figure S 10. Impact of co-feeding water on DME STY for aromatic aldehyde promoted methanol dehydration using H-ZSM-5 SAR 80. Conditions: 110 °C, methanol WHSV 17.1 h^{-1}, methanol partial pressure 110 kPa, water partial pressure 5.5 kPa, benzaldehyde partial pressure 5.5 kPa and 4-n-pentylbenzaldehyde partial pressure 0.011 kPa. Black bar methanol only data.

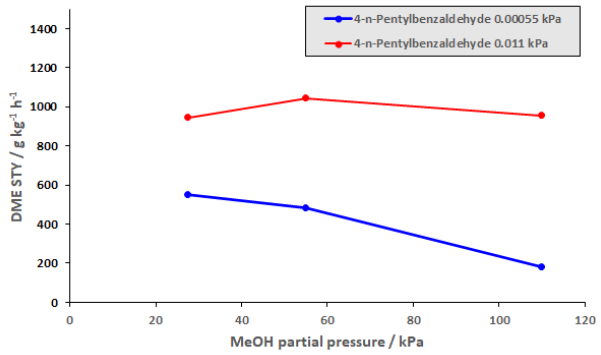

Figure S 11. Impact of methanol partial pressure on DME STY for 4-n-pentylbenzaldehyde promoted methanol dehydration using H-ZSM-5 SAR 80. Conditions: 110 °C, aldehyde partial pressure 0.00055 and 0.011 kPa, methanol WHSV 4.3, 8.5 and 17.1 h^{-1}.

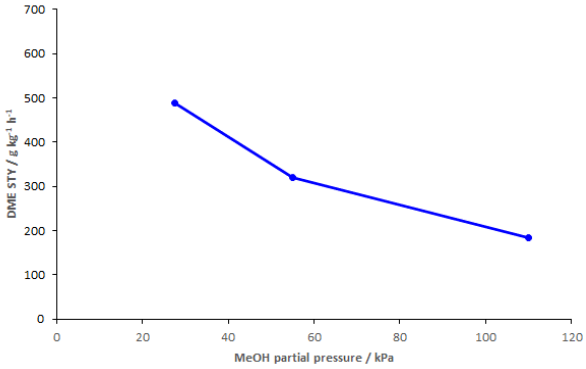

Figure S 12. Impact of methanol partial pressure on DME STY for benzaldehyde promoted methanol dehydration using H-ZSM-5 SAR 80. Conditions: 110 °C, benzaldehyde partial pressure 0.11 kPa, methanol WHSV 4.3, 8.5 and 17.1 h^{-1}.

3.5 **Comparison of zeolite and mesoporous catalysts**

A mesoporous silica-alumina MCM-41 (SAR 79) catalyst was tested for methanol dehydration in the absence and presence of 0.1 mol % benzaldehyde at 150 °C, under the same conditions as the zeolite catalysts tested in Figure 1 in the main paper and the H-ZSM-5 catalysts tested in Figure S 4. The MCM-41 catalyst made very little DME under these conditions, giving a DME STY of < 10 g kg^{-1} h^{-1} with or without benzaldehyde in the methanol feed. In contrast the H-ZSM-5 SAR 80 catalyst tested in Figure S 4 gave a DME STY of 3215 g kg^{-1} h^{-1} with 0.1 mol % benzaldehyde in the feed.

The importance of the zeolite micropores in boosting the potency of the aldehyde promoters was further explored by comparing H-ZSM-5 SAR 80 with a molecular acid, silicotungstic acid (STA), supported on mesoporous silica. Both catalysts were tested at 110 °C with 0.01 mol % of benzaldehyde and a series of 4-alkyl substituted benzaldehydes, see Figure S 13. As the alkyl group was lengthened from methyl to n-pentyl there was a significant increase in DME STY across the series for the H-ZSM-5 SAR 80 catalyst. The DME STY increased from 16 g kg^{-1} h^{-1} for the unpromoted reaction to 946 g kg^{-1} h^{-1} for the most potent promoter tested, 4-n-pentylbenzaldehyde, representing a 59-fold increase in STY. In contrast beyond 4-methylbenzaldehyde there was no strong effect of alkyl chain length on DME STY for the STA on silica catalyst, with the DME STY increasing

from 43 g kg^{-1} h^{-1} for the unpromoted reaction to 116 g kg^{-1} h^{-1} for the 4-n-pentylbenzaldehyde promoted reaction. The Brønsted acid (BA) sites in the H-ZSM-5 SAR catalyst were found on average to turning over 10 times faster for making DME than those on the STA on silica catalyst when tested with 0.01 mol % 4-n-pentylbenzaldehyde, see Figure S 14, illustrating the significance of the zeolite confinement effect on promoter potency.

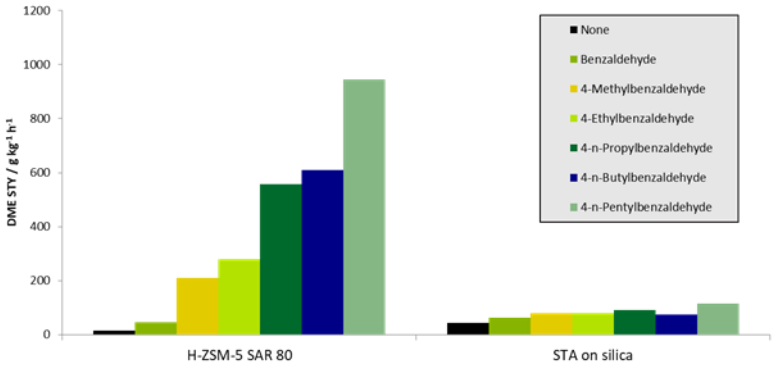

Figure S 13. Impact of co-feeding benzaldehyde and 4-alkylbenzaldehydes on DME STY for H-ZSM-5 SAR 80 and silicotungstic acid (STA) supported on silica. Conditions: 110 °C, methanol WHSV 17.1 h^{-1}, methanol partial pressure 110 kPa and aldehyde partial pressure 0.011 kPa. Black bar methanol only data.

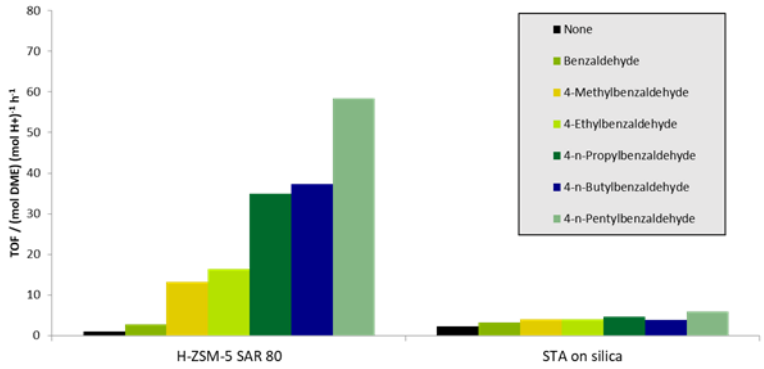

Figure S 14. Impact of co-feeding benzaldehyde and 4-alkylbenzaldehydes on Brønsted acid site turnover frequency to DME for H-ZSM-5 SAR 80 and silicotungstic acid (STA) supported on silica. Conditions: 110 °C, methanol WHSV 17.1 h^{-1}, methanol partial pressure 110 kPa and aldehyde partial pressure 0.011 kPa. Black bar methanol only data.

The water tolerance of the H-ZSM-5 SAR 80 versus STA on silica catalyst was tested for the M2D reaction in the presence of 0.01 mol % of 4-n-pentylbenzaldehyde, Figure S 15. Addition of 5 mol % water to the promoted STA on silica M2D reaction reduced the DME STY from 116 g kg^{-1} h^{-1} to 44 g kg^{-1} h^{-1}. In the absence of water and promoter the STA on silica catalyst gives a DME STY of 43 g kg^{-1} h^{-1}, whilst with methanol plus 5 mol % water it gives a DME STY of 36 g kg^{-1} h^{-1}. This indicates a relatively small promotion for the STA on silica catalyst in the presence of added water. For the H-ZSM-5 SAR 80 catalyst, as noted previously, addition of 5 mol % water reduced the DME STY for the promoted reaction from 946 to 237 g kg^{-1} h^{-1}. This is still substantially above the DME STY's seen for the methanol only reaction, of 16 g kg^{-1} h^{-1}, and the methanol only reaction plus 5 mol % water, of 10 g kg^{-1} h-^{1}. Indeed for the H-ZSM-5 catalyst, with 5 mol % water in the methanol feed, addition of 0.01 mol % of 4-pentylbenzaldehyde significantly increased the DME STY, from 10 to 237 g mol kg^{-1} h^{-1}, resulting in a 24-fold increase in DME STY. This suggests that the

confines of the zeolite, combined with its high SAR, and structure of the promoter, create a more favourable environment for methanol dehydration to methanol.

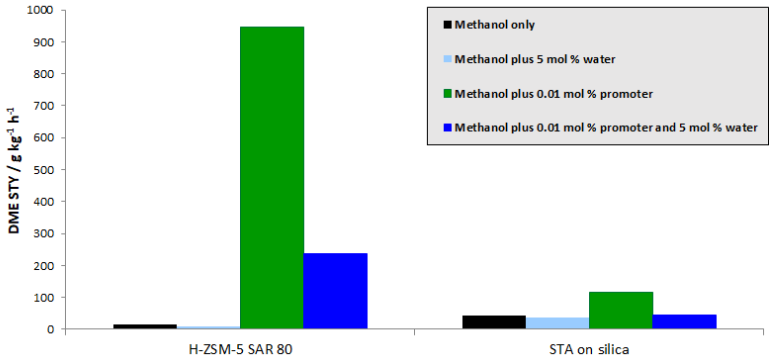

Figure S 15. Impact of co-feeding water and 4-n-pentylbenzaldehyde on DME STY for H-ZSM-5 SAR 80 and silicotungstic acid (STA) supported on silica. Conditions: 110 °C, methanol WHSV 17.1 h^{-1}, methanol partial pressure 110 kPa, water partial pressure 5.5 kPa and aldehyde partial pressure 0.011 kPa. Black bar methanol only data.

4. *IN-SITU* FT-IR-MS STUDIES

4.1 **Experimental**

Fourier transform infra-red (FT-IR) spectra were collected using a high temperature reaction cell from Harrick Scientific. The reaction cell was equipped with ZnSe windows, with the reaction cell operated at ambient pressure. FT-IR spectra were collected with a Thermo Scientific™ Nicolet™ iS50 spectrometer equipped with an MCT detector and KBr beam-splitter and were measured in the transmission mode. The gaseous effluent from the reaction cell was sampled with a capillary connected to a Dycor mass spectrometer (Ametek), with the evolution of DME from the zeolite sample being determined by monitoring the m/z signal at 46. In a typical experiment approximately 10 mg of zeolite powder was made into a disk by pressing, which was then placed in a sample holder in the reaction cell. The zeolite sample was then degassed of air and dried under flowing nitrogen at 450 °C for 2 hours, with sample having been heated to 450 °C at a ramp rate of 5 °C per minute. The zeolite sample was then cooled to 110 °C. The reactant under study (e.g. methanol or aromatic aldehyde) was then introduced into the reaction cell by sparging nitrogen through the liquid reactant placed in a saturator operated at room temperature. The partial pressure of each reactant is determined by its saturated vapor pressure at ambient temperature. The flowrate of nitrogen was 50 mL per minute in all cases. After an appropriate reaction time the reaction cell was then purged with nitrogen only at 110 °C for 2 hours to remove any weakly held physiosorbed surface species from the zeolite. An additional reactant (methanol, aromatic aldehyde or water) was optionally introduced into the reaction cell, with the sample still at 110 °C following the nitrogen purge, by changing the liquid in the saturator. FT-IR spectra of the zeolite sample were recorded with wavenumbers ranging from 1200 cm^{-1} to 4000 cm^{-1}. Spectra were collected at a frequency of one per minute, using 32 scans per spectrum. The time resolved plots of the FT-IR spectra were created based on desirable time intervals to show the major changes occurring.

4.2 **Studies with benzaldehyde and H-ZSM-5 (MFI) and silicalite-1 (MFI)**

The interaction of benzaldehyde with H-ZSM-5 SAR 80 was investigated in a high temperature reaction cell by *in-situ* FT-IR spectroscopy. At 110 °C treatment of H-ZSM-5 SAR 80 with flowing N_2 saturated with benzaldehyde vapour resulted in complete titration of the Bronsted acid (BA) sites at 3608 cm^{-1}, Figure S 16.

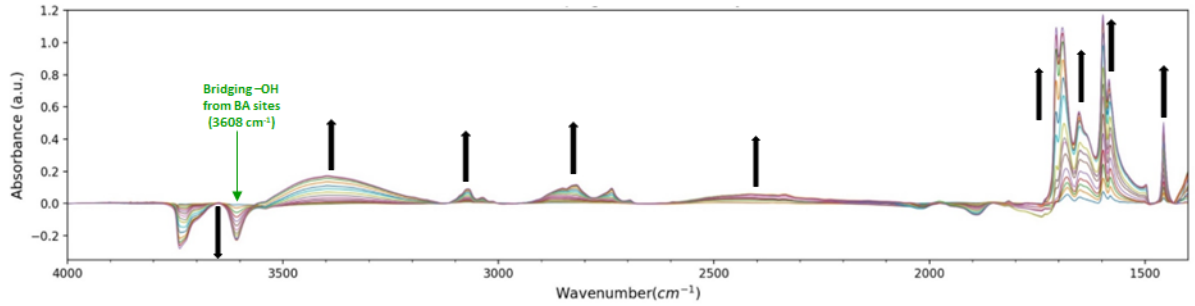

Figure S 16. IR difference spectra of benzaldehyde adsorption on H-ZSM5 SAR 80 at 110 °C. Spectra displayed with 1 min intervals, over 17 minute period. The arrows indicate the trend of change in IR band intensity with time at different regions.

Concurrent with titration of the BA sites a strong IR band appeared at 1580 cm^{-1}, associated with a protonated C=O bond vibration strongly coupled with aromatic ring vibrations. A strong and sharp IR band at 1597 cm^{-1}, associated with an aromatic carbon-carbon bond vibration strongly coupled with protonated formyl group vibrations, was also evident. A medium intensity and sharp IR at 1459 cm^{-1}, associated with an aromatic carbon-carbon bond vibration, was also observed. The assignments above were guided by simulated spectra generated by DFT molecular modelling, see Table S 10 and Table S 11, and gas and liquid phase spectra reported in the literature and NIST database.[3, 4] A isotopic labelling study was also performed, using benzaldehyde enriched with ^{13}C in the formyl group, see later, Figure S 22. A liquid phase IR spectrum, recorded using an ATR FT-IR spectrometer, is provided below for ease of reference, Figure S 17. The simulated spectra indicate that protonation of the C=O group greatly increases the intensity of the aromatic ring carbon-carbon bond vibrations, which are normally of low intensity in benzaldehyde alone. The simulated spectra indicate that the C=O group and aromatic carbon-carbon bond vibrations become strongly coupled upon protonation, giving rise to the intense and sharp bands reported above at 1580 and 1597 cm^{-1}. In Figure S 16 a broad IR band in the ca. 2200 to 2600 cm^{-1} region was also present, indicative of perturbation of BA site O-H bonds via a strong interaction with the aldehyde C=O group. During the benzaldehyde dosing of the zeolite sample a new quite broad IR band also appeared at ca. 1635 cm^{-1}, characteristic of C=O group attached to an aromatic ring interacting with Al^{3+} Lewis acid (LA) sites.[5, 6] Consistent with adsorption of benzaldehyde on the zeolite IR bands associated with aromatic C-H bond vibrations, 3070 cm^{-1}, and formyl C-H bond vibrations, broad bands ca. 2650 to 2900 cm^{-1}, were also observed. The silanol groups in the zeolite, centred at 3740 cm^{-1}, were also titrated, concurrent with the appearance of an IR band at 1692 cm^{-1}, indicative of silanol groups H-bonded to the C=O group of the aldehyde. An IR band at 1706 cm^{-1} was also observed, assigned to either a C=O vibration in a) physisorbed benzaldehyde and/or b) benzaldehyde weakly interacting with silanol -OH groups on the external surface of the zeolite crystals. After exposure to benzaldehyde purging the zeolite sample with N_2 at 110 °C for 2 hours partially regenerated the silanol groups, indicating a relatively weak interaction between the zeolite and some of the

silanol groups. With the N_2 purge the IR band at 1706 cm^{-1} disappeared, indicating loss of physisorbed benzaldehyde or benzaldehyde weakly H-bonded to some of the silanol -OH groups. In contrast the IR bands at 1580 and 1597 cm^{-1} remained largely intact after the N_2 purge, with the BA sites remaining titrated, indicating a strong interaction between benzaldehyde and the BA sites.

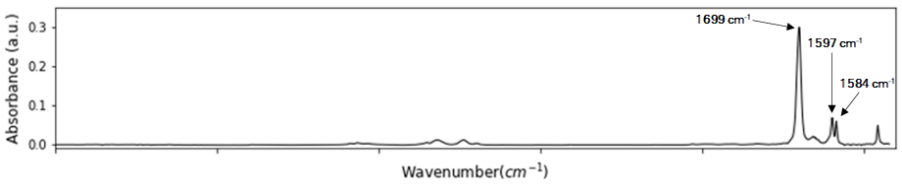

Figure S 17. ATR IR spectrum of liquid benzaldehyde.

At 110 °C treatment of silicalite-1 (MFI) with flowing N_2 saturated with benzaldehyde vapour resulted in adsorption of benzaldehyde, with titration of the silanol groups at 3736 and 3687 cm^{-1}, Figure S 18. An IR band at 1707 cm^{-1} was also observed, assigned to either a C=O vibration in a) physisorbed benzaldehyde and/or b) benzaldehyde weakly interacting with silanol -OH groups on the external surface of the zeolite crystals. The IR band at 1707 cm^{-1} also had a shoulder at ca. 1690 cm^{-1}, indicative of a C=O vibration weakly H-bonded to silanol -OH groups. A broad IR band centred at ca. 3345 cm^{-1} was also apparent, indicative of perturbation of silanol O-H bonds via a weak interaction with the aldehyde C=O group. IR bands at 1597 and 1585 cm^{-1}, due to aromatic ring carbon-carbon bond vibrations, were also apparent. As in the spectrum above of liquid phase benzaldehyde these IR bands were also low in intensity versus the IR band associated with the C=O group vibration. The sample was then purged with N_2 for 2 hours to remove weakly adsorbed species, this greatly reduced the intensity of the IR band at 1707 cm^{-1}, Figure S 19. The IR band at ca. 1690 cm^{-1} did not reduce as much in intensity, suggesting that this IR band is associated with C=O group H-bonded to an internal silanol -OH group.

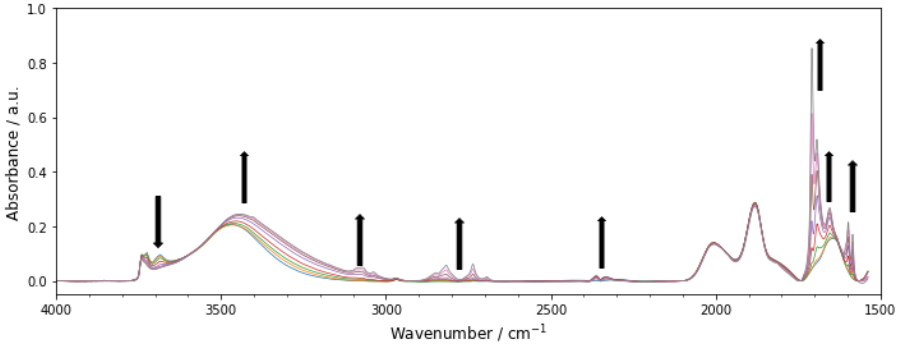

Figure S 18. Time resolved IR spectra of benzaldehyde adsorption on silicalite-1 at 110 °C. Spectra displayed with 1 min intervals, over a 7 minute period. The arrows indicate the trend of change in IR band intensity with time at different regions.

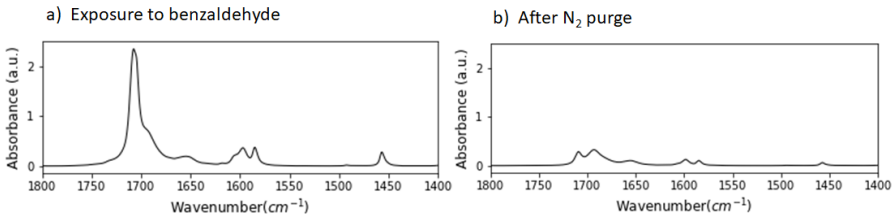

Figure S 19. IR difference spectra of benzaldehyde adsorbed on silicalite-1 at 110 °C, focussed on the 1400 to 1800 cm^{-1} region a) exposed to benzaldehyde for 7 minutes and b) after purging with N_2 for 2 hours.

The IR difference spectra of MFI samples with varying amounts of alumina (H-ZSM-5 of SAR 23, 80 and 280; silicalite-1) that have been exposed to benzaldehyde and then purged with N_2 for 2 hours are shown below in Figure S 20. These spectra indicate an increase in band intensities in the 1580 to 1640 cm^{-1} region, as the alumina content of the materials increases. Simulated spectra, Table S 11, indicate that the IR band intensity increase in the 1580 to 1600 cm^{-1} region is related to IR vibrations in protonated benzaldehyde, of carbon-carbon bonds in the aromatic ring, and the C=O group, which become strongly coupled upon protonation. The broad IR band at ca. 1635 cm^{-1}, assigned to a vibration in C=O interacting with a LA site, also increases in intensity as the alumina content of the materials is increased.

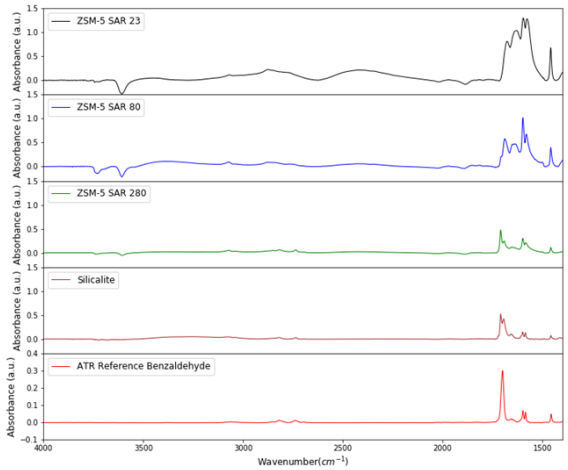

Figure S 20. IR difference spectra of MFI samples exposed to benzaldehyde at 110 °C and then purged with N_2 for 2 hours. For reference the bottom spectrum shows an ambient temperature FT-IR spectrum of liquid phase benzaldehyde recorded in ATR mode.

To examine further the nature of IR bands in the 1500 to 1700 cm^{-1} region an isotopic shift study was performed with ^{13}C enriched benzaldehyde (supplied by Cambridge Isotope), with the ^{13}C label present in the formyl group. The FT-IR measurements were performed in a different high temperature reaction cell (from Harrick Scientific) of a similar design and set-up as to the one described above. The experimental set-up used argon (Ar) as the carrier and purge gas, instead of N_2. Firstly, a disk made from H-ZSM-5 SAR 23 was placed in the reaction cell and heated to 110 ^oC whilst purging the reaction cell with Ar gas. A background spectrum was recorded. The disk was then removed from the reaction cell and a small drop of benzaldehyde (normal or ^{13}C enriched at the formyl group) added to it. It was then placed back in the reaction cell and heated back to 110 ^oC under flowing Ar. The spectra below were then recorded, Figure S 21.

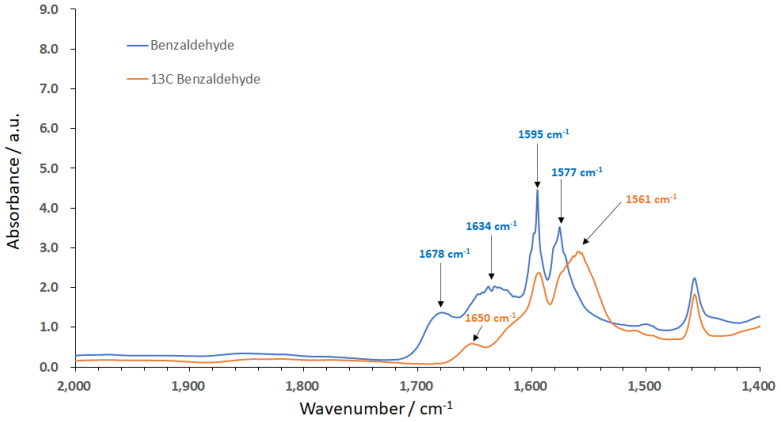

Figure S 21. IR difference spectra of benzaldehyde adsorbed on H-ZSM-5 SAR 23 at 110 °C. Blue spectrum shown used normal benzaldehyde; orange spectrum shown used benzaldehyde ^{13}C enriched at the formyl group carbon.

The IR spectrum for the H-ZSM-23 sample exposed to normal benzaldehyde showed sharp IR bands at 1577 and 1595 cm^{-1}, previously assigned to a protonated C=O bond vibration and an aromatic carbon-carbon bond vibration, which are strongly coupled. These two IR bands had shoulders at approximately 1571, 1580, 1598 and 1602 cm^{-1}. The shoulders are likely due to aromatic ring carbon-carbon vibrations associated with benzaldehyde adsorbed on LA sites (C=O vibration at 1634 cm^{-1}) and silanol -OH groups (C=O vibration at 1678 cm^{-1}). The sharp bands at 1577 and 1595 cm^{-1} were not evident in the sample with ^{13}C enriched benzaldehyde, instead a broad IR band centred at ca. 1561 cm^{-1} was observed. Simulated IR spectra, see Table S 11, using ^{13}C enriched benzaldehyde indicates two vibrations in approximately this region for protonated benzaldehyde, of similar intensity, one associated with an aromatic ring carbon-carbon bond vibration, the other with a C=O bond vibration; these vibrations are strongly coupled. There may be other undiscernible IR bands in this region from the various adsorbed benzaldehyde species, contributing to the width and shape of the band at 1561 cm^{-1}. The IR band at 1678 cm^{-1}, associated with a C=O group interacting with silanol -OH groups, moved, as expected, to 1650 cm^{-1}, when the formyl group was ^{13}C labelled. The broad IR band at ca. 1634 cm^{-1}, associated with C=O group interacting with LA sites, moved to a lower wavenumber, appearing as a shoulder under the IR bands in the 1600 cm^{-1} region. The breadth and noisy nature of the band at ca. 1634 cm^{-1} suggests it is associated with rather amorphous Al^{3+} LA sites, from extra-framework aluminium species.

The IR disk exposed to ^{13}C enriched benzaldehyde was removed from the reaction cell and a small amount of methanol was added to it. The disk was then placed back in the reaction cell and heated back to 110 ^{o}C under flowing Ar. The IR spectrum showed the presence of a new IR band at 1540 cm^{-1}, Figure S 22. This is shifted by 24 cm^{-1} from the IR band at 1564 cm^{-1}, see main paper, ascribed to vibrations from the C=O-Me group in the methyl oxonium species, $[PhC(H)(C{=}O{-}Me)]^{+}$. The ^{12}C to ^{13}C isotopic shift in the frequency of this IR band is in line with expectations.

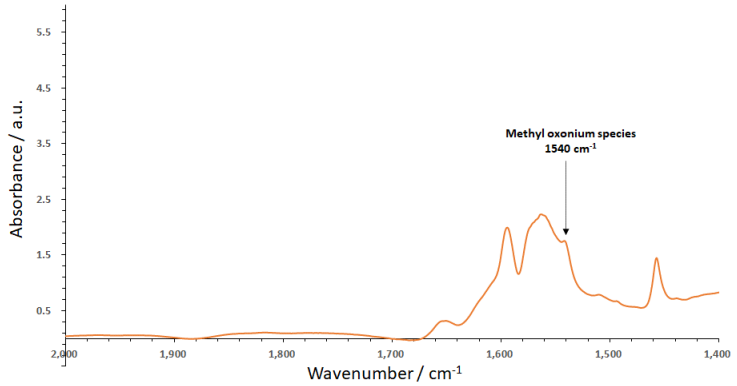

Figure S 22. IR difference spectra of ^{13}C enriched benzaldehyde adsorbed on H-ZSM-5 SAR 23 at 110 °C, after addition of methanol and purging with Ar.

4.3 **Studies with 4-methylbenzaldehyde and H-ZSM-5**

At 110 °C treatment of H-ZSM-5 SAR 80 with flowing N_2 saturated with 4-methylbenzaldehyde vapour resulted in complete titration of the BA sites. A strong unsymmetrical IR band at 1605 cm^{-1} was observed, with a shoulder IR band at 1576 cm^{-1} clearly present. These IR bands are assigned to C=O and aromatic carbon-carbon bond vibrations in protonated 4-methylbenzaldehyde, see Table S 11 for simulated IR bands, with underlying weaker IR bands from other 4-methylbenzaldehyde species e.g. C=O and aromatic ring vibrations from the aldehyde weakly bound to a silanol -OH group and LA sites.

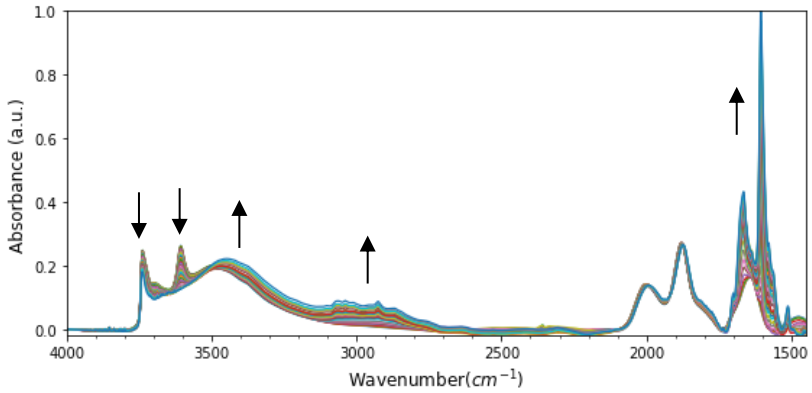

Figure S 23. Time resolved IR spectra of 4-methyl benzaldehyde adsorption on H-ZSM5 SAR 80 at 110 °C. Spectra displayed with 1 min intervals, over a 30 minute period. The arrows indicate the trend of change in IR band intensity with time at different regions. The BA sites were fully titrated.

The 4-methylbenzaldehyde treated H-ZSM-5 SAR 80 sample above was purged with N_2 at 110 °C and then exposed to flowing N_2 saturated with methanol vapour, generating a distinctive IR band at 1554 cm^{-1}, see Figure S 24, attributed to the methyl oxonium species, $[4\text{-Me-}C_6H_4\text{-C(H)(C=O-Me)}]^+$; see Table S 10 for simulated IR bands. Subsequent treatment of the sample with a stream of N_2 saturated with water vapour resulted in disappearance of the band at 1554 cm^{-1}. Re-exposure of the sample to methanol vapour regenerated the IR band at 1554 cm^{-1}. This experiment demonstrates the reversible and facile nature of formation of methyl oxonium species.

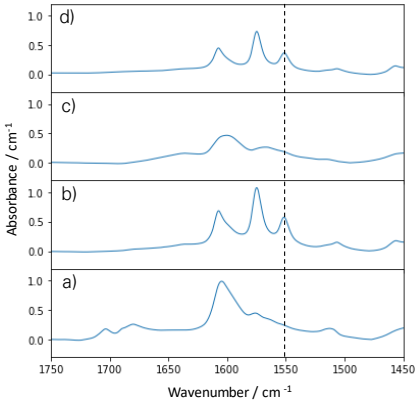

Figure S 24. IR difference spectra for sequential reactions of H-ZSM-5 SAR 80 at 110 °C with a) 4-methylbenzaldehyde b) followed by methanol c) followed by water d) followed by methanol. Black hashed line shows position of distinctive peak at 1554 cm^{-1} assigned to the methyl oxonium species.

4.4 Studies with 2-methylbenzaldehyde and 3-methylbenzaldehyde and H-ZSM-5

At 110 °C treatment of H-ZSM-5 SAR 80 with flowing N_2 saturated with either 2-methylbenzaldehyde or 3-methylbenzaldehyde vapour resulted in complete titration of the BA sites, see Figure S 25 and Figure S 26. Both these aldehydes took longer to fully titrate the BA sites, suggesting a tighter fit in the zeolite pores and slower diffusion; the time differences to achieve full BA site titration are not due to the small differences in volatility of the 3 aldehydes.

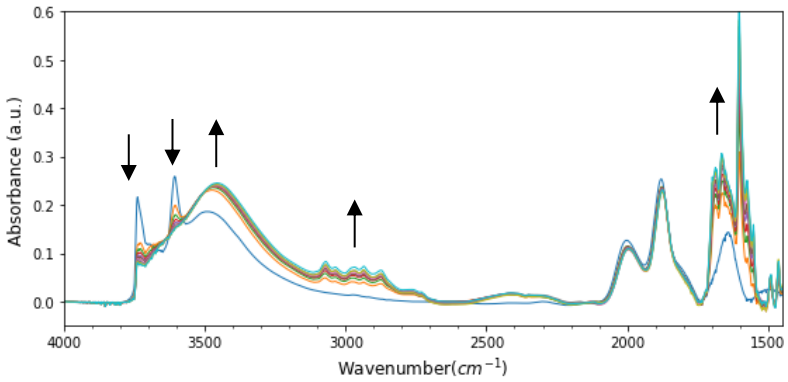

Figure S 25. Time resolved IR spectra of 2-methyl benzaldehyde adsorption on H-ZSM5 SAR 80 at 110 °C. Spectra displayed with 50 min intervals, over 450 minute period. The arrows indicate the trend of change in IR band intensity with time at different regions. The BA sites were fully titrated.

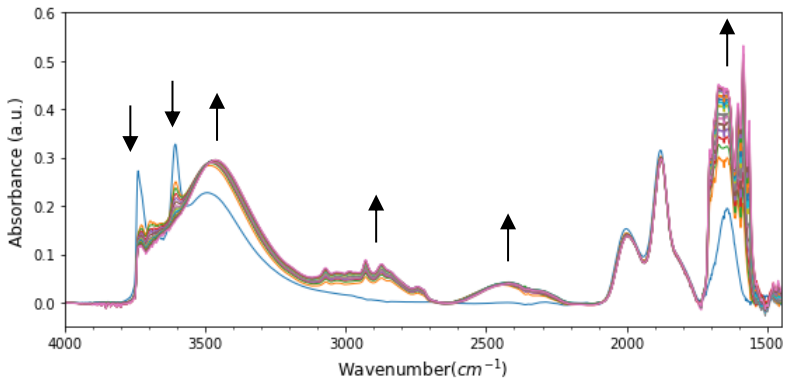

Figure S 26. Time resolved IR spectra of 3-methyl benzaldehyde adsorption on H-ZSM5 SAR 80 at 110 °C. Spectra displayed with 30 minute intervals, over a 480 minute period. The arrows indicate the trend of change in IR band intensity with time at different regions. The BA sites were fully titrated.

4.5 **Studies with 4-n-alkylbenzaldehydes and H-ZSM-5**

At 110 ^{o}C treatment of H-ZSM-5 SAR 23 with flowing N_2 saturated with 4-n-pentylbenzaldehyde vapour for 24 hours resulted in complete titration of the BA sites, Figure S 27. 4-n-pentylbenzaldeyde has a very low vapour pressure at ambient temperature, hence the time to titrate the BA sites is much longer than for the more volatile benzaldehyde described in the FT-IR experiments above and in the main paper for H-ZSM-5 SAR 23 and SAR 80. The sample was then purged with N_2 at 110 ^{o}C to remove any weakly held species. Strong IR bands at 1596 and 1578 cm^{-1} were observed in the sample, assigned to strongly coupled C=O and aromatic ring carbon-carbon vibrations in a protonated 4-n-pentylbenzaldehyde. There are likely weaker underlying aromatic ring vibrations from aldehyde weakly absorbed on other sites too in this region. A weaker shoulder IR Band at 1561 cm^{-1} was also observed. The broad IR band at ca. 1629 cm^{-1} was assigned to a C=O group interacting with a LA site. The IR band at 1675 cm^{-1} was assigned to a C=O group interacting with silanol -OH groups via H-bonding.

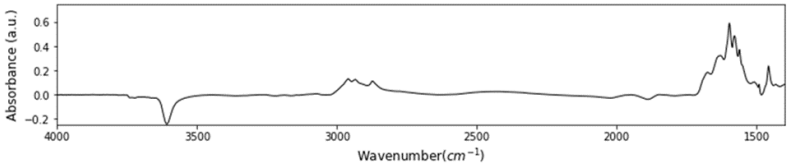

Figure S 27. IR difference spectrum of 4-n-pentylbenzaldehyde adsorbed on H-ZSM-5 SAR 23 at 110 °C, taken after 24 hours of exposure to 4-n-pentylbenzaldehyde, followed by purging with N_2 for 2 hours to remove any weakly adsorbed species. The BA sites were fully titrated.

The 4-n-pentylbenzaldehyde treated H-ZSM-5 SAR 23 sample above was then exposed to flowing N_2 saturated with methanol vapour for 130 minutes. This initiated the M2D reaction (the formation of significant amounts of DME was observed by MS analysis of the reactor effluent, see Figure S 29) and generated a distinctive IR band at 1547 cm^{-1}, attributed to the methyl oxonium species, [4-n-pentyl-C_6H_4-C(H)(C=O-Me)]$^{+}$. This band was present both during the M2D reaction and after the M2D reaction and purging the sample with N_2 for 2 hours, see Figure S 28. IR bands at 1605 and 1575 cm^{-1} were also present during and after the M2D reaction. The prominence and longevity of the promoter IR bands during this M2D experiment illustrates the anchoring effect of the pendant n-pentyl group on promoter competitive adsorption versus methanol, via zeolite pore wall van der Waal interactions cf. Figure 9 in the main paper with benzaldehyde. The absence of the IR bands at 1629 and 1675 cm^{-1} suggests that during the M2D reaction that methanol has totally displaced the weakly held aldehyde bound to the LA sites and silanol -OH groups. A lot of the aldehyde however remains bond to/associated with the BA sites, either in its protonated form or as a methyl oxonium species. The BA sites remain largely titrated by the aldehyde and associated species under the conditions (low partial pressure of methanol, no promoter in the methanol feed cf. HTE catalytic tests) and short duration of this FT-IR experiment.

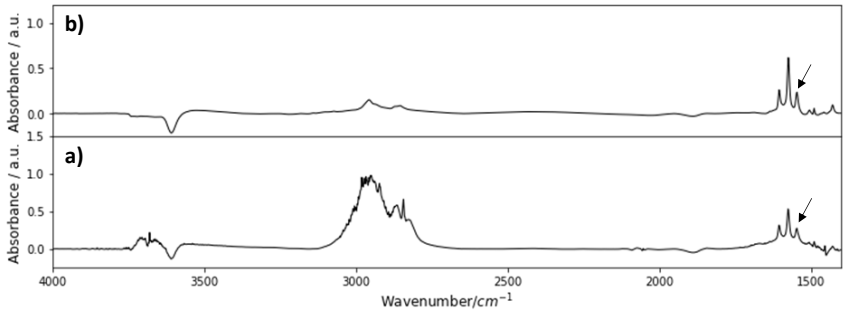

Figure S 28. IR difference spectra for H-ZSM-5 SAR 23 at 110 °C after a) titration with 4-n-pentylbenzaldehyde, followed by reaction with methanol, spectrum shown after 2 hours of reaction b) purging with N_2 after the M2D reaction. Black arrow shows position of distinctive peak at 1547 cm^{-1}, assigned to a methyl oxonium species.

In the above experiment with the 4-n-pentylbenzalhyde titrated H-ZSM-5 SAR 23 catalyst the effluent from the IR reaction cell was monitored for DME by MS, Figure S 29. After a short induction period of ca. 8 minutes DME started to be evolved from the catalyst, reaching a maximum at around 50 to 60 minutes. The DME evolved from the catalyst in the remainder of the experiment remained relatively constant, suggesting a relatively strong adsorption of the promoter species versus the methanol fed and products formed (DME and water), at the reduced methanol partial pressure of the FT-IR experiments versus the standard HTE catalytic tests.

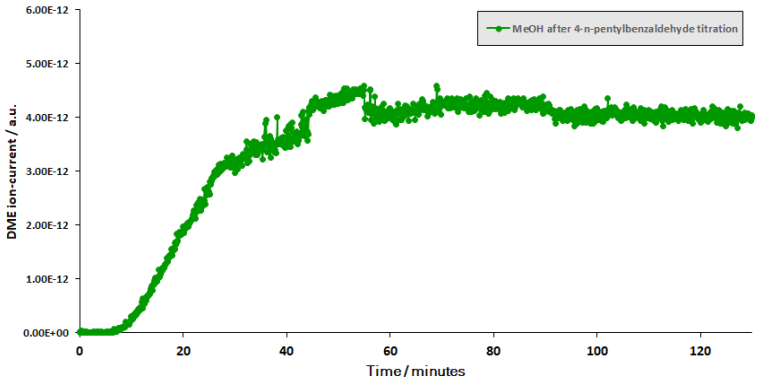

Figure S 29. DME evolved from sample of H-ZSM-5 SAR 23 at 110 °C exposed to 4-n-pentylbenzaldehyde, followed by methanol.

Similar M2D FT-IR-MS experiments to the above were performed with 4-n-propylbenzaldehyde and 4-n-butylbenzaldehyde, with H-ZSM-5 SAR 80 catalyst. Again the BA sites were titrated with the aldehyde, using an appropriate amount of time to achieve full titration of the BA sites. The samples were purged with N_2 at 110 °C and the M2D reaction was then initiated by exposing the zeolite samples to flowing N_2 saturated with methanol vapour. The FT-IR spectra for the experiment with 4-n-propylbenzaldehyde are shown in Figure S 30 and show a very similar 3-fingerprint pattern in the 1500 to 1650 cm^{-1} region after the M2D reaction and purging with N_2. A distinctive IR band, attributed to the methyl oxonium species, is seen at 1549 cm^{-1}. For the experiment with 4-n-butylbenzaldehyde, after the M2D reaction and purging with N_2, the distinctive IR band associated with the methyl oxonium species was seen at 1551 cm^{-1}.

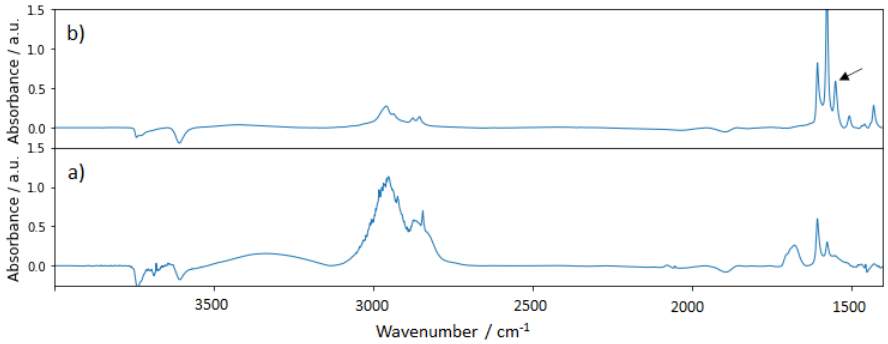

Figure S 30. IR difference spectra for H-ZSM-5 SAR 80 at 110 °C after a) titration with 4-n-propylbenzaldehyde, followed by reaction with methanol, spectrum shown after 2 hours of reaction b) purging with N_2 after the M2D reaction. Black arrow shows position of distinctive peak at 1549 cm^{-1}, assigned to a methyl oxonium species.

4.6 Studies with benzaldehyde and H-SSZ-13 and H-beta

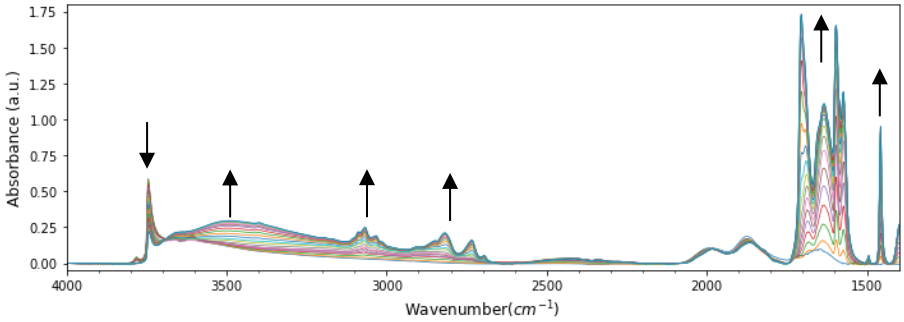

Figure S 31. Time resolved IR spectra of benzaldehyde adsorption on H-Beta zeolite at 110 °C. Spectra shown at 1 minute intervals over a 20 minute period, showing titration of the BA sites.

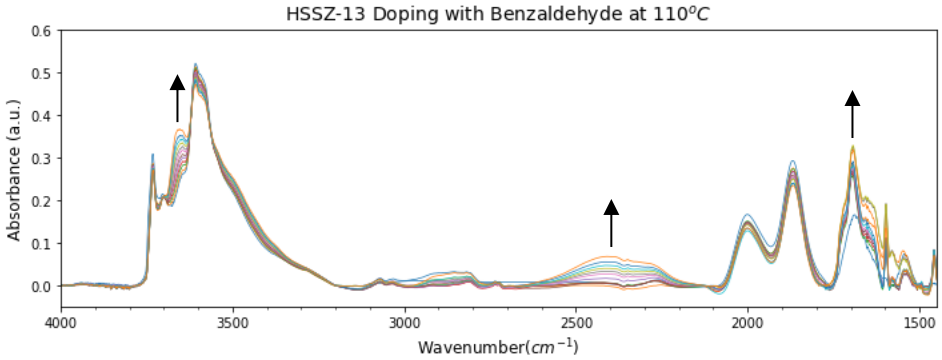

Figure S 32. Time resolved IR spectra of benzaldehyde adsorption on H-SSZ-13 zeolite at 110 °C. Spectra recorded over a 120 min period, showing little change in the BA site region, with the BA sites remaining largely intact (> 95%). This is in alignment with the small promotion observed when this catalyst is tested with benzaldehyde for the M2D reaction, see Figure 1 in main paper.

This version replaces the originally published version where two numbers on pg. 20 regarding the IRwere incorrectly quoted.

S. AMMONIA TPD

Ammonia temperature programmed desorption analysis was carried out using a fully automated Altamira AMI-200 Chemisorption Analyser. Approximately 50mg of sample was accurately weighed into a quartz U-shaped reactor tube. The reactor tube outlet was plugged using quartz wool that had been pre-treated in an oven at 120°C. The reactor tube was then placed in the AMI-200 unit and pre-treated in-situ under a flow of dry argon, heating from room temperature to 400 °C at 10°C/min and dwelling for 60mins. Following drying, the sample was cooled to 100 °C and NH_3 loading was carried out by flowing a 1% NH_3/Ar mix (30ml/min) for 60 minutes (or until saturation was reached). Whilst maintaining the bed temperature at 100 °C, any physisorbed and other weakly adsorbed material was then purged from the surface by treating with water vapour for 60 minutes. Once physisorbed and other weakly adsorbed material had been removed, the sample was further treated with a flow of dry argon at 100 °C for 60 minutes in order to remove any residual water from the sample bed. Finally, TPD analysis was carried out by heating the sample from 100 °C to 800 °C at a rate of 5°C/min under flowing argon (30ml/min). NH_3 desorption was continually monitored throughout using a Mettler Toledo T50 acid-base auto-titrator. This mode of detection utilises a Kjeldahl-style pH stat method whereby ammonia that desorbs from the sample is delivered to a dilute boric acid receiver solution. The pH of this solution is constantly maintained at 5 by adding a 0.02M HCl titrant. The volume of HCl required to sustain a constant pH can be used to calculate the amount of NH_3 that has desorbed from the sample. Results are expressed as µmoles of H^+ per gramme of catalyst based upon the NH_3 desorbed per loaded mass of sample and are given in Table S 4 below for the zeolite and silicotungstic acid/silica catalysts tested in Table S 2, Table S 3, Figure S 5 and Figure S 14.

Table S 4. Ammonia TPD data for various catalysts.

Catalyst	**Acidity / µmoles H^+ g^{-1}**
H-ZSM-5 SAR 80 batch 1	346
H-ZSM-5 SAR 80 batch 2	370
H-ZSM-11 SAR 50	440
H-ZSM-5 SAR 23 (2016)	910
H-ZSM-5 SAR 280 (2016)	140
STA/silica	426

6. Computational Methods

6.1 Calculation of transition states and adsorption energy calculations

The methodology used for the calculation of the energies of reaction intermediates and transition states and the adsorption energies of the aldehydes in H-ZSM-5 is the same as that used in a previous publication.[1]

The optimized geometries and corresponding energies were calculated using VASP[7-9] package. A 400eV cut-off energy and PREC = Accurate were set for plane wave basis set, while consistent PAW potentials[10] were used for each atom. The optB86b-vdW DFT functional[11, 12] was used to calculate the non-local exchange and correlation energies, as well as dispersion interaction contributions. A 1 x 1 x 1 Monkhorst-Pack was used to sample the Brillouin zone. All the geometries were converged until forces on all the atoms were below 0.05 eV/A, while the relaxation in electronic energy within the SCF loop was lower than 10^{-6}. The transition state geometry was firstly initiated using Nudged Elastic Band (NEB) method[13, 14] and further refined using DIMER technique.[15]

The MFI crystallographic structure was retrieved from database of zeolites structures[16] and the Brønsted acid location was selected at zig-zag/straight pore intersection (see below). Each adsorption energy was calculated as the energy difference between the zeolite with adsorbate versus the zeolite and adsorbate in the gas phase. The adsorption values reported here are associated with enthalpy contributions at 0 K, without any temperature corrections applied. ZSM-5 (MFI) molecular modelling simulations used 288 framework atoms, compromised of 95 Si and 192 O atoms, with one of the T-atoms in the framework substituted with an Al atom to create a BA site. For the molecular modelling work a representative BA site was selected at the intersection of the straight and sinusoidal channels, selecting the O2 site located between the T1 and T2 sites with the T1 site selected for the Al location,[16] see Figure S 33.

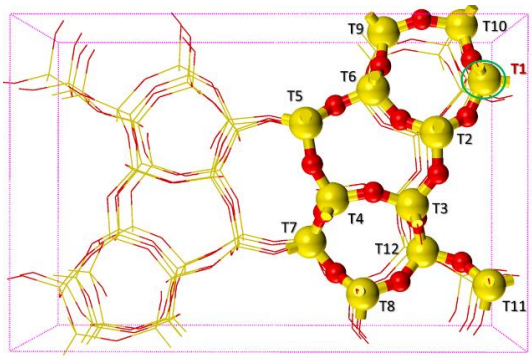

Figure S 33. MFI unit cell showing T1 site used for molecular modelling calculations in this manuscript; the T-atom circled in green was substituted with an Al atom to create the BA site.

Initial modelling was performed on oxygen atoms adjacent to the T1 site and the adsorption energies were calculated using multiple starting point orientations. The O2 location was found to be more favourable for benzaldehyde adsorption by allowing the benzene ring to be aligned with the ellipsoidal straight pore of ZSM-5, see Figure S 34. In the H-bonded mode the carbonyl group of the aldehyde breaks conjugation with the aromatic ring and orients perpendicular relative to the ring, having its O atom pointing toward BA2. In the second adsorption mode the proton was desorbed from the BA site and placed on the oxygen of the formyl group, with

the positively charged molecule kept planar and similarly placed in the centre of the zeolite pore. In this case the protonated formyl group retained its conjugation with the aromatic ring.

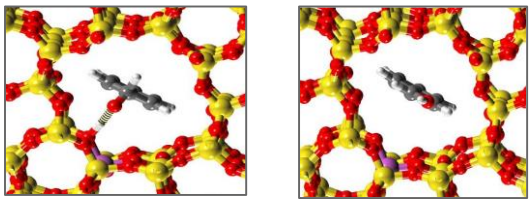

Figure S 34. Comparison between modes of benzaldehyde adsorption explored through molecular modelling. (a) adsorption of benzaldehyde to O2 location in H-ZSM-5 through hydrogen bonding to BA site; (b) Protonation of benzaldehyde.

The adsorption energy of methanol H-bonded to the BA site described above (see left-hand side figure in Figure S 35) was also determined and found to be -118 kJ mol^{-1}; water H-bonded to the same BA site had an adsorption energy of -99 kJ mol^{-1}. We previously reported an adsorption energy of -82 kJ mol^{-1} for methanol,[1] which was calculated using the adjacent BA site, with the Al in the same T-site (see right-hand side figure in Figure S 35). Both methanol adsorption energies are lower than all of those determined for benzaldehyde and its 4-substituted derivatives, see main paper. The water adsorption energy is lower than that calculated for methanol and all the 4-susbtituted benzaldehyde derivatives, however competitive adsorption of water on the BA site (and on the charged zeolite framework if the BA site is deprotonated, see Scheme S 1) at high methanol conversions may increasingly become a factor in determining catalyst activity, especially given the sensitivity of the promoted reaction pathway to water.

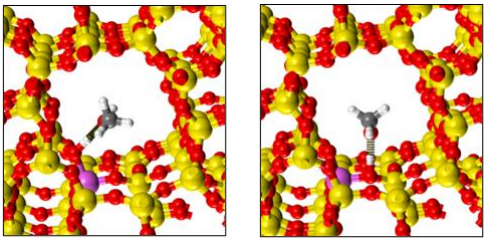

Figure S 35. Adsorption of methanol on two BA sites via H-bonding.

The adsorption energy of 4-pentylbenzaldehyde to the BA site chosen above for benzaldehyde adsorption was determined using two conformations for the n-pentyl chain, as shown in Figure S 36. The conformations chosen allowed the aldehyde to be favourably accommodated in the zeolite pore, giving adsorption energies of -192 kJ mol^{-1}, for conformation a), and -199 kJ mol^{-1}, for conformation b). In Figure 17 in the main paper the lower energy absorption number is shown, for conformer where the n-pentyl chain is traversing the intersection of the straight and sinusoidal channels.

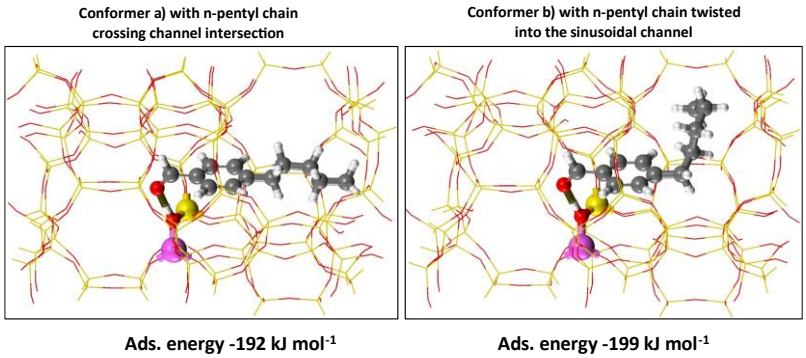

Figure S 36. Adsorption modes for 4-pentylbenzaldehdye H-bonded to a BA site, with the n-pentyl chain in two different conformations.

The adsorption energy of 4-ethylbenzaldehyde on the same BA site as chosen above for 4-n-pentylbenzaldehyde adsorption was also determined. Geometry optimised structures are shown in Figure S 37 below. Initially two conformations were selected, with the ethyl group placed in plain with aromatic ring before geometry optimization, conformers a) and b) in Figure S 37. The geometry optimised adsorption energies were -166 kJ mol^{-1} for conformer a) and -177 kJ mol^{-1} for conformer b). These adsorption energies are lower than those determined for 4-n-pentylbenzaldehyde.

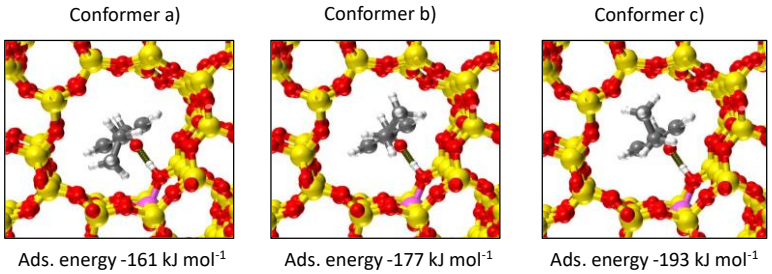

Figure S 37. Adsorption modes for 4-ethylbenzaldehdye H-bonded to a BA site, with the ethyl group in three different conformations.

The adsorption energy of a third conformer was also determined, conformer c) in Figure S 37. In this conformer the ethyl group is twisted 90 degrees out of plain before geometry optimisation. The geometry optimized conformer c) has an adsorption energy of -193 kJ mol^{-1}, which is considerably larger than that found for the other ethyl conformers and intermediate in adsorption energy between the adsorption energies found for the two 4-n-pentylbenzaldehyde conformers.

The absorption energies determined above for 4-ethylbenzaldehyde and 4-pentylbenzaldehyde indicate that there is considerable degree of variability in the adsorption energy calculated dependent on the conformer selected for geometry optimisation. In contrast for 4-methylbenzaldehyde there is no such conformational variability for the C1 alkyl chain, which is also centralised in the zeolite channel, see Figure S 38 below. The absorption energy for 4-methylbenzaldehdye is -168 kJ mol^{-1}, which is significantly lower than found for the most strongly adsorbed conformers of 4-ethylbenzaldehyde and 4-n-pentylbenzaldehyde, of -193 and -199 kJ mol^{-1} respectively. Ascertaining a clear trend for the absorption energy of 4-alkylbenzaldehydes with C2 to C5 alkyl groups is however fraught with complexity due to the large number of possible conformations of the alkyl

groups and their steric environment with respect to the zeolite pore walls. Furthermore the number of conformational possibilities in the zeolite pores increase when the linear alkyl chain has 3 or more carbon atoms, as the alkyl chain then enters the intersection of the straight channel with the sinusoidal channel in the zeolite. In addition, static simulations of this nature have their limitations and molecular dynamic simulations may provide additional insight to determine the factors at the molecular level involved in the experimental observations described in this work.

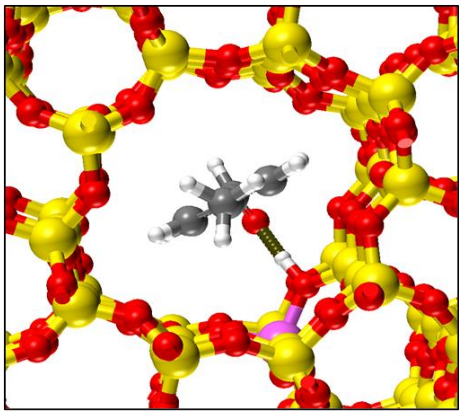

Ads. energy -168 kJ mol^{-1}

Figure S 38. Adsorption mode for 4-methylbenzaldehdye H-bonded to a BA site.

6.2 Energy profile for the catalytic cycle with H-ZSM-5

The full reaction and mechanistic pathway for benzaldehyde promoted M2D reaction with H-ZSM-5 is shown in the Scheme S 1 below.

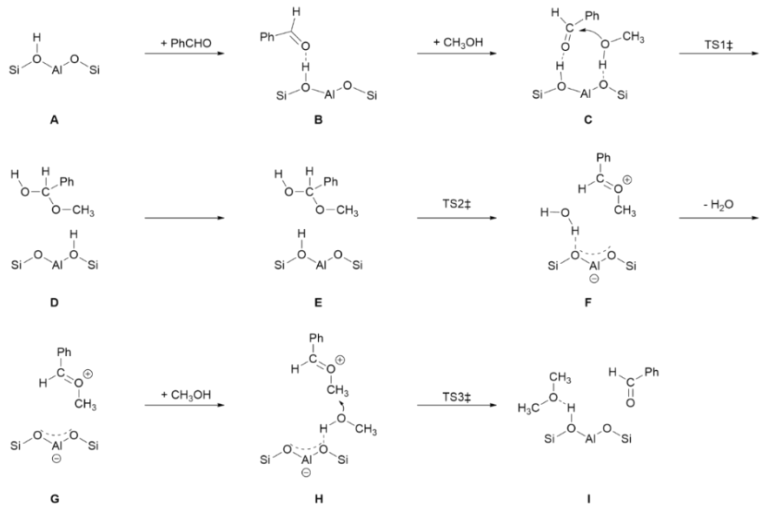

Scheme S 1. Proposed reaction scheme for catalytic cycle for formation of DME with benzaldehyde promoter in the vicinity of zeolite active site.

The above scheme describes the steps in the energy profile diagram below, Figure S 39, which was created using the mechaSVG python package.[17] The apparent activation energy barrier for the overall catalytic cycle is 88 kJ mol^{-1} and is associated with the reaction of the methyl oxonium species with adsorbed methanol,

transition state 3. The intermediates associated with the methyl oxonium species (F, G and H) are all higher in energy than those associated with the adsorbed benzaldehyde and hemi-acetal precursors (B, C, D and E). This, together with the transition state energy barriers for the forward and reverse reactions, is consistent with the observations in the FT-IR experiments of the transient nature of the methyl oxonium species, especially at elevated methanol and water concentrations present in the zeolite pores during catalysis.

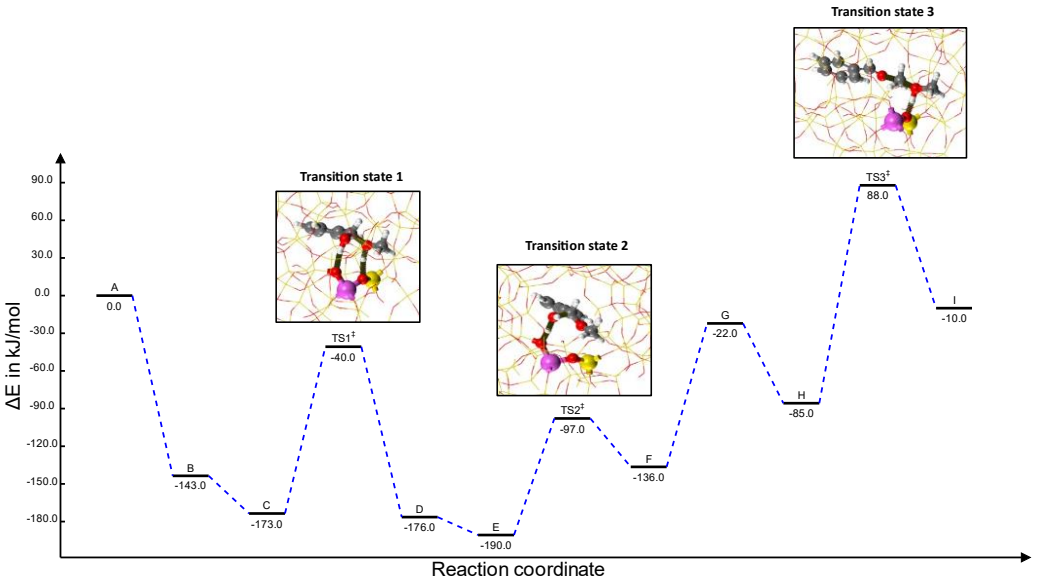

Figure S 39. Energy profile for the catalytic cycle with benzaldehyde promoter.

6.3 **Generation of gas phase conformers**

The rotational conformers for all the benzaldehyde derivatives in the gas phase were prepared using the Materials and Processes Simulations platform of Scienomics.[18] All conformers were optimised at the DFT level and the chemical properties are reported for the lowest energy conformer.

6.4 **DFT calculations and descriptors**

All the benzaldehyde derivatives were optimized in the gas phase starting from a planar configuration of the carbonyl to the benzene ring using Q-CHEM 5.3 & 5.4 software[19] and all QCHEM defaults unless stated otherwise. The DFT calculations were performed using the B3LYP functional[20, 21] and def2-TZVP basis set.[22] The natural bond orbital (NBO) analysis was calculated at the same level of theory using NBO 5.0.[23] Vibrational frequencies were calculated to confirm stationary points represent a ground state. Isotropic and anisotropic polarizabilities were calculated using the MOProp module at the same level of theory. A scf convergence of 10^{-8} has been used for all steps described above. The Verloop Sterimol parameters[24, 25] B_1, B_5, and L for ring substituents were calculated for the geometry optimized structures using the MORFEUS package.[26] Uncorrected L parameters were obtained and all other defaults were used for the calculation (radii = crc).

The following electronic and steric parameters were extracted from the geometry optimized structures:

- Isotropic and Anisotropic polarizability

- HOMO/LUMO energies
- Dipole moment
- IR frequencies and intensities
- Molecular volume and molecular surface area
- NBO charges

Hammett substituent constants were obtained from the review by Taft et al.[27] All steric and electronic parameters are displayed in Table S 5 and Sterimol parameters are contained in Table S 6.

Table S 5 part 1. Values of relative molecular mass (M_r, amu), isotropic polarizability (^{iso}pol, bohr3), anisotropic polarizability (^{aniso}pol, bohr3), dipole moment (μ, debye), HOMO_energy and LUMO_energy (hartree), infrared frequency of carbonyl group (Vc=o, cm-1), natural charges of aldehyde atoms (NBO_C, NBO_O, NBO_H), molecular volume (MV, Å^3), molecular surface area (S, Å^2), Hammett values (σ_p for para-substituted benzaldehydes, σ_m for meta-substituted benzaldehydes).

Molecule	M_r	μ	^{iso}Pol	$^{aniso}Pol$	$V_{C=O}$	HOMO_energy	LUMO_energy
Benzaldehyde	106.12	3.45	82.14	60.28	1770.11	-0.2674	-0.0768
4-Methylbenzaldehyde	120.15	4.01	97.32	74.32	1767.60	-0.2632	-0.0716
4-Ethylbenzaldehyde	134.17	4.06	110.37	78.69	1767.23	-0.2630	-0.0718
4-n-Propylbenzaldehyde	148.20	4.11	123.85	88.84	1766.75	-0.2626	-0.0713
4-n-Butylbenzaldehyde	162.23	4.19	136.72	92.13	1765.95	-0.2624	-0.0709
4-n-Pentylbenzaldehyde	176.25	4.21	149.74	101.70	1767.27	-0.2623	-0.0709
4-MeO-benzaldehyde	136.15	5.18	104.34	86.79	1759.52	-0.2465	-0.0639
4-CF_3-benzaldehyde	174.12	1.77	96.26	68.82	1777.94	-0.2814	-0.0966
4-F-benzaldehyde	124.11	2.33	82.94	62.80	1769.38	-0.2718	-0.0786
4-Cl-benzaldehyde	140.56	2.27	97.91	85.14	1771.84	-0.2715	-0.0846
4-Br-benzaldehyde	185.02	2.23	106.58	95.45	1772.05	-0.2686	-0.0858
4-CO_2Me-benzaldehyde	164.16	2.23	117.90	98.31	1767.71	-0.2748	-0.0974
3-MeO-benzaldehyde	136.15	2.39	101.41	67.21	1766.35	-0.2448	-0.0750
3-Methylbenzaldehyde	120.15	3.55	95.99	65.18	1768.10	-0.2646	-0.0744
3-F-benzaldehyde	124.11	3.70	82.59	60.46	1775.08	-0.2753	-0.0860
3-Cl-benzaldehyde	140.56	2.06	95.96	73.80	1774.79	-0.2703	-0.0866
3-Br-benzaldehyde	185.02	2.02	104.21	81.23	1775.86	-0.2673	-0.0874

Table S 5 part 2. Values of relative molecular mass (M_r, amu), isotropic Polarizability (^{iso}Pol, Bohr^3), anisotropic Polarizability ($^{aniso}Pol$, Bohr^3), dipole moment (μ, Debye), $HOMO\_energy$ and $LUMO\_energy$ (Hartree), Infrared frequency of carbonyl group ($V_{C=O}$, cm^{-1}), natural charges of aldehyde atoms (NBO_C, NBO_O, NBO_H), molecular volume (MV, Å^3), molecular surface area (S, Å^2), Hammett values (σ_p for para-substituted benzaldehydes, σ_m for meta-substituted benzaldehydes) (continued).

Molecule	NBO_C	NBO_O	NBO_H	MV	S	$\sigma_{p\ or\ m}$
Benzaldehyde	0.4080	-0.5078	0.1009	102.574	132.931	0
4-Methylbenzaldehyde	0.4070	-0.5129	0.0995	119.246	154.574	-0.17
4-Ethylbenzaldehyde	0.4072	-0.5128	0.0994	136.064	176.422	-0.15
4-n-Propylbenzaldehyde	0.4071	-0.5131	0.0993	152.834	198.205	-0.13
4-n-Butylbenzaldehyde	0.4071	-0.5133	0.0993	169.611	219.973	-0.16
4-n-Pentylbenzaldehyde	0.4072	-0.5134	0.0992	186.393	241.8	-0.15
4-MeO-benzaldehyde	0.4038	-0.5208	0.0979	127.633	164.265	-0.27
4-CF_3-benzaldehyde	0.4077	-0.4956	0.1051	133.371	170.853	0.54
4-F-benzaldehyde	0.4067	-0.5090	0.1021	107.26	139.046	0.06
4-Cl-benzaldehyde	0.4066	-0.5052	0.1026	116.44	149.616	0.23
4-Br-benzaldehyde	0.4068	-0.5041	0.1028	120.77	154.306	0.23
4-CO_2Me-benzaldehyde	0.4067	-0.4993	0.1037	146.803	187.035	0.45

3-MeO-benzaldehyde	0.4079	-0.5132	0.1027	127.665	164.179	0.12
3-Methylbenzaldehyde	0.4084	-0.5103	0.1003	119.256	154.493	-0.07
3-F-benzaldehyde	0.4071	-0.5006	0.1045	107.293	139.114	0.34
3-Cl-benzaldehyde	0.4088	-0.4998	0.1044	116.479	149.654	0.37
3-Br-benzaldehyde	0.4091	-0.4993	0.1048	120.794	154.312	0.39

Table S 6. Verloop Sterimol parameters for para- and meta-substituents.

Molecule	B_1	B_5	L
Benzaldehyde	1.1	1.1	2.18
4-Methylbenzaldehyde	1.7	2.12	3.2
4-Ethylbenzaldehyde	1.7	3.26	4.29
4-n-Propylbenzaldehyde	1.7	3.53	5.33
4-n-Butylbenzaldehyde	1.7	4.6	6.44
4-n-Pentylbenzaldehyde	1.7	4.9	7.48
4-MeO-benzaldehyde	1.52	3.13	4.2
4-CF_3-benzaldehyde	2.09	2.73	3.49
4-F-benzaldehyde	1.47	1.47	2.81
4-Cl-benzaldehyde	1.75	1.75	3.49
4-Br-benzaldehyde	1.85	1.85	3.75
4-CO_2Me-benzaldehyde	1.76	3.49	5.14
3-MeO-benzaldehyde	1.52	3.14	4.2
3-Methylbenzaldehyde	1.7	2.12	3.21
3-F-benzaldehyde	1.47	1.47	2.82
3-Cl-benzaldehyde	1.75	1.75	3.5
3-Br-benzaldehyde	1.85	1.85	3.76

6.5 **Descriptors and Sterimol values for 2-substituted benzaldehydes**

Molecular descriptors were calculated for 2-substituted (*ortho*-substituted) benzaldehydes as outlined in section 6.4. The values are displayed in Table S 7. *Ortho*-Sterimol values describe the size of the substituent in the ortho-position of the aromatic ring.[28] Where the *ortho*-substituent is a H atom the Sterimol values for hydrogen are used. Sterimol values are displayed in Table S 8.

Table S 7. Values of relative molecular mass (M_r, amu), isotropic polarizability (^{iso}pol, bohr3), anisotropic polarizability (^{aniso}pol, bohr3), dipole moment (μ, debye), HOMO_energy and LUMO_energy (hartree), infrared frequency of carbonyl group (Vc=o, cm-1), natural charges of aldehyde atoms (NBO_C, NBO_O, NBO_H), molecular volume (MV, Å^3), molecular surface area (S, Å^2), Hammett values (σ_p for para-substituted benzaldehydes, σ_m for meta-substituted benzaldehydes).

Molecule	M_r	μ	^{iso}Pol	$^{aniso}Pol$	$V_{C=O}$	HOMO_energy	LUMO_energy
2-Methylbenzaldehyde	120.15	3.07	95.28	64.81	1763.35	-0.2614	-0.073
2-MeO-benzaldehyde	136.15	4.93	100.80	66.13	1751.78	-0.2455	-0.0709
2-F-benzaldehyde	124.11	3.52	82.11	59.94	1761.98	-0.2715	-0.0842
2-Cl-benzaldehyde	140.56	3.38	94.66	66.80	1761.42	-0.2709	-0.0864
2-Br-benzaldehyde	185.02	3.35	102.54	76.17	1760.49	-0.2686	-0.0872

Table S 7. Values of relative molecular mass (M_r, amu), isotropic polarizability (^{iso}pol, bohr3), anisotropic polarizability (^{aniso}pol, bohr3), dipole moment (μ, debye), HOMO_energy and LUMO_energy (hartree), infrared frequency of carbonyl group (Vc=o, cm-1), natural charges of aldehyde atoms (NBO_C, NBO_O, NBO_H), molecular volume (MV, Å^3), molecular surface area (S, Å^2), Hammett values (σ_p for para-substituted benzaldehydes, σ_m for meta-substituted benzaldehydes) continued.

Molecule	NBO_C	NBO_O	NBO_H	MV	S	$\sigma_{p\ or\ m}$
2-Methylbenzaldehyde	0.40409	-0.51683	0.09945	119.01	151.494	-
2-MeO-benzaldehyde	0.40045	-0.51981	0.12476	127.503	162.325	-
2-F-benzaldehyde	0.40147	-0.50546	0.1243	107.252	137.987	-
2-Cl-benzaldehyde	0.40269	-0.50412	0.12656	116.324	147.344	-
2-Br-benzaldehyde	0.40365	-0.50293	0.12657	120.599	151.665	-

Table S 8. Sterimol and *Ortho*-Sterimol values for benzaldehyde promoters.

Molecule	B_1	B_5	L	B_{1ortho}	B_{5ortho}	L_{ortho}
Benzaldehyde	1.1	1.1	2.18	1.1	1.1	2.18
4-Methylbenzaldehyde	1.7	2.12	3.2	1.1	1.1	2.18
4-Ethylbenzaldehyde	1.7	3.26	4.29	1.1	1.1	2.18
4-n-Propylbenzaldehyde	1.7	3.53	5.33	1.1	1.1	2.18
4-n-Butylbenzaldehyde	1.7	4.6	6.44	1.1	1.1	2.18
4-n-Pentylbenzaldehyde	1.7	4.9	7.48	1.1	1.1	2.18
4-MeO-benzaldehyde	1.52	3.13	4.2	1.1	1.1	2.18
4-CF_3-benzaldehyde	2.09	2.73	3.49	1.1	1.1	2.18
4-F-benzaldehyde	1.47	1.47	2.81	1.1	1.1	2.18
4-Cl-benzaldehyde	1.75	1.75	3.49	1.1	1.1	2.18
4-Br-benzaldehyde	1.85	1.85	3.75	1.1	1.1	2.18
4-CO_2Me-benzaldehyde	1.76	3.49	5.14	1.1	1.1	2.18
3-MeO-benzaldehyde	1.52	3.14	4.2	1.1	1.1	2.18
3-Methylbenzaldehyde	1.7	2.12	3.21	1.1	1.1	2.18
3-F-benzaldehyde	1.47	1.47	2.82	1.1	1.1	2.18
3-Cl-benzaldehyde	1.75	1.75	3.5	1.1	1.1	2.18

3-Br-benzaldehyde	1.85	1.85	3.76	1.1	1.1	2.18
2-Methylbenzaldehyde	1.7	2.12	3.2	1.7	2.12	3.2
2-MeO-benzaldehyde	1.52	3.13	4.21	1.52	3.13	4.21
2-F-benzaldehyde	1.47	1.47	2.82	1.47	1.47	2.82
2-Cl-benzaldehyde	1.75	1.75	3.5	1.75	1.75	3.5
2-Br-benzaldehyde	1.85	1.85	3.76	1.85	1.85	3.76

6.6 **Calculation of protonation and methylation energies**

The gas phase protonation and methylation energies for benzaldehyde derived species were calculated using Q-CHEM 5.3 & 5.4 software[19] with the B3LYP functional[20, 21] and def2-TZVP basis set.[22] The geometry optimized structure of the benzaldehyde derivative was reacted with H_3O^+ or $MeOH_2^+$ for the protonation and methylation reactions respectively, as in Scheme S 2. The proton or methyl group was placed cis to the hydrogen on the adjacent carbon atom[4, 29] and the geometry re-optimized. All the protonated or methylated species have a +1 charge. An energy of -76.4630 Hartree was used for H_2O, -76.7376 Hartree for H_3O^+, and -116.0737 Hartree for $MeOH_2^+$. Energy values at 0 K were extracted in Hartree and converted to kJ/mol. The protonation and methylation energies are displayed in Table S 9.

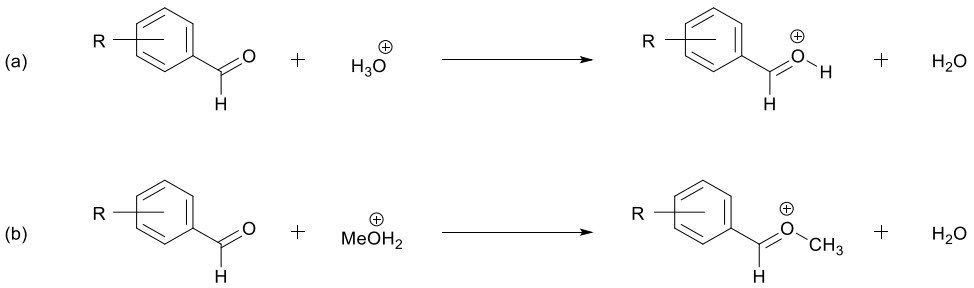

Scheme S 2. (a) Reaction used for calculation of gas phase protonation energies (b) Reaction used for calculation of gas phase methylation energies.

Table S 9. Calculated protonation and methylation energies for benzaldehyde derived molecules in the gas phase at 0 K. All values in kJ mol^{-1}.

Molecule	*Protonation energy*	*Methylation energy*
Benzaldehyde	-159.19	-132.37
4-Methylbenzaldehyde	-178.89	-149.11
4-Ethylbenzaldehyde	-181.70	-151.26
4-n-Propylbenzaldehyde	-184.31	-153.60
4-n-Butylbenzaldehyde	-185.50	-154.70
4-n-Pentylbenzaldehyde	-186.55	-155.33
4-MeO-benzaldehyde	-204.02	-170.37
4-CF_3-benzaldehyde	-128.10	-103.81
4-F-benzaldehyde	-155.88	-128.14
4-Cl-benzaldehyde	-157.37	-128.81

4-Br-benzaldehyde	-157.80	-128.89
4-CO_2Me-benzaldehyde	-150.44	-123.79
3-MeO-benzaldehyde	-170.01	-140.99
3-Methylbenzaldehyde	-169.21	-141.05
3-F-benzaldehyde	-140.95	-116.23
3-Cl-benzaldehyde	-141.97	-116.12
3-Br-benzaldehyde	-142.35	-116.58

As expected, the calculated protonation and methylation energies are highly correlated with an $R^2 = 1$, see a) in Figure S 40. The correlation between calculated protonation energy and DME STY, $R^2 = 0.67$, see b) in Figure S 40, is comparable to that observed for other electronic descriptors of the benzaldehyde based promoters, see Figure S 41. Indeed, there is a high degree of correlation between the protonation energy and the other electronic descriptors, most notably NBO charge on carbonyl oxygen, see a) in Figure S 41. The NBO charge and other electronic descriptors were selected for further data analytics approaches because they are more facile to calculate than the protonation and methylation energies.

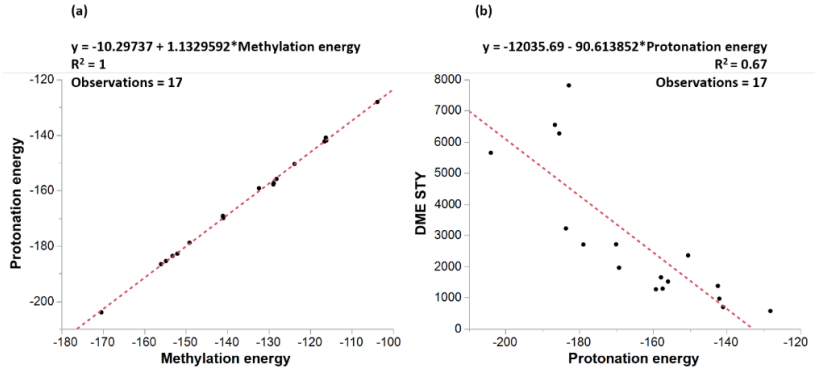

Figure S 40. (a) Correlation between calculated protonation and methylation energy (kJ/mol); (b) Correlation between protonation energy (kJ/mol) and DME STY (g $kg^{-1}h^{-1}$).

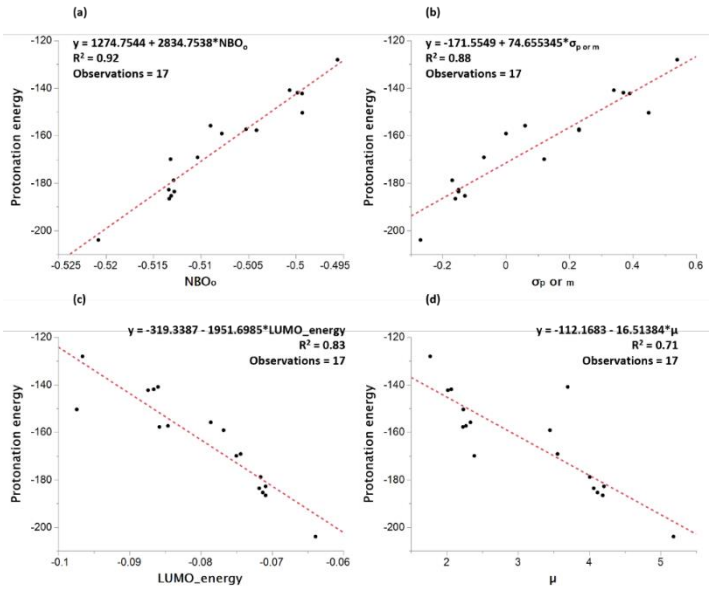

Figure S 41. Correlation of calculated protonation energy with (a) NBO charge on oxygen; (b) Hammett substituent values; (c) LUMO_energy; (d) dipole moment.

6.7 Calculation of IR frequencies for benzaldehyde and 4-methylbenzaldehyde and related species

The IR frequencies were calculated for the benzaldehyde, 4-methylbenzaldehyde and related methyl oxonium species using Q-CHEM 5.3 & 5.4 software[19] with the B3LYP functional[20, 21] and def2-TZVP basis set.[22] A methyl group was added to the carbonyl oxygen of the initial geometry optimized structure of benzaldehyde and 4-methylbenzaldehyde. The methyl group was placed *cis* to the hydrogen atom on the adjacent carbon atom (see Figure S 42),[4, 29] and the geometry re-optimized, followed by frequency calculations. Both steps were performed using scf convergence of 10^{-8}. The calculated IR frequencies are shown in Table S 10. In addition the vibrational modes calculated by molecular modelling were visualised using IQmol software to assist in assigning the experimentally observed IR bands.

Figure S 42. Benzaldehyde and 4-methylbenzaldehyde methyl oxonium species.

Table S 10. Calculated Infrared (IR) vibrational frequencies (cm^{-1}) for benzaldehyde and 4-methylbenzaldehyde and their respective methyl oxonium analogues. The IR frequencies are reported for the 1450 – 1720 cm^{-1} region (after correction) along with intensities. A scaling factor of 0.9671 was used to correct the IR frequencies obtained from DFT calculations.[30]

Molecule	Aldehyde		
	IR frequency	Corrected IR frequency[a]	Intensity
Benzaldehyde	1527 (ring)	1477	0.70
	1625 (ring)	1572	13.80
	1642 (ring)	1588	31.01
	1770 (C=O)	1712	268.95
4-Methylbenzaldehyde	1542 (ring)	1491	0.16
	1611 (ring)	1558	15.75
	1649 (ring)	1595	102.32
	1768 (C=O)	1710	295.70

Molecule	Methyl oxonium		
	IR frequency	Corrected IR frequency[a]	Intensity
Benzaldehyde	1530	1480	9.92
	1595	1543	130.44
	1618	1565	611.39
	1643	1589	81.27
4-Methylbenzaldehyde	1539	1488	44.08
	1570	1518	49.05
	1620	1567	827.76
	1651	1597	164.22

[a] Corrected frequency calculated using a scaling factor of 0.9671.[30]

The above calculations were repeated for protonated benzaldehyde, [PhC(H)(=O-H)]$^+$, both for normal benzaldehyde and for benzaldehyde ^{13}C enriched at the formyl group, and protonated 4-methylbenzadlehyde, [4-Me-C_6H_4C(H)(=O-H)]$^+$, see Table S 11.

Table S 11 Calculated Infrared (IR) vibrational frequencies (cm^{-1}) for protonated normal and ^{13}C formyl group enriched benzaldehyde and 4-methylbenzaldehyde. The IR frequencies are reported for the 1450 – 1600 cm^{-1} region along with intensities. A scaling factor of 0.9671 was used to correct the IR frequencies obtained from DFT calculations

Molecule	Protonated aldehyde		
	IR frequency	Corrected IR frequency[a]	Intensity
Benzaldehyde unlabelled	1522 (ring)	1472	23.97
	1593 (ring)	1541	9.79
	1627 (C=O)	1573	245.98
	1645 (ring)	1591	330.93
Benzaldehyde ^{13}C enriched in formyl group	1520 (ring)	1470	26.65
	1589 (ring)	1537	124.32
	1601 (C=O)	1548	159.14
	1643 (ring)	1589	223.07
4-Methylbenzaldehyde	1528 (ring)	1478	56.54
	1564 (ring)	1513	4.53
	1635 (C=O)	1581	350.07
	1651 (ring)	1597	428.14

[a] Corrected frequency calculated using a scaling factor of 0.9671.

7. DATA ANALYSIS AND MULTIVARIATE LINEAR REGRESSION (MLR)

7.1 **Correlation analysis**

The correlation between the molecular descriptors determined for benzaldehyde and its 3- and 4-substituted (meta- and para-substituted) derivatives and DME STY for the promoted M2D reaction was explored, using the 150 ^oC DME STY data collected (Table S 2) for H-ZSM-5 SAR 80. The Pearson correlation coefficient was calculated using KNIME version 4.6.1[31] and a univariate correlation matrix heatmap was generated, see Figure S 43 and Table S 12.

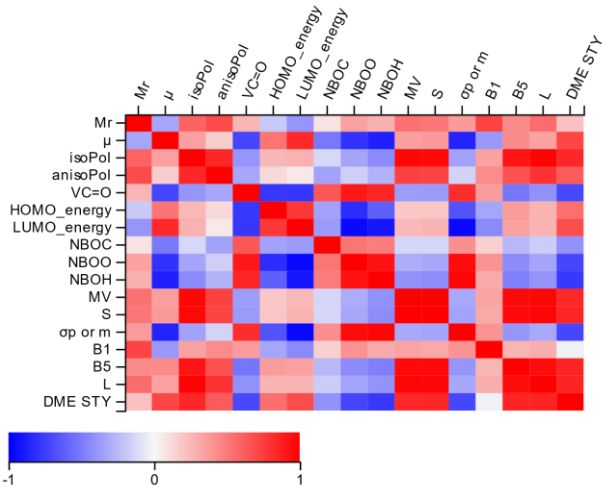

Figure S 43. Correlation heatmap for aromatic aldehyde molecular descriptors and DME STY (g kg^{-1} h^{-1}) for H-ZSM-5 SAR 80 tested at 150 °C with benzaldehyde and 3- and 4-substituted benzaldehydes.

The best Pearson correlation coefficients for steric descriptors with DME STY are:

- Isotropic Polarizability (^{iso}Pol) = 0.85
- Molecular Surface Area (S) = 0.85
- B_5 = 0.86
- L = 0.86

The best correlation for electronic descriptors with DME STY:

- Dipole Moment ($\boldsymbol{\mu}$) = 0.72
- NBO charge on oxygen (NBO_O) = -0.72
- NBO charge on hydrogen (NBO_H) = -0.77
- Hammett substituent constant ($\sigma_{p\ or\ m}$) = -0.72

	Mr	μ	isoPol	anisoPol	VC=O	HOMO_energy	LUMO_energy	NBOC	NBOO	NBOH	MV	S	$\sigma_{p \text{ or } m}$	B1	B5	L	DME STY
Mr	1.00	-0.33	0.60	0.70	0.27	-0.18	-0.40	0.08	0.35	0.29	0.55	0.52	0.38	0.73	0.44	0.56	0.22
μ	-0.33	1.00	0.35	0.17	-0.72	0.53	0.83	-0.52	-0.80	-0.87	0.36	0.38	-0.86	-0.38	0.44	0.35	0.72
isoPol	0.60	0.35	1.00	0.84	-0.39	0.26	0.28	-0.13	-0.33	-0.44	0.97	0.97	-0.35	0.34	0.92	0.98	0.85
anisoPol	0.70	0.17	0.84	1.00	-0.33	0.13	0.06	-0.34	-0.16	-0.28	0.74	0.72	-0.15	0.43	0.67	0.80	0.63
VC=O	0.27	-0.72	-0.39	-0.33	1.00	-0.77	-0.78	0.65	0.90	0.85	-0.37	-0.38	0.82	0.37	-0.52	-0.41	-0.71
HOMO_energy	-0.18	0.53	0.26	0.13	-0.77	1.00	0.77	-0.34	-0.82	-0.62	0.20	0.20	-0.67	-0.33	0.37	0.28	0.55
LUMO_energy	-0.40	0.83	0.28	0.06	-0.78	0.77	1.00	-0.37	-0.96	-0.91	0.25	0.28	-0.97	-0.44	0.35	0.27	0.69
NBOC	0.08	-0.52	-0.13	-0.34	0.65	-0.34	-0.37	1.00	0.53	0.50	-0.13	-0.13	0.42	0.16	-0.25	-0.17	-0.41
NBOO	0.35	-0.80	-0.33	-0.16	0.90	-0.82	-0.96	0.53	1.00	0.93	-0.31	-0.33	0.95	0.41	-0.44	-0.34	-0.72
NBOH	0.29	-0.87	-0.44	-0.28	0.85	-0.62	-0.91	0.50	0.93	1.00	-0.41	-0.44	0.98	0.31	-0.49	-0.40	-0.77
MV	0.55	0.36	0.97	0.74	-0.37	0.20	0.25	-0.13	-0.31	-0.41	1.00	1.00	-0.32	0.34	0.96	0.98	0.84
S	0.52	0.38	0.97	0.72	-0.38	0.20	0.28	-0.13	-0.33	-0.44	1.00	1.00	-0.34	0.32	0.96	0.98	0.85
$\sigma_{p \text{ or } m}$	0.38	-0.86	-0.35	-0.15	0.82	-0.67	-0.97	0.42	0.95	0.98	-0.32	-0.34	1.00	0.40	-0.39	-0.32	-0.72
B1	0.73	-0.38	0.34	0.43	0.37	-0.33	-0.44	0.16	0.41	0.31	0.34	0.32	0.40	1.00	0.27	0.29	-0.03
B5	0.44	0.44	0.92	0.67	-0.52	0.37	0.35	-0.25	-0.44	-0.49	0.96	0.96	-0.39	0.27	1.00	0.95	0.86
L	0.56	0.35	0.98	0.80	-0.41	0.28	0.27	-0.17	-0.34	-0.40	0.98	0.98	-0.32	0.29	0.95	1.00	0.86
DME STY	0.22	0.72	0.85	0.63	-0.71	0.55	0.69	-0.41	-0.72	-0.77	0.84	0.85	-0.72	-0.03	0.86	0.86	1.00

Table S 12: Pearson Correlation coefficients for molecular descriptors and DME STY (g kg^{-1} h^{-1}) for H-ZSM-5 SAR 80 tested at 150 °C with benzaldehyde and 3- and 4-substituted benzaldehydes.

7.2 **Relationship of molecular descriptors to Hammett constant values**

Univariate correlations between computationally derived molecular descriptors and the Hammett constants were explored (Figure S 44) for benzaldehyde and the 3- and 4-substituted (meta- and para-substituted) benzaldehyde derivatives tested in this work. The correlation analysis was performed in JMP® Pro version 16.1.0.[32] There is a moderate linear correlation (R^2 = 0.67) between IR carbonyl stretching frequency ($V_{C=O}$) and the Hammett constant , see Figure S 44 a). However, a strong linear relationship between the Hammett constant and both the LUMO-energy and NBO charge on carbonyl oxygen (NBO_O) was found, see Figure S 44, b) and c). These results confirm that certain calculated electronic descriptors can be used as alternatives to Hammett substituent values for substituted benzaldehydes.

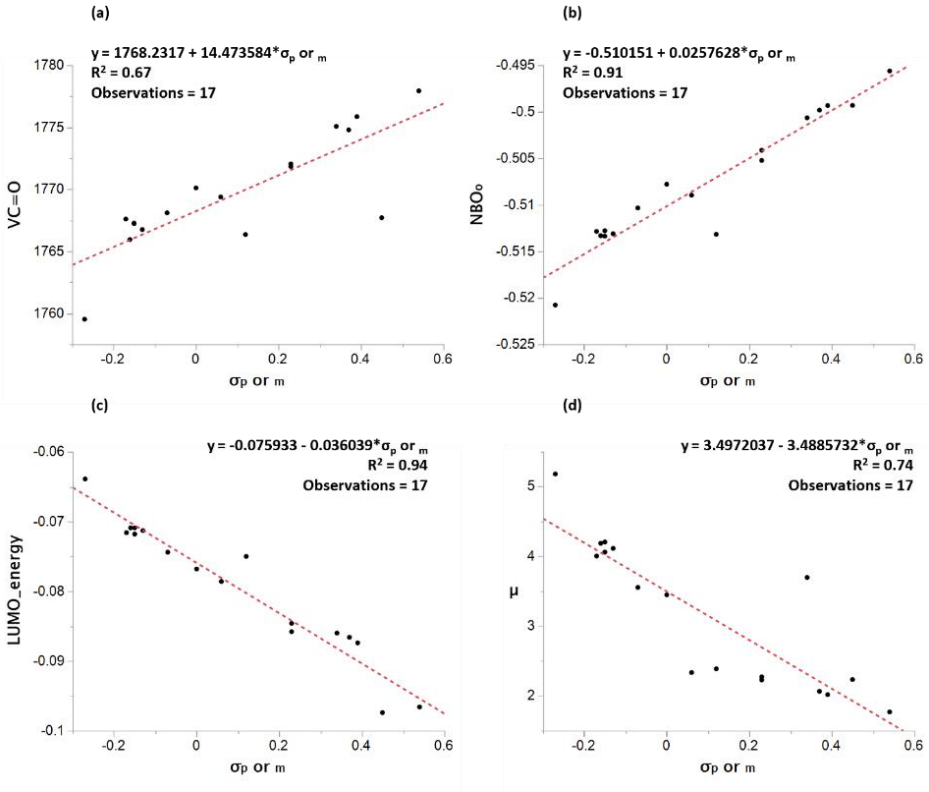

Figure S 44. Univariate correlation between electronic parameters and Hammett values; (a) $V_{C=O}$ correlation with σ_p or $_m$; (b) NBO_O correlation with σ_p or $_m$; (c) LUMO_energy correlation with σ_p or $_m$; (d) dipole moment (μ) correlation with σ_p or $_m$.

7.3 **Correlation between steric descriptors**

The steric descriptors ^{iso}Pol, S, B_5 and L, for benzaldehyde and 3- and 4-substituted benzaldehydes in the methanol dehydration reaction with H-ZSM-5 SAR 80 at 150 ^oC, are highly correlated as they are all related to the size of the benzaldehyde promoter as a whole or the size of the substituent. An example of the high degree of correlation is displayed in Figure S 45 for the steric descriptors L and S.

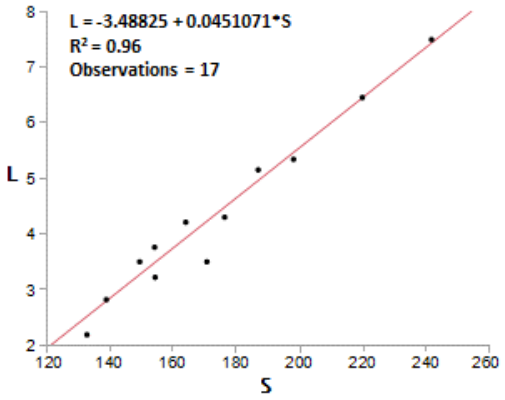

Figure S 45. Univariate correlation between molecular surface area (S) and Sterimol parameter (L).

7.4 Univariate correlation of molecular descriptors to DME STY for H-ZSM-5 SAR 80

Univariate linear correlations between molecular descriptors and DME STY were next explored for benzaldehyde and 3- and 4-substituted benzaldehydes in the methanol dehydration reaction with H-ZSM-5 SAR 80 at 150 °C, using data from Table S 2. No correlation was observed between the relative molecular mass and DME STY (R^2 = 0.048, see Figure S 46). The Sterimol parameters L and B_5 together with ^{iso}Pol and molecular surface area display a fairly strong positive correlation with DME STY (R^2 = 0.73 and 0.72) for the 17 aromatic aldehyde promoter molecules, see Figure S 47.

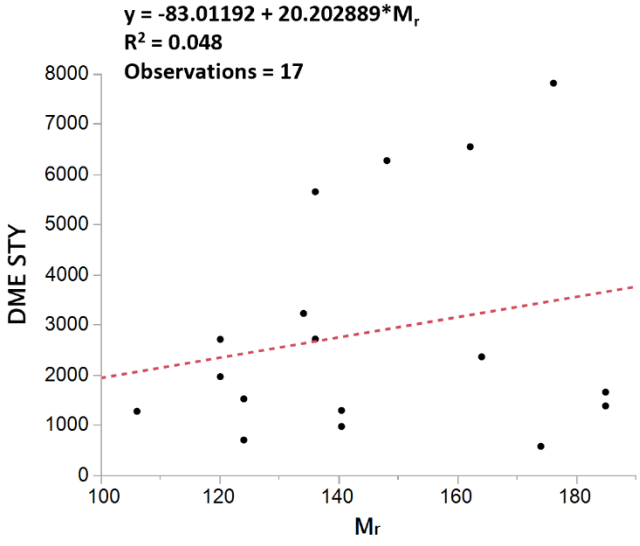

Figure S 46. Univariate correlation of relative molecular mass with DME STY. H-ZSM-5 SAR 80 tested at 150 °C with benzaldehyde and 3- and 4-substituted benzaldehydes.

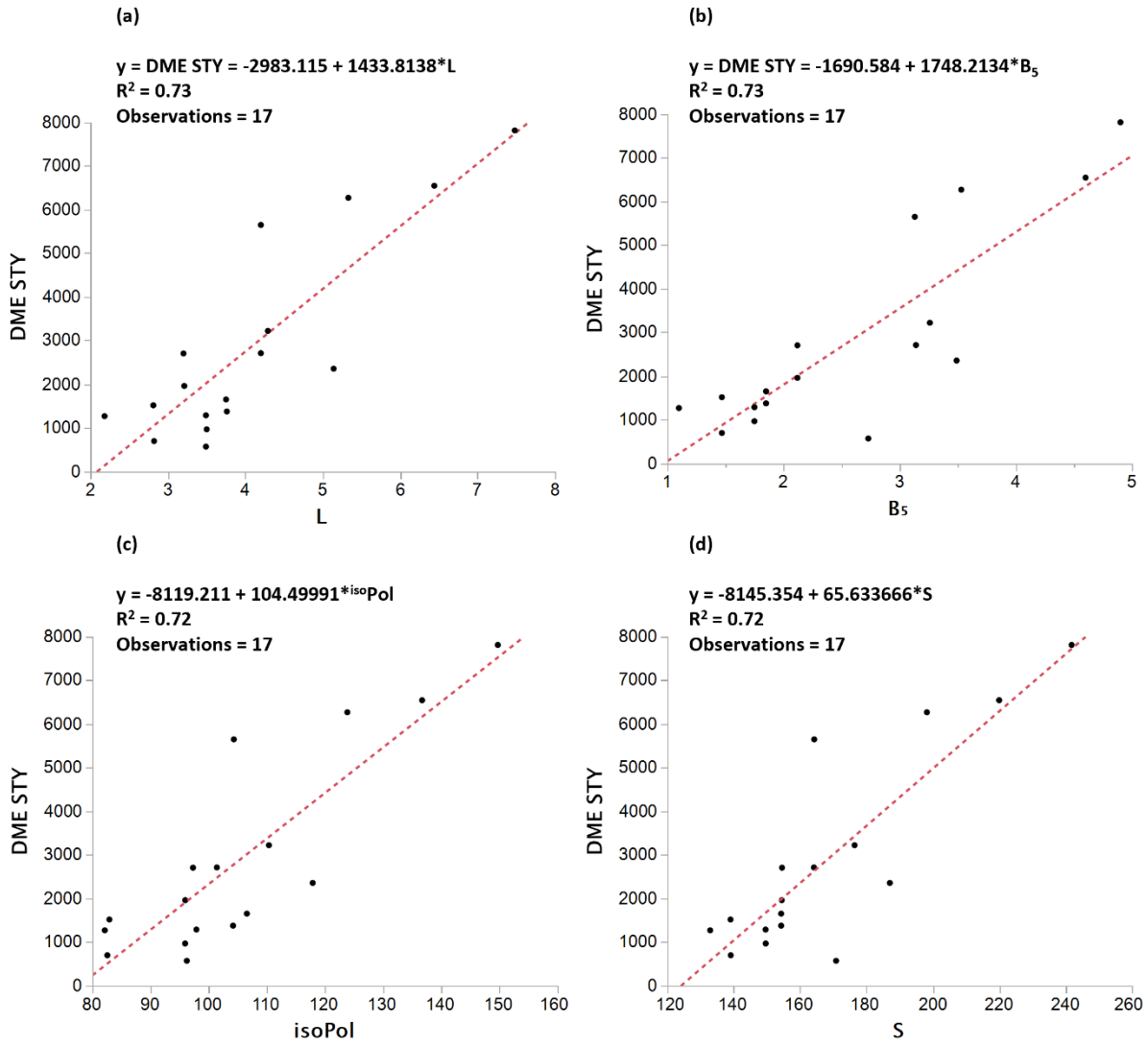

Figure S 47. Univariate correlation between DME STY and (a) Sterimol L; (b) Sterimol B_5; (c) Isotropic polarizability (^{iso}Pol); (d) dmolecular surface area (S). H-ZSM-5 SAR 80 tested at 150 °C with benzaldehyde and 3- and 4-substituted benzaldehydes.

A weaker correlation was found with electronic parameters NBO_o, μ, $V_{C=O}$, and LUMO_energy (R^2 = 0.52, 0.51, 0.50, 0.47 respectively), see Figure S 48 a) to d). The Hammett substituent values display the same level of correlation with DME STY as the other electronic parameters (R^2 = 0.51, Figure S 49) which is not unsurprising given that for 3- and 4-substituted (meta- and para-substituted) species the Hammett values largely describe the same electronic effect.

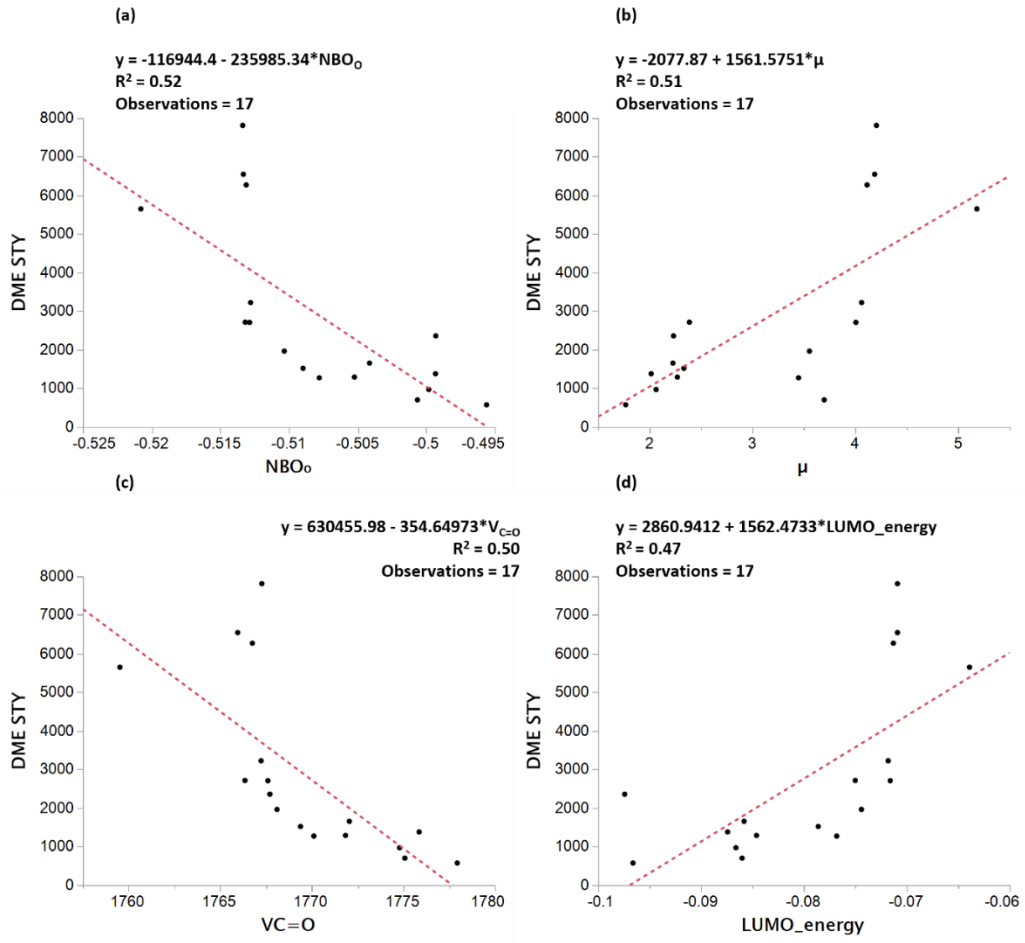

Figure S 48. Correlation of DME STY with (a) NBO charge on carbonyl oxygen (NBO$_O$); (b) dipole moment (μ); (c) IR frequency of carbonyl group (V$_{C=O}$); (d) LUMO_energy. H-ZSM-5 SAR 80 tested at 150 °C with benzaldehyde and 3- and 4-substituted benzaldehydes.

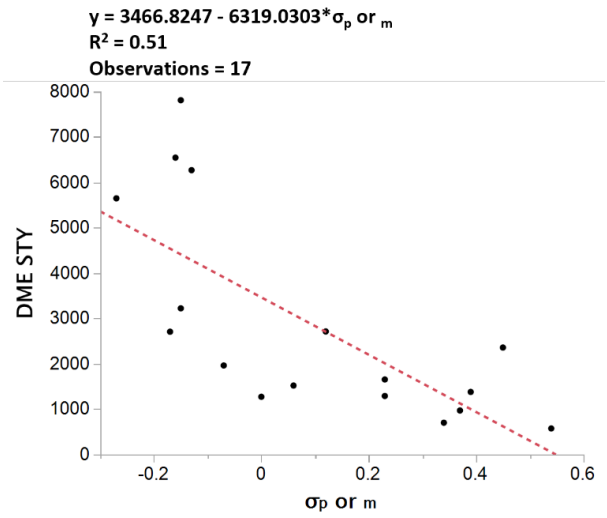

Figure S 49. Correlation of DME STY with Hammett substituent values ($\sigma_{p\ or\ m}$). H-ZSM-5 SAR 80 tested at 150 °C with benzaldehyde and 3- and 4-substituted benzaldehydes.

7.5 MLR models for DME STY with benzaldehyde and 3- and 4-substituted benzaldehyde derivatives as promoters

The descriptor values were normalized using the Z-score normalisation node in KNIME, see Equation S 1.

$$\frac{x - mean}{std.dev.}$$

Equation S 1. Z-score normalization.

Initially, the forward stepwise regression feature in JMP® Pro version 16.1.0 was used to construct models for the 3- and 4-substituted benzaldehydes which were analysed using standard metrics (RMSE and R^2). Due to the small size of the dataset cross-validation was performed using the leave-one-out (LOO) method.[33] The Sterimol L parameter and the LUMO energy were selected as the most important features. Cross-validation was performed with KNIME version 4.6.1.

Multivariate correlations between molecular descriptors and DME STY were next explored for benzaldehyde and 3- and 4-substituted benzaldehydes in the methanol dehydration reaction with H-ZSM-5 SAR 80 at 150 °C, using data from Table S 2**.** An excellent correlation (R^2 = 0.95) was observed with just L and LUMO_energy. These parameters describe the steric and electronic properties of the benzaldehyde derived promoter molecules. The model with LUMO_energy and L was also applicable to benzaldehyde promotion of methanol dehydration with another 3-demensional medium pore zeolite, H-ZSM-11 (MEL), see Figure S 51 . Similar models for the 3- and 4-substitued benzaldehyde derivatives can also be obtained using either NBO_O or Hammett values combined with L or molecular surface area (Section 7.6).

H-ZSM-5 SAR 80 at 150 °C, model details using LUMO_energy and L

DME STY = 2677.10412913711 + 1489.37251167584 * :L + 1047.96749102824 * :LUMO_energy

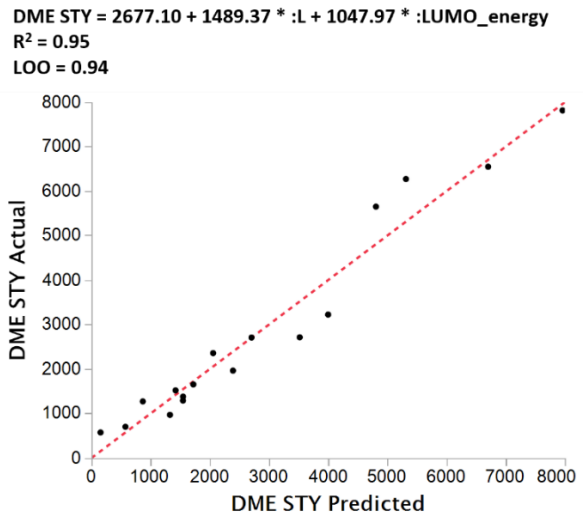

Figure S 50. Multivariate linear regression model to predict DME STY (g kg^{-1} h^{-1}) using LUMO_energy and L. H-ZSM-5 SAR 80 tested at 150 °C with benzaldehyde and 3- and 4-substituted benzaldehydes.

Summary of Fit

RSquare	0.954182
RSquare Adj	0.947636
Root Mean Square Error	520.0819
Mean of Response	2860.941
Observations (or Sum Wgts)	17

Analysis of Variance

Source	DF	Sum of Squares	Mean Square	F Ratio
Model	2	78861232	39430616	145.7773
Error	14	3786793	270485.22	**Prob > F**
C. Total	16	82648025		<.0001*

Parameter Estimates

Term	Estimate	Std Error	t Ratio	Prob>|t|
Intercept	2677.1041	126.7655	21.12	<.0001*
L	1489.3725	122.7816	12.13	<.0001*
LUMO_energy	1047.9675	127.5191	8.22	<.0001*

Table S 13. Predicted values for DME STY (g kg^{-1} h^{-1}) from model with L and LUMO_energy. H-ZSM-5 SAR 80 tested at 150 °C with benzaldehyde and 3- and 4-substituted benzaldehydes.

Molecule	Experimental DME STY	Predicted DME STY	LOO Predicted DME STY
Benzaldehyde	1274	870	763
4-Methylbenzaldehyde	2709	2706	2705
4-Ethylbenzaldehyde	3225	4000	4085
4-n-Propylbenzaldehyde	6272	5315	5165
4-n-Butylbenzaldehyde	6548	6703	6758
4-n-Pentylbenzaldehyde	7815	7960	8081
4-MeO-benzaldehyde	5651	4808	4555
4-CF_3-benzaldehyde	576	156	7
4-F-benzaldehyde	1522	1422	1409
4-Cl-benzaldehyde	1292	1548	1571
4-Br-benzaldehyde	1656	1723	1730
4-CO_2Me-benzaldehyde	2360	2057	1860
3-MeO-benzaldehyde	2715	3520	3583
3-Methylbenzaldehyde	1965	2393	2450
3-F-benzaldehyde	703	576	558
3-Cl-benzaldehyde	972	1328	1367
3-Br-benzaldehyde	1381	1550	1569

H-ZSM-11 SAR 50 at 150 °C, model details using LUMO_energy and L

2969.86121607027 + 1787.76027927822 * :L + 1189.16527569202 * :LUMO_energy

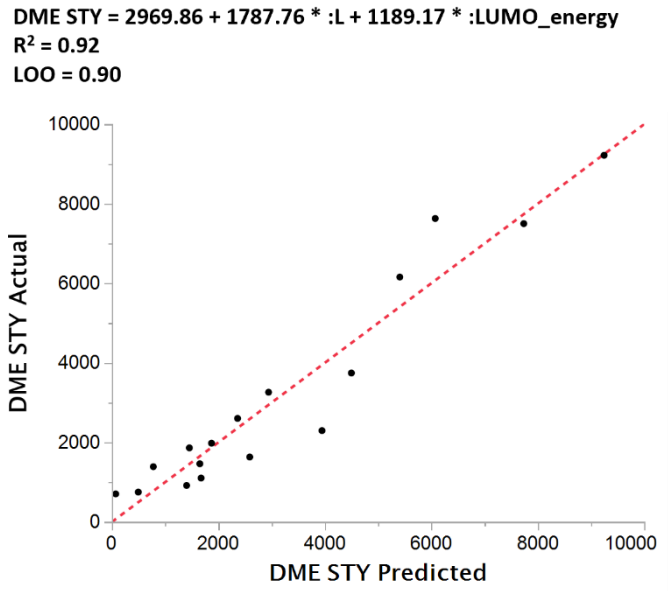

Figure S 51. Multivariate linear regression model to predict DME STY (g kg^{-1} h^{-1}) using LUMO_energy and L. H-ZSM-11 SAR 50 tested at 150 °C with benzaldehyde and 3- and 4-substituted benzaldehydes.

Summary of Fit

RSquare	0.923821
RSquare Adj	0.912938
Root Mean Square Error	802.4869
Mean of Response	3188.882
Observations (or Sum Wgts)	17

Analysis of Variance

Source	DF	Sum of Squares	Mean Square	F Ratio
Model	2	109334290	54667145	84.8888
Error	14	9015793	643985.24	**Prob > F**
C. Total	16	118350084		<.0001*

Parameter Estimates

Term	Estimate	Std Error	t Ratio	Prob>|t|
Intercept	2969.8612	195.5993	15.18	<.0001*
L	1787.7603	189.4521	9.44	<.0001*
LUMO_energy	1189.1653	196.7621	6.04	<.0001*

Table S 14. Predicted values for DME STY (g kg^{-1} h^{-1}) from model with L and LUMO_energy. H-ZSM-11 SAR 50 tested at 150 °C with benzaldehyde and 3- and 4-substituted benzaldehydes.

Molecule	Experimental DME STY	Predicted DME STY	LOO Predicted DME STY
Benzaldehyde	1390	779	617
4-Methylbenzaldehyde	3261	2944	2887
4-Ethylbenzaldehyde	3744	4499	4581
4-n-Propylbenzaldehyde	7628	6073	5829
4-n-Butylbenzaldehyde	7499	7736	7819
4-n-Pentylbenzaldehyde	9217	9245	9269
4-MeO-benzaldehyde	6156	5408	5184
4-CF_3-benzaldehyde	705	73	-150
4-F-benzaldehyde	1863	1456	1400
4-Cl-benzaldehyde	1463	1653	1670
4-Br-benzaldehyde	1980	1872	1862
4-CO_2Me-benzaldehyde	2603	2361	2204
3-MeO-benzaldehyde	2296	3947	4075
3-Methylbenzaldehyde	1633	2589	2716
3-F-benzaldehyde	751	496	460
3-Cl-benzaldehyde	918	1404	1456
3-Br-benzaldehyde	1104	1676	1741

7.6 Alternative MLR models for DME STY with benzaldehyde and 3- and 4-substituted benzaldehydes as promoters

H-ZSM-5 SAR 80 at 150 °C, model details using Hammett constant values and L

3124.62409298434 + 1442.90197246724 * :L + -4353.97190619861 * :σ_p or $_m$

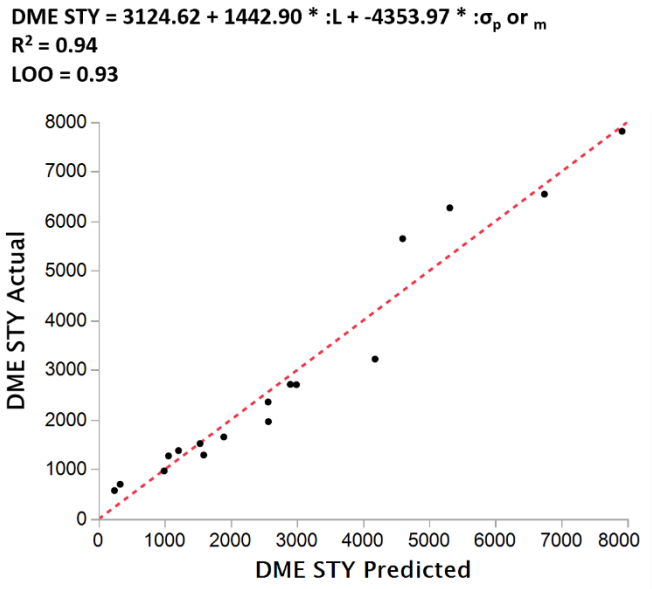

Figure S 52. Multivariate linear regression model to predict DME STY (g kg^{-1} h^{-1}) for H-ZSM-5 SAR 80 at 150 °C, using σ_p or $_m$ and L.

Summary of Fit

RSquare	0.951731
RSquare Adj	0.944836
Root Mean Square Error	533.8074
Mean of Response	2860.941
Observations (or Sum Wgts)	17

Analysis of Variance

Source	DF	Sum of Squares	Mean Square	F Ratio
Model	2	78658721	39329360	138.0218
Error	14	3989304	284950.32	**Prob > F**
C. Total	16	82648025		<.0001*

Parameter Estimates

Term	Estimate	Std Error	t Ratio	Prob>|t|
Intercept	3124.6241	141.9543	22.01	<.0001*
L	1442.902	127.8117	11.29	<.0001*
σ_p or $_m$	-4353.972	546.8226	-7.96	<.0001*

Table S 15. Predicted values for DME STY (g kg^{-1} h^{-1}) from model using L and σ_p or $_m$. H-ZSM-5 SAR 80 tested at 150 °C with benzaldehyde and 3- and 4-substituted benzaldehydes.

Molecule	Experimental DME STY	Predicted DME STY	LOO Predicted DME STY
Benzaldehyde	1274	1058	995
4-Methylbenzaldehyde	2709	2993	3060
4-Ethylbenzaldehyde	3225	4182	4309
4-n-Propylbenzaldehyde	6272	5313	5162
4-n-Butylbenzaldehyde	6548	6743	6813
4-n-Pentylbenzaldehyde	7815	7917	8003
4-MeO-benzaldehyde	5651	4599	4346
4-CF_3-benzaldehyde	576	241	132
4-F-benzaldehyde	1522	1535	1537
4-Cl-benzaldehyde	1292	1591	1617
4-Br-benzaldehyde	1656	1895	1915
4-CO_2Me-benzaldehyde	2360	2565	2645
3-MeO-benzaldehyde	2715	2901	2913
3-Methylbenzaldehyde	1965	2569	2663
3-F-benzaldehyde	703	328	265
3-Cl-benzaldehyde	972	993	996
3-Br-benzaldehyde	1381	1210	1182

H-ZSM-5 SAR 80 at 150 °C, model details using LUMO_energy and S

DME STY = 2860.94 + 1115.77 * :LUMO_energy + 1623.57 * :S

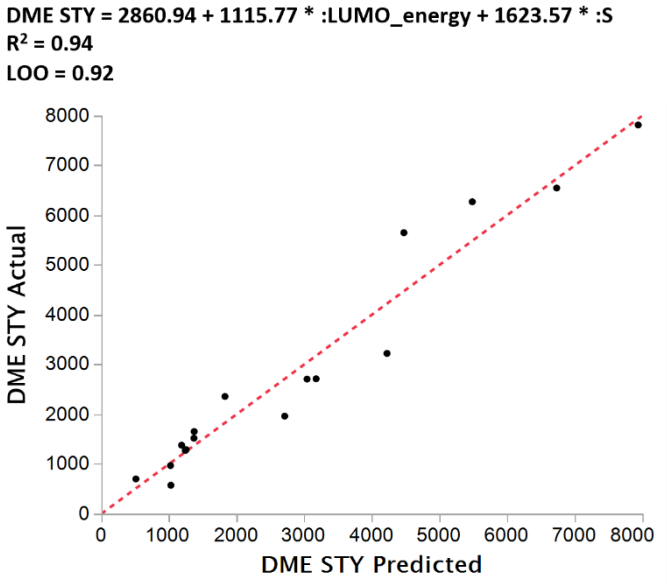

Figure S 53. Multivariate linear regression model to predict DME STY (g kg^{-1} h^{-1}) using LUMO_energy and S. H-ZSM-5 SAR 80 tested at 150 °C with benzaldehyde and 3- and 4-substituted benzaldehydes.

Summary of Fit

RSquare	0.944294
RSquare Adj	0.936336
Root Mean Square Error	573.461
Mean of Response	2860.941
Observations (or Sum Wgts)	17

Parameter Estimates

Term	Estimate	Std Error	t Ratio	Prob>|t|
Intercept	2860.9412	139.0847	20.57	<.0001*
LUMO_energy	1115.7738	149.1205	7.48	<.0001*
S	1623.5667	149.1205	10.89	<.0001*

Analysis of Variance

Source	DF	Sum of Squares	Mean Square	F Ratio
Model	2	78044020	39022010	118.6593
Error	14	4604005	328857.53	**Prob > F**
C. Total	16	82648025		<.0001*

Table S 16. Predicted values for DME STY (g kg^{-1} h^{-1}) from model using S and LUMO_energy. H-ZSM-5 SAR 80 tested at 150 °C with benzaldehyde and 3- and 4-substituted benzaldehydes.

Molecule	Experimental DME STY	Predicted DME STY	LOO Predicted DME STY
Benzaldehyde	1274	1244	1237
4-Methylbenzaldehyde	2709	3044	3094
4-Ethylbenzaldehyde	3225	4227	4336
4-n-Propylbenzaldehyde	6272	5487	5352
4-n-Butylbenzaldehyde	6548	6735	6804
4-n-Pentylbenzaldehyde	7815	7940	8046
4-MeO-benzaldehyde	5651	4476	4098
4-CF_3-benzaldehyde	576	1030	1212
4-F-benzaldehyde	1522	1372	1350
4-Cl-benzaldehyde	1292	1256	1252
4-Br-benzaldehyde	1656	1375	1347
4-CO_2Me-benzaldehyde	2360	1830	1515
3-MeO-benzaldehyde	2715	3178	3216
3-Methylbenzaldehyde	1965	2713	2796
3-F-benzaldehyde	703	513	485
3-Cl-benzaldehyde	972	1025	1031
3-Br-benzaldehyde	1381	1189	1166

H-ZSM-11 SAR 50 at 150 °C, model details using Hammett constant values and L

3495.41116702407 + -5111.42601947812 * : σ_p or $_m$ + 1722.31896590153 * :L

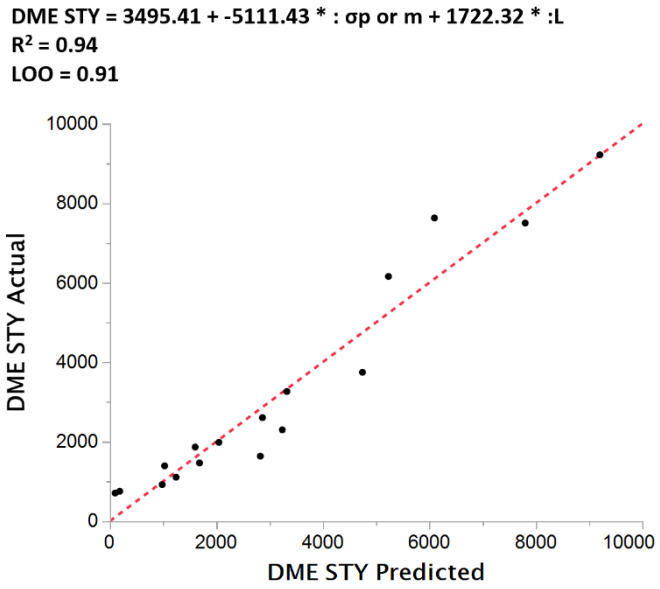

Figure S 54. Multivariate linear regression model to predict DME STY (g kg^{-1} h^{-1}) using σ_p or $_m$ and L. H-ZSM-11 SAR 50 tested at 150 °C with benzaldehyde and 3- and 4-substituted benzaldehydes.

Summary of Fit

RSquare	0.935444
RSquare Adj	0.926222
Root Mean Square Error	738.7349
Mean of Response	3188.882
Observations (or Sum Wgts)	17

Analysis of Variance

Source	DF	Sum of Squares	Mean Square	F Ratio
Model	2	110709875	55354937	101.4330
Error	14	7640209	545729.21	**Prob > F**
C. Total	16	118350084		<.0001*

Parameter Estimates

Term	Estimate	Std Error	t Ratio	Prob>|t|
Intercept	3495.4112	196.4503	17.79	<.0001*
σ_p or $_m$	-5111.426	756.7466	-6.75	<.0001*
L	1722.319	176.8783	9.74	<.0001*

Table S 17. Predicted values for DME STY (g kg^{-1} h^{-1}) from model using L and σ_p or $_m$. H-ZSM-11 SAR 50 tested at 150 °C with benzaldehyde and 3- and 4-substituted benzaldehydes.

Molecule	Experimental DME STY	Predicted DME STY	LOO Predicted DME STY
Benzaldehyde	1390	1029	923
4-Methylbenzaldehyde	3261	3324	3339
4-Ethylbenzaldehyde	3744	4745	4878
4-n-Propylbenzaldehyde	7628	6096	5856
4-n-Butylbenzaldehyde	7499	7801	7908
4-n-Pentylbenzaldehyde	9217	9204	9192
4-MeO-benzaldehyde	6156	5233	5010
4-CF_3-benzaldehyde	705	100	-97
4-F-benzaldehyde	1863	1603	1565
4-Cl-benzaldehyde	1463	1684	1704
4-Br-benzaldehyde	1980	2048	2053
4-CO_2Me-benzaldehyde	2603	2866	2969
3-MeO-benzaldehyde	2296	3239	3300
3-Methylbenzaldehyde	1633	2827	3012
3-F-benzaldehyde	751	186	92
3-Cl-benzaldehyde	918	983	993
3-Br-benzaldehyde	1104	1244	1267

7.7 MLR DME STY models incorporating 2-substituted benzaldehyde derivatives as well as benzaldehyde and 3- and 4-substituted benzaldehyde derivatives as promoters

The model with ZSM-5 SAR80 150 °C was expanded to incorporate the 2-substituted benzaldehyde derivatives tested in Table S 3. Somewhat surprisingly, a high correlation for DME STY was obtained with just L and LUMO_energy (R^2 = 0.90, see Figure S 55), however, prediction accuracy for benzaldehyde, 2-methylbenzaldehyde and 2-methoxybenzaldehyde was low. This could be a consequence of the dataset being heavily weighted towards 3- and 4-substituted benzaldehyde derivatives so that the influence of having a

substituent at the 2-position (ortho-position) is underestimated when building the model. The model and prediction could be greatly improved by adding the B_{5ortho} Sterimol parameter which describes the maximum width of the substituent in the 2-position, Figure S 56.

Model details for H-ZSM-5 SAR 80 at 150 °C with 2-, 3- and 4-substituted benzaldehyde derivatives

2442.63636363636 + 1566.11138510218 * :L + 966.251165975859 * :LUMO_energy

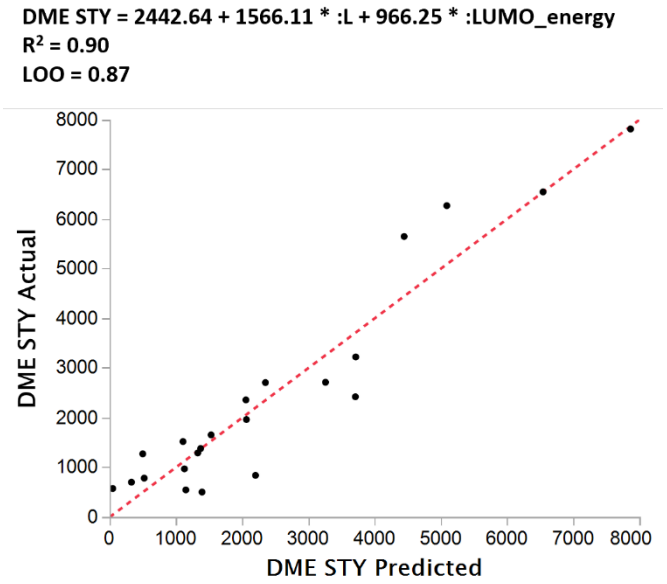

Figure S 55. Multivariate linear regression model to predict DME STY (g kg^{-1} h^{-1}) using LUMO_energy and L. H-ZSM-5 SAR 80 tested at 150 °C with benzaldehyde and 2-, 3- and 4-substituted benzaldehydes.

Summary of Fit

RSquare	0.902499
RSquare Adj	0.892236
Root Mean Square Error	710.1655
Mean of Response	2442.636
Observations (or Sum Wgts)	22

Analysis of Variance

Source	DF	Sum of Squares	Mean Square	F Ratio
Model	2	88697766	44348883	87.9354
Error	19	9582365	504335.01	**Prob > F**
C. Total	21	98280131		<.0001*

Parameter Estimates

Term	Estimate	Std Error	t Ratio	Prob>|t|
Intercept	2442.6364	151.4078	16.13	<.0001*
L	1566.1114	161.266	9.71	<.0001*
LUMO_energy	966.25117	161.266	5.99	<.0001*

Table S 18. Predicted values for DME STY (g kg^{-1} h^{-1}) from model using L and LUMO_energy. H-ZSM-5 SAR 80 tested at 150 °C with benzaldehyde and 2-, 3- and 4-substituted benzaldehydes.

Molecule	Experimental DME STY	Predicted DME STY	LOO Predicted DME STY
Benzaldehyde	1274	500	343
4-Methylbenzaldehyde	2709	2353	2304
4-Ethylbenzaldehyde	3225	3717	3760
4-n-Propylbenzaldehyde	6272	5092	4924
4-n-Butylbenzaldehyde	6548	6545	6544
4-n-Pentylbenzaldehyde	7815	7867	7908
4-MeO-benzaldehyde	5651	4447	4159
4-CF_3-benzaldehyde	576	47	-98
4-F-benzaldehyde	1522	1108	1066
4-Cl-benzaldehyde	1292	1331	1333
4-Br-benzaldehyde	1656	1533	1524
4-CO_2Me-benzaldehyde	2360	2058	1897
3-MeO-benzaldehyde	2715	3260	3293
3-Methylbenzaldehyde	1965	2066	2076
3-F-benzaldehyde	703	329	290
3-Cl-benzaldehyde	972	1129	1142
3-Br-benzaldehyde	1381	1374	1374
2-Methylbenzaldehyde	841	2203	2362
2-MeO-benzaldehyde	2423	3711	3838
2-F-benzaldehyde	785	522	496
2-Cl-benzaldehyde	548	1151	1199
2-Br-benzaldehyde	505	1396	1472

Model details for H-ZSM-5 SAR 80 at 150 °C with 2-, 3- and 4-substituted benzaldehyde derivatives, adding in B_{5ortho}

2442.63636363636 + 1049.00661464201 * :LUMO_energy + 1502.81106081504 * :L +-490.263440606259 * :B_{5ortho}

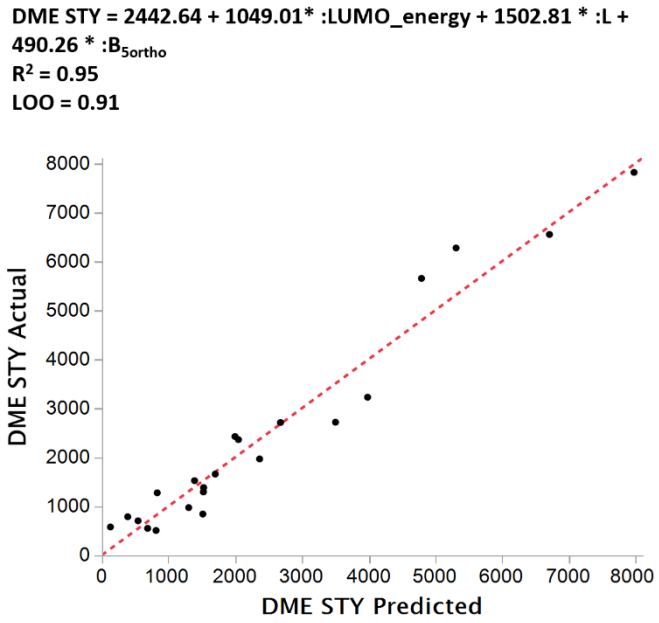

Figure S 56. Multivariate linear regression model to predict DME STY (g kg^{-1} h^{-1}) using LUMO_energy, L and B_{5ortho}. H-ZSM-5 SAR 80 tested at 150 °C with benzaldehyde and 2-, 3- and 4-substituted benzaldehydes.

Summary of Fit

RSquare	0.952158
RSquare Adj	0.944184
Root Mean Square Error	511.0954
Mean of Response	2442.636
Observations (or Sum Wgts)	22

Analysis of Variance

Source	DF	Sum of Squares	Mean Square	F Ratio
Model	3	93578198	31192733	119.4124
Error	18	4701933	261218.51	**Prob > F**
C. Total	21	98280131		<.0001*

Parameter Estimates

Term	Estimate	Std Error	t Ratio	Prob>|t|
Intercept	2442.6364	108.9659	22.42	<.0001*
LUMO_energy	1049.0066	117.6293	8.92	<.0001*
L	1502.8111	116.981	12.85	<.0001*
B5ortho	-490.2634	113.4233	-4.32	0.0004*

Table S 19. Predicted values for DME STY (g kg^{-1} h^{-1}) from model containing ortho-substituents using L, LUMO_energy and B_{5ortho}. H-ZSM-5 SAR 80 tested at 150 °C with benzaldehyde and 2-, 3- and 4-substituted benzaldehydes.

Molecule	Experimental DME STY	Predicted DME STY	LOO Predicted DME STY
Benzaldehyde	1274	832	727
4-Methylbenzaldehyde	2709	2680	2675
4-Ethylbenzaldehyde	3225	3986	4066
4-n-Propylbenzaldehyde	6272	5312	5163
4-n-Butylbenzaldehyde	6548	6712	6768
4-n-Pentylbenzaldehyde	7815	7981	8111
4-MeO-benzaldehyde	5651	4793	4555
4-CF_3-benzaldehyde	576	130	6
4-F-benzaldehyde	1522	1391	1375
4-Cl-benzaldehyde	1292	1523	1541
4-Br-benzaldehyde	1656	1701	1705
4-CO_2Me-benzaldehyde	2360	2049	1883
3-MeO-benzaldehyde	2715	3504	3564
3-Methylbenzaldehyde	1965	2367	2416
3-F-benzaldehyde	703	544	525
3-Cl-benzaldehyde	972	1303	1333
3-Br-benzaldehyde	1381	1527	1541
2-Methylbenzaldehyde	841	1515	1685
2-MeO-benzaldehyde	2423	1998	1045
2-F-benzaldehyde	785	389	349
2-Cl-benzaldehyde	548	688	706
2-Br-benzaldehyde	505	814	868

Model details for H-ZSM-11 SAR 50 150 °C with 2-, 3- and 4-substituted benzaldehyde derivatives, adding in B_{5ortho}

2703.45454545455 + -609.750850641697 * :B_{5ortho} + 1787.79042064996 * :L+1175.98612227048 * :LUMO_energy

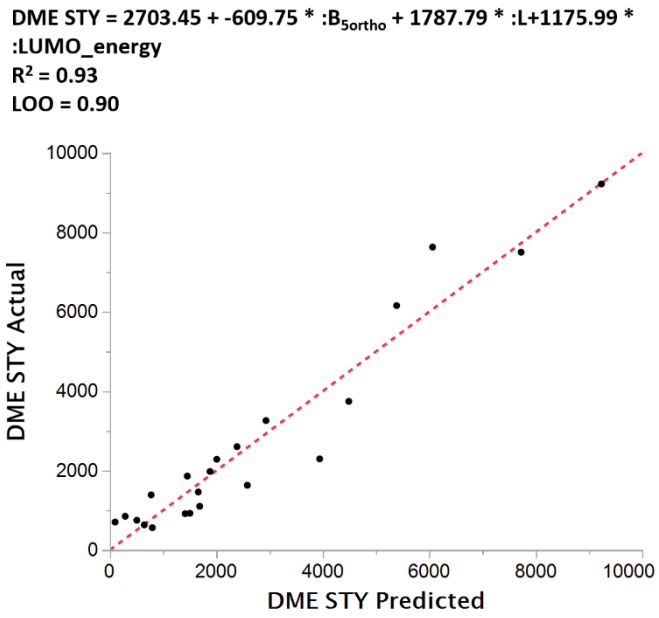

Figure S 57. Multivariate linear regression model to predict DME STY (g kg^{-1} h^{-1}) using LUMO_energy, L and B_{5ortho}. H-ZSM-11 SAR 50 tested at 150 °C with benzaldehyde and 2-, 3- and 4-substituted benzaldehydes.

Summary of Fit

RSquare	0.928974
RSquare Adj	0.917136
Root Mean Square Error	737.8334
Mean of Response	2703.455
Observations (or Sum Wgts)	22

Analysis of Variance

Source	DF	Sum of Squares	Mean Square	F Ratio
Model	3	128165804	42721935	78.4755
Error	18	9799166	544398.1	**Prob > F**
C. Total	21	137964969		<.0001*

Parameter Estimates

Term	Estimate	Std Error	t Ratio	Prob>|t|
Intercept	2703.4545	157.3066	17.19	<.0001*
B5ortho	-609.7509	163.7415	-3.72	0.0016*
L	1787.7904	168.8775	10.59	<.0001*
LUMO_energy	1175.9861	169.8133	6.93	<.0001*

Table S 20. Predicted values for DME STY (g kg^{-1} h^{-1}) from model using L, LUMO_energy and B_{5ortho}. H-ZSM-11 SAR 50 tested at 150 °C with benzaldehyde and 2-, 3- and 4-substituted benzaldehydes.

Molecule	Experimental DME STY	Predicted DME STY	LOO Predicted DME STY
Benzaldehyde	1390	776	631
4-Methylbenzaldehyde	3261	2933	2879
4-Ethylbenzaldehyde	3744	4489	4568
4-n-Propylbenzaldehyde	7628	6063	5819
4-n-Butylbenzaldehyde	7499	7725	7802
4-n-Pentylbenzaldehyde	9217	9234	9247
4-MeO-benzaldehyde	6156	5387	5172
4-CF_3-benzaldehyde	705	99	-69
4-F-benzaldehyde	1863	1456	1406
4-Cl-benzaldehyde	1463	1661	1676
4-Br-benzaldehyde	1980	1882	1875
4-CO_2Me-benzaldehyde	2603	2389	2274
3-MeO-benzaldehyde	2296	3941	4066
3-Methylbenzaldehyde	1633	2583	2700
3-F-benzaldehyde	751	507	478
3-Cl-benzaldehyde	918	1415	1459
3-Br-benzaldehyde	1104	1688	1744
2-Methylbenzaldehyde	927	1504	1650
2-MeO-benzaldehyde	2286	2009	1388
2-F-benzaldehyde	851	289	232
2-Cl-benzaldehyde	636	647	649
2-Br-benzaldehyde	565	798	839

7.8 Example of alternative MLR DME STY model with benzaldehyde and 2-, 3- and 4-substituted benzaldehyde derivatives as promoters with H-ZSM-11 SAR 50

Model details for H-ZSM-11 SAR 50 at 150 °C, using S, B_{1ortho} and μ

2703.45454545454 + 1729.88616064391 * :S + -635.652395004289 * :B_{1ortho} +1030.47953736518 * :μ

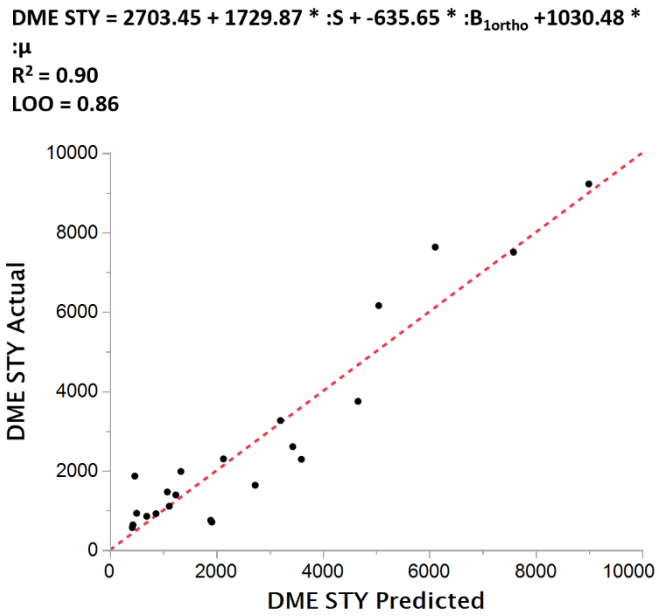

Figure S 58. Multivariate linear regression model to predict DME STY (g kg^{-1} h^{-1}) using S, B_{1ortho} and μ. H-ZSM-11 SAR 50 tested at 150 °C with benzaldehyde and 2-, 3- and 4-substituted benzaldehydes.

Summary of Fit

RSquare	0.901143
RSquare Adj	0.884667
Root Mean Square Error	870.4654
Mean of Response	2703.455
Observations (or Sum Wgts)	22

Analysis of Variance

Source	DF	Sum of Squares	Mean Square	F Ratio
Model	3	124326189	41442063	54.6938
Error	18	13638781	757710.05	**Prob > F**
C. Total	21	137964969		<.0001*

Parameter Estimates

Term	Estimate	Std Error	t Ratio	Prob>|t|
Intercept	2703.4545	185.5839	14.57	<.0001*
S	1729.8862	211.1289	8.19	<.0001*
B1ortho	-635.6524	203.5031	-3.12	0.0059*
μ	1030.4795	206.1781	5.00	<.0001*

Table S 21. Predicted values for DME STY (g kg^{-1} h^{-1}) from model using S, B_{1ortho} and μ. H-ZSM-11 SAR 50 tested at 150 °C with benzaldehyde and 2-, 3- and 4-substituted benzaldehydes.

Molecule	Experimental DME STY	Predicted DME STY	LOO Predicted DME STY
Benzaldehyde	1390	1239	1208
4-Methylbenzaldehyde	3261	3205	3197
4-Ethylbenzaldehyde	3744	4662	4758
4-n-Propylbenzaldehyde	7628	6111	5867
4-n-Butylbenzaldehyde	7499	7582	7610
4-n-Pentylbenzaldehyde	9217	8997	8819
4-MeO-benzaldehyde	6156	5051	4591
4-CF_3-benzaldehyde	705	1916	2188
4-F-benzaldehyde	1863	469	266
4-Cl-benzaldehyde	1463	1080	1034
4-Br-benzaldehyde	1980	1335	1259
4-CO_2Me-benzaldehyde	2603	3436	3609
3-MeO-benzaldehyde	2296	2134	2118
3-Methylbenzaldehyde	1633	2730	2833
3-F-benzaldehyde	751	1895	2110
3-Cl-benzaldehyde	918	867	860
3-Br-benzaldehyde	1104	1115	1117
2-Methylbenzaldehyde	927	504	376
2-MeO-benzaldehyde	2286	3598	3980
2-F-benzaldehyde	851	694	671
2-Cl-benzaldehyde	636	434	364
2-Br-benzaldehyde	565	422	343

8. Preliminary Solid State NMR Studies

8.1 Materials

Benzaldehyde (99%, AR) was purchased from Sigma-Aldrich. ^{13}C-enriched methanol ($^{13}CH_3OH$) and ^{13}C-enriched benzaldehyde ($O=^{13}CH\text{-}C_6H_5$) were purchased from Cambridge Isotope.

8.2 *In-situ* solid state NMR experiments

The NMR experiments were carried out using a BRUKER AVANCE III 400 MHz NMR spectrometer using a 4 mm double resonance probe with a sample spinning rate of 8 kHz. The ^{13}C CP/MAS NMR experiments were performed with a ramped CP (90-110% RF modulation on ^{1}H, 1000 steps) with Hartmann-Hahn condition optimized with glycine. The ^{13}C chemical shifts were referenced to adamantane (δ ^{13}C = 38.5 ppm for $-CH_2$).

For the *in-situ* NMR study of methanol dehydration to DME, 0.2 g of the H-ZSM-5 SAR 23 sample was dehydrated under high vacuum (10^{-4} Pa) at 420 °C for 12 hours. The sample was then exposed to 1 kPa methanol vapour and equilibrated at room temperature (RT) for 1 hour. The excess methanol was removed by evacuating the sample for 30 minutes at RT. The sample was then transferred into NMR rotors in a glove-box for the NMR experiment. ^{13}C Cross-Polarization Magic-Angle-Spinning (CP/MAS) NMR spectra were taken whilst the temperature was increased in steps to 65, 95 and 110 °C. NMR spectra are shown in Figure S 59 and show that significant amounts of DME (signal at 61.1 ppm) are only formed on the surface of the zeolite under the conditions of this experiment once the temperature reaches 110 °C.

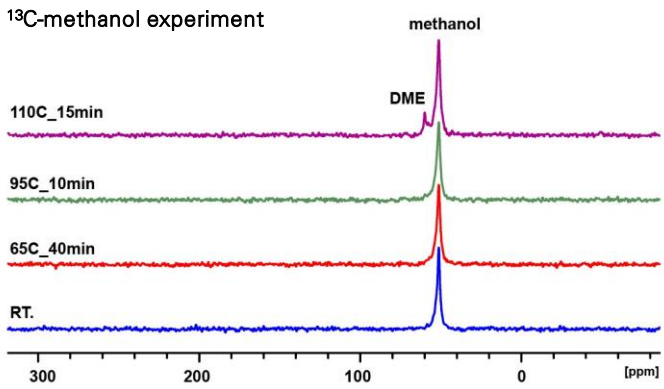

Figure S 59. ^{13}C NMR spectra of H-ZSM-5 SAR 23 exposed to ^{13}C-enriched methanol at room temperature, 65 °C (after 40 minutes), 95 °C (after 10 minutes) and 110 °C (after 15 minutes).

For the *in-situ* NMR study of methanol dehydration to DME over ^{13}C-enriched benzaldehyde doped H-ZSM-5 SAR 23, benzaldehyde adsorption was conducted by exposing 0.2 g of pre-dehydrated H-ZSM-5 SAR 23 (10^{-4} Pa/ 420°C/ 12 hours) to 0.5 kPa of benzaldehyde for 30 minutes at RT. Subsequently, excess benzaldehyde was desorbed under vacuum for 30 minutes. The benzaldehyde adsorbed sample was further exposed to 2 kPa of ^{13}C-methanol and equilibrated. Finally, physically adsorbed methanol was removed by evacuation of the sample under vacuum for 30 minutes. The sample was then transferred into NMR rotors in a glove-box for the NMR experiment. ^{13}C CP/MAS NMR spectra were taken whilst the temperature was increased in steps to 65, 95 and

110 °C. In contrast to the experiment with methanol only in the presence of benzaldehyde small amounts of DME (signal at 61.1 ppm) were already present on the surface of the zeolite catalyst at room temperature, Figure S 60, with increasingly significant amounts being formed at 65, 95 and 110 °C. This NMR experiment illustrates that benzaldehyde promotes DME formation on the surface of H-ZSM-5 at temperatures even lower than those used in the HTE and FT-IR-MS catalytic experiments. The broad signal at 200.2 ppm is in the position expected for the formyl group carbon in protonated benzaldehyde, $[Ph^{13}C(H)(=O\text{-}H)]^+$. A relatively weak and sharp signal at 192.8 ppm is assigned to the formyl group carbon in free benzaldehyde.

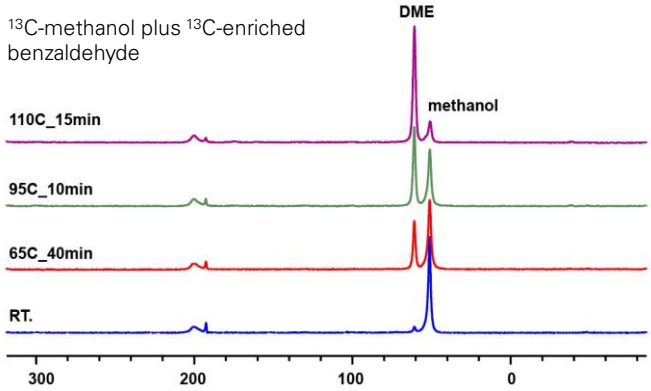

Figure S 60. ^{13}C NMR spectra of H-ZSM-5 SAR 23 exposed to ^{13}C-enriched benzaldehyde and ^{13}C-enriched methanol at room temperature, 65 °C (after 40 minutes), 95 °C (after 10 minutes) and 110 °C (after 15 minutes).

A similar experiment was also conducted with H-ZSM-5 SAR 80, this time using normal benzaldehyde and ^{13}C-enriched methanol. The NMR spectrum at room temperature is shown in Figure S 61. A very weak NMR signal was observed at 72.7 ppm and was tentatively assigned to the methyl group in the methyl oxonium species $[PhC(H)(C=O\text{-}Me)]^+$. Further experiments are in progress to enhance and confirm the provenance of this signal.

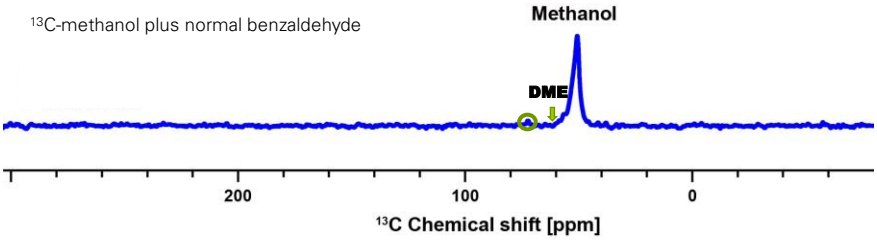

Figure S 61. ^{13}C NMR spectrum of H-ZSM-5 SAR 80 exposed to benzaldehyde and ^{13}C-enriched methanol at room temperature. Green circle highlights the position of new signal at 73 ppm, tentatively assigned to the methyl group in the methyl oxonium species $[PhC(H)(C=O\text{-}Me]^+$. Green arrow indicates the expected position for DME.

9. Cartesian Coordinates

Lowest energy conformers for benzaldehydes

Benzaldehyde

H	3.2753070624	-0.4134434090	0.0004241423
C	2.2067872490	-0.2374784532	0.0002275970
C	1.3250926717	-1.3181711747	0.0000053859
C	-0.0420072996	-1.0968254949	-0.0002372456
C	-0.5371837193	0.2104610711	-0.0002640273
C	0.3495240405	1.2879295859	-0.0000498669
C	1.7205694770	1.0651471293	0.0002007322
H	1.7106873570	-2.3298445152	0.0000201074
H	-0.7461179428	-1.9188352657	-0.0004031017
C	-1.9932067981	0.4647493578	-0.0005040325
H	-0.0403484308	2.2998915558	-0.0000761450
H	2.4078354136	1.9015071464	0.0003748561
O	-2.8462942054	-0.3907907161	-0.0006181737
H	-2.2727683329	1.5392290609	-0.0005238270

4-Methylbenzaldehyde

C	2.5150312044	0.3599207058	0.0001898612
C	1.0487068766	0.2008790147	0.0001820035
C	0.4587972143	-1.0680500741	0.0001864258
C	-0.9172310215	-1.1925430064	0.0001507318
C	-1.7470110366	-0.0624938842	0.0001173353
C	-1.1506787431	1.1982320443	0.0001113648
C	0.2316322226	1.3297640700	0.0001457703
H	1.1005497016	-1.9397516288	0.0002030978
H	-1.3657830157	-2.1794026077	0.0001467159
C	-3.2432375680	-0.2174329989	0.0001800688
H	-1.7752285531	2.0836516511	0.0000625262
H	0.6822540917	2.3160640206	0.0001304084
O	3.3143730542	-0.5472469090	0.0002135375
H	2.8615970855	1.4150573993	0.0002133561
H	-3.7454705222	0.7496602317	-0.0009823299
H	-3.5801223622	-0.7739448515	-0.8778930827
H	-3.5802183450	-0.7718424113	0.8795593233

4-Ethylbenzaldehyde

C	-2.7719332432	-0.0829624564	0.5302522553
C	-3.5291569996	-0.2024107384	-0.8006842113
C	-1.2790726785	0.0150886782	0.3429114316
C	-0.6483142660	1.2551957398	0.2297613375
C	0.7199260447	1.3368464587	0.0142820131
C	1.4896748312	0.1785793475	-0.0911894055
C	2.9435609243	0.2859787649	-0.3165904827
O	3.7026528049	-0.6488801948	-0.4252602540
C	0.8672714450	-1.0680045442	0.0250917422
C	-0.4968111914	-1.1425010647	0.2403600195
H	-3.1308984333	0.7959812948	1.0710616993
H	-3.0010356987	-0.9514508407	1.1531742785
H	-3.2089084263	-1.0856631544	-1.3562173907

H	-4.6040149963	-0.2820203213	-0.6273914879
H	-3.3509865729	0.6700806178	-1.4321069969
H	-1.2350716859	2.1624739288	0.3147102937
H	1.2005389413	2.3054487922	-0.0694737379
H	3.3212459162	1.3280847397	-0.3828686986
H	1.4727468582	-1.9619457583	-0.0522513796
H	-0.9719919780	-2.1121773670	0.3364503123

4-n-propylbenzaldehyde

C	-2.2280037948	0.2143580577	0.6548681610
C	-3.0354148679	-0.0416926609	-0.6301945246
C	-4.5395889993	0.1143589039	-0.4199355989
C	-0.7424473406	0.0671441336	0.4534850495
C	0.0382561581	1.1566859117	0.0468638168
C	1.3947090553	1.0175021133	-0.1850233124
C	2.0113402641	-0.2252726155	-0.0127907797
C	3.4557610857	-0.3987991953	-0.2564241929
O	4.2120470635	0.4743878191	-0.6138995084
C	1.2434816017	-1.3151115193	0.3979783412
C	-0.1164448461	-1.1688895353	0.6283735597
H	-2.5622146316	-0.4818395208	1.4295236658
H	-2.4525578370	1.2211744365	1.0181023067
H	-2.6955627369	0.6487391762	-1.4077904059
H	-2.8117336905	-1.0476006620	-0.9967961057
H	-5.0887847087	-0.0602053598	-1.3469381751
H	-4.9114218887	-0.5932410293	0.3252269659
H	-4.7864205255	1.1204091852	-0.0716741165
H	-0.4303999608	2.1252133840	-0.0841865762
H	1.9994442542	1.8590426095	-0.4976649604
H	3.8286390938	-1.4308834274	-0.0864043388
H	1.7177384700	-2.2799466088	0.5394797093
H	-0.7016576847	-2.0221403626	0.9513644060

4-n-butylbenzaldehyde

C	-1.6546648686	0.2533818757	0.9621073985
C	-2.5741915511	-0.0836561276	-0.2237895266
C	-4.0573559760	-0.0541929396	0.1444399803
C	-4.9715302622	-0.4098954357	-1.0263370637
C	-0.1912727215	0.2274993480	0.6043897729
C	0.5031712697	1.4066072016	0.3302448903
C	1.8448005890	1.3756281991	-0.0245751217
C	2.5222578837	0.1605511179	-0.1161634540
C	3.9471962921	0.1443061668	-0.4964860406
O	4.6261534614	-0.8495407575	-0.6125097817
C	1.8353686355	-1.0265494934	0.1577477346
C	0.4999931816	-0.9884640623	0.5135319646
H	-1.9180386540	1.2414953134	1.3484750301
H	-1.8451382646	-0.4600154818	1.7697454920
H	-2.3827671970	0.6228317880	-1.0381898805
H	-2.3121987088	-1.0731706766	-0.6119125628
H	-4.3156304613	0.9407485756	0.5220576242
H	-4.2374471187	-0.7485320132	0.9721416645
H	-4.7620085745	-1.4158746790	-1.3977048807
H	-4.8352929486	0.2842250091	-1.8592680462
H	-6.0229475699	-0.3758369321	-0.7345646446
H	-0.0121594550	2.3572634049	0.4035042132
H	2.3748421476	2.2993130797	-0.2297368761

H	4.3840529936	1.1483801262	-0.6817545952
H	2.3707517815	-1.9647771101	0.0877250388
H	-0.0218052059	-1.9133366224	0.7315968566

4-n-pentylbenzaldehyde

C	1.0625178443	-0.6458084019	0.8731294981
C	2.0157076352	0.0315503362	-0.1261976938
C	3.4871440207	-0.1167284419	0.2603247123
C	4.4475093381	0.5263575630	-0.7405096861
C	5.9146367921	0.3936511345	-0.3362190513
H	1.2533381434	-0.2453146681	1.8726387801
H	1.2906475728	-1.7149305239	0.9133056456
H	1.7601414041	1.0933630792	-0.2013305720
H	1.8528793103	-0.3924109490	-1.1224279087
H	3.7314673326	-1.1804919764	0.3627021215
H	3.6463507772	0.3269474826	1.2499589030
H	4.1937928019	1.5855928632	-0.8538321033
H	4.2983350022	0.0717092522	-1.7255540369
H	6.5740155868	0.8597066641	-1.0709109280
H	6.2067334391	-0.6557347172	-0.2471324169
H	6.1025947847	0.8713906829	0.6285748429
C	-0.3919162198	-0.4539958961	0.5292506492
C	-1.1245177729	0.6014349992	1.0868580993
C	-2.4527094117	0.8035818141	0.7575864034
C	-3.0870252818	-0.0526473095	-0.1469880647
C	-2.3657056820	-1.1070899863	-0.7081051874
C	-1.0347262392	-1.3054153944	-0.3717742336
H	-0.6402133654	1.2648922946	1.7940933026
H	-3.0211985424	1.6163133792	1.1911928287
C	-4.5030547244	0.1400015753	-0.5119301867
H	-2.8554553605	-1.7753631027	-1.4078776786
H	-0.4866459039	-2.1334768418	-0.8063408006
O	-5.2199597980	1.0155171085	-0.0857160770
H	-4.8943305595	-0.6026747322	-1.2389320752

4-Methoxybenzaldehyde

C	1.2731294848	-0.2528551076	-0.0012630039
C	0.8006255410	1.0610015302	0.0130754176
C	-0.5685217877	1.2888515309	0.0662083365
C	-1.4754751953	0.2327861982	0.1048236980
C	-0.9866170727	-1.0820997864	0.0899231872
C	0.3669204322	-1.3247486015	0.0374964088
O	2.5816736620	-0.5933704904	-0.0508497429
C	3.5609259100	0.4360430670	-0.0920958519
C	-2.9186523193	0.5052960740	0.1592280007
O	-3.7879210094	-0.3364953356	0.1929553095
H	-3.1816119592	1.5845321285	0.1674292724
H	1.4820911493	1.8978468925	-0.0155351272
H	-0.9383617159	2.3084266997	0.0769433020
H	-1.6959928153	-1.8990565268	0.1204028901
H	0.7605375804	-2.3326270404	0.0260281188
H	4.5224958307	-0.0698310284	-0.1271133393
H	3.4447733662	1.0581671445	-0.9836138909
H	3.5129673379	1.0648455304	0.8009920865

4-CF_3-benzaldehyde

F	-2.7330707099	0.2895980497	1.1674924607

C	-2.1958690949	0.0134623091	-0.0419539132
C	-0.6895173535	-0.0056265462	0.0187133595
C	-0.0008523332	1.2082939436	0.0760147482
C	1.3785563211	1.2129351024	0.1662015109
C	2.0806566006	0.0045247935	0.1981991969
C	3.5592682672	-0.0096247327	0.2950360284
O	4.2529988458	0.9756075063	0.3568511030
C	1.3861249631	-1.2014334288	0.1383059581
C	0.0002490695	-1.2116238657	0.0490451791
F	-2.7086016763	-1.1650040335	-0.4401611441
F	-2.6505704121	0.9563581054	-0.8919858993
H	-0.5497080055	2.1399783644	0.0456884119
H	1.9325576993	2.1412261573	0.2117277755
H	4.0101086660	-1.0231402664	0.3065706774
H	1.9335658240	-2.1365858810	0.1614630971
H	-0.5389149819	-2.1470344056	-0.0008325349

4-Fluorobenzaldehyde

C	2.4641809179	0.3699439223	0.0000768633
C	0.9978375602	0.2043704961	0.0000601188
C	0.4217591604	-1.0706068342	0.0000481158
C	-0.9537330076	-1.2174109523	-0.0000089674
C	-1.7412534406	-0.0736916830	-0.0000497275
C	-1.2053742249	1.2030671782	-0.0000368485
C	0.1759355765	1.3324264922	0.0000312380
H	1.0723213329	-1.9353188253	0.0000709366
H	-1.4249573726	-2.1909102396	-0.0000236255
F	-3.0785604386	-0.2134425007	-0.0001255148
H	-1.8623032991	2.0619661823	-0.0000772910
H	0.6224893737	2.3200144922	0.0000445796
O	3.2639182433	-0.5362460688	0.0007078234
H	2.8076926026	1.4254114547	0.0007835428

4-Chlorobenzaldehyde

Cl	3.0517738935	-0.1340293056	-0.0000220007
C	1.3154734938	-0.0038734287	-0.0000065685
C	0.5441116703	-1.1650573102	-0.0000006643
C	-0.8351143359	-1.0583542375	0.0000117328
C	-1.4473897836	0.1987066761	0.0000190965
C	-2.9191308304	0.3268636121	0.0000364158
O	-3.6944107884	-0.5994898395	-0.0000382045
C	-0.6564651856	1.3474037083	0.0000122795
C	0.7275124961	1.2551382446	0.0000002009
H	1.0278341029	-2.1320553711	-0.0000057315
H	-1.4591306916	-1.9426678083	0.0000171957
H	-3.2887835041	1.3734832439	-0.0000412110
H	-1.1280175793	2.3234029739	0.0000175891
H	1.3465433603	2.1410303915	-0.0000043027

4-Bromobenzaldehyde

Br	2.5325655454	-0.0591956767	0.0018440133
C	0.6329333252	0.0500567853	0.0005350556
C	-0.1156812501	-1.1258168854	0.0001456131
C	-1.4976012080	-1.0438332986	-0.0008051622
C	-2.1317647357	0.2027806412	-0.0014482491
C	-3.6072665495	0.3079130549	-0.0027815435
O	-4.3671563392	-0.6297562391	0.0039496544

C	-1.3614025603	1.3664052565	-0.0009683875
C	0.0255139693	1.2990604304	-0.0000225205
H	0.3824140702	-2.0854081681	0.0005793530
H	-2.1059681304	-1.9394260117	-0.0011719003
H	-3.9934311883	1.3488222858	0.0037876393
H	-1.8509251958	2.3335029804	-0.0014286427
H	0.6255706068	2.1979315241	0.0002854689

4-CO_2Me-benzaldehyde

C	0.5663760701	-0.1992430956	0.0315688732
C	-0.1053544875	1.0284284075	0.0050038648
C	-1.4879919413	1.0610399844	-0.0307432297
C	-2.2163425555	-0.1314633249	-0.0402858169
C	-1.5445285347	-1.3542453210	-0.0137217098
C	-0.1597903063	-1.3902366828	0.0224264968
H	0.4625347135	1.9474835469	0.0122157646
H	-2.0241424315	2.0007530193	-0.0518012503
H	-2.1131050538	-2.2772487189	-0.0216634617
H	0.3767977068	-2.3286806129	0.0433764288
C	-3.6966041237	-0.1152816373	-0.0791264438
O	-4.3751176154	0.8829349810	-0.1052181671
H	-4.1671356433	-1.1200562439	-0.0832940734
C	2.0561810594	-0.2950224865	0.0694238784
O	2.6672770482	-1.3355079222	0.0956634202
O	2.6500057072	0.9121283846	0.0704251200
C	4.0864383222	0.9030713052	0.1029309466
H	4.3845166304	1.9477261939	0.1074004942
H	4.4434795016	0.3972088358	0.9990641521
H	4.4829322154	0.3942200667	-0.7749205586

3-Methoxybenzaldehyde

C	2.6339896136	-1.6053926069	0.0101522165
O	2.4275025818	-0.2001612134	-0.0241443915
C	1.1535578967	0.2682264097	0.0017417465
C	0.0190114364	-0.5288095827	0.0703975336
C	-1.2447579060	0.0731288662	0.0912791569
C	-2.4584860022	-0.7669673814	0.1642699829
O	-2.4648634837	-1.9749293987	0.2102839026
C	-1.3759707380	1.4572224464	0.0437988996
C	-0.2330597025	2.2502550730	-0.0246098157
C	1.0196125002	1.6641947283	-0.0459340406
H	3.7112106706	-1.7490275792	-0.0235838180
H	2.2371605914	-2.0433094320	0.9302035691
H	2.1742207542	-2.0952728552	-0.8526676274
H	0.0695642546	-1.6070431111	0.1095655628
H	-3.4102693640	-0.1969261334	0.1748432218
H	-2.3614305780	1.9067473208	0.0612311474
H	-0.3189410452	3.3286196784	-0.0626961253
H	1.9184659994	2.2647891814	-0.0998479623

3-Methylbenzaldehyde

C	2.4049842134	-1.5971794995	-0.0000200910
C	1.3755182006	-0.4975258470	-0.0000250037
C	0.0164227392	-0.7807794752	-0.0001932463
C	-0.9336405545	0.2454576373	-0.0002179892
C	-2.3782201539	-0.0646534001	-0.0003828483
O	-2.8520539971	-1.1765144623	-0.0004782026

C	-0.5209768424	1.5758998575	-0.0000716995
C	0.8358606131	1.8747957085	0.0001211552
C	1.7692265679	0.8473819104	0.0001404776
H	1.9333870722	-2.5795710169	-0.0001540809
H	3.0501384452	-1.5328400806	-0.8794184885
H	3.0499643292	-1.5329994353	0.8795184780
H	-0.3358362956	-1.8051751569	-0.0003019605
H	-3.0382821180	0.8282474406	-0.0006440670
H	-1.2606051525	2.3684599985	-0.0001086448
H	1.1676847875	2.9053827926	0.0002534123
H	2.8262362774	1.0896526387	0.0002860201

3-Fluorobenzaldehyde

F	2.1745135775	-1.6454679215	0.0001322029
C	1.3311029637	-0.5941935565	0.0000479216
C	-0.0274458517	-0.8238876725	-0.0001622239
C	-0.8855792182	0.2791229377	-0.0002548895
C	-2.3527216922	0.0802302395	-0.0004688348
O	-2.9023047774	-0.9944405938	-0.0004142002
C	-0.3672154675	1.5737666631	-0.0001330238
C	1.0079595260	1.7749587769	0.0000900339
C	1.8701581278	0.6857069980	0.0001805183
H	-0.4272288791	-1.8289409906	-0.0002490995
H	-2.9434381721	1.0193597953	-0.0005499562
H	-1.0435117132	2.4201749361	-0.0002128843
H	1.4128379376	2.7784783656	0.0001905987
H	2.9446876867	0.8102806760	0.0003494540

3-Chlorobenzaldehyde

Cl	2.7489248412	-0.7727897847	0.0514123786
C	1.1824112385	-0.0031269269	0.0447311014
C	0.0354341547	-0.7811098785	0.1023472026
C	-1.2136082959	-0.1609757146	0.0961219039
C	-2.4314147590	-1.0021472755	0.1583856481
O	-3.5609409183	-0.5771919918	0.1595654961
C	-1.3075081286	1.2313526948	0.0321940247
C	-0.1526873714	1.9937185198	-0.0244997924
C	1.0991644212	1.3816067857	-0.0189542985
H	0.1111779970	-1.8601711190	0.1520149434
H	-2.2364771703	-2.0933367514	0.2064292264
H	-2.2878602352	1.6886570637	0.0287361626
H	-0.2140972394	3.0732435655	-0.0741257620
H	2.0033232902	1.9728532371	-0.0640444615

3-bromobenzaldehyde

Br	2.3357284579	-0.4124154290	0.0770086340
C	0.5391079867	0.2334697462	0.0587585479
C	-0.5116084830	-0.6694924545	0.1136897864
C	-1.8228509086	-0.1940138347	0.0986750858
C	-2.9393612956	-1.1661350314	0.1577201550
O	-4.1090801688	-0.8691829626	0.1524450446
C	-2.0729044532	1.1783347539	0.0287082107
C	-1.0116349536	2.0664377326	-0.0255797551
C	0.3019267944	1.5999760864	-0.0108976245
H	-0.3206225126	-1.7337109257	0.1682102974
H	-2.6236745262	-2.2284612698	0.2095371381
H	-3.0985744650	1.5224544480	0.0189156367

H	-1.1939534337	3.1320298386	-0.0804486535
H	1.1308009381	2.2932650575	-0.0532813211

2-methylbenzaldehyde

C	1.1171202615	-1.9015060982	0.0002294000
C	0.0399372466	-0.8529762898	0.0001499590
C	0.3197086699	0.5322436184	0.0003623538
C	1.6855889030	1.0932076022	0.0006907361
O	2.7246199585	0.4732781534	0.0002076746
C	-0.7280978204	1.4591533320	0.0002734445
C	-2.0518984520	1.0521139208	-0.0000259104
C	-2.3332407035	-0.3083742138	-0.0002324370
C	-1.2989805206	-1.2386355298	-0.0001388003
H	0.6737907421	-2.8975904170	0.0002042391
H	1.7677039901	-1.8031174559	-0.8696187495
H	1.7676071258	-1.8031010456	0.8701435845
H	1.7030273220	2.2040612327	0.0003631967
H	-0.4865774120	2.5162878042	0.0004518522
H	-2.8518784388	1.7809400384	-0.0000926847
H	-3.3606821422	-0.6512843523	-0.0004626460
H	-1.5370725122	-2.2957042662	-0.0002925326

2-Methoxybenzaldehyde

C	2.8642597167	0.9282559132	0.1411396320
O	1.4590004632	1.1249796293	0.0811363812
C	0.6371505026	0.0455420740	0.0662664159
C	-0.7481584110	0.3035002225	0.0063551896
C	-1.2769780087	1.6834637787	-0.0375953898
O	-2.4584276434	1.9503187176	-0.0866273773
C	-1.6382565691	-0.7718645693	-0.0113268249
C	-1.1869601556	-2.0798210712	0.0285580304
C	0.1820268900	-2.3210581397	0.0875588883
C	1.0943820464	-1.2727967162	0.1068563129
H	3.3021510769	1.9234106051	0.1431332855
H	3.1535472659	0.4028460233	1.0551112251
H	3.2260597861	0.3746177809	-0.7293199261
H	-0.5221031747	2.4864971280	-0.0230417157
H	-2.6952505421	-0.5431115525	-0.0577496825
H	-1.8879130770	-2.9037274165	0.0141639693
H	0.5519002113	-3.3386401301	0.1186619499
H	2.1511954070	-1.4887915517	0.1537531070

2-F-benzaldehyde

F	0.1141064414	-2.1969970948	-0.0751149367
C	-0.3598043957	-0.9346812254	-0.0471751340
C	0.5368311882	0.1315517055	-0.0866675797
C	2.0006240781	-0.0796034678	-0.1560706264
O	2.8043861372	0.8236637082	-0.1892313043
C	0.0063883436	1.4268817646	-0.0560238168
C	-1.3596145567	1.6352538035	0.0123490777
C	-2.2262853120	0.5429781024	0.0511483506
C	-1.7295234678	-0.7533333430	0.0211815274
H	2.3336041518	-1.1314670331	-0.1751095925
H	0.7023771430	2.2551166791	-0.0869843478
H	-1.7554081728	2.6419059514	0.0351358922
H	-3.2959581249	0.7002254703	0.1054245279

H -2.3801747910 -1.6167253937 0.0500087969

2-Cl-benzaldehyde
Cl 1.6223863467 -1.5965688429 -0.0839508510
C 0.1107743299 -0.7153366543 -0.0489581458
C 0.0827700237 0.6827701430 -0.0858682611
C 1.3061361650 1.5210571888 -0.1599025513
O 1.2834549759 2.7295752403 -0.1902402716
C -1.1632867057 1.3201985250 -0.0521250277
C -2.3384873692 0.5949443572 0.0147914583
C -2.2852334364 -0.7966056680 0.0500216947
C -1.0634861136 -1.4546858790 0.0183965171
H 2.2629809089 0.9751090982 -0.1872328281
H -1.1694892083 2.4021564267 -0.0811237029
H -3.2926660424 1.1045040854 0.0403778700
H -3.1981327120 -1.3762837245 0.1028560084
H -1.0136873773 -2.5343480681 0.0459594237

2-Br-benzaldeyde
Br 1.9423800536 0.0900084920 0.0021717129
C 0.0636063106 0.4566690660 0.0010719061
C -0.8881003293 -0.5674901871 0.0003183082
C -0.5445266152 -2.0130069465 0.0008916424
O -1.3725271355 -2.8935188498 -0.0001342946
C -2.2426737074 -0.2107257559 -0.0007412557
C -2.6353347038 1.1148280440 -0.0009677592
C -1.6684567422 2.1169745853 -0.0001095762
C -0.3183245565 1.7917891282 0.0008823259
H 0.5316109782 -2.2511366370 0.0023729849
H -2.9682249365 -1.0141835587 -0.0012969742
H -3.6865293656 1.3718813373 -0.0018342730
H -1.9629041484 3.1590023171 -0.0001935710
H 0.4339309272 2.5679460966 0.0015381610

Lowest energy conformers for benzaldehyde methyl oxonium species

Benzaldehyde methyl oxonium
H 3.8472021478 -0.4603863213 -0.0066311052
C 2.7820216715 -0.2659317570 -0.0021261824
C 1.8886127275 -1.3423001674 -0.0786694201
C 0.5329453489 -1.1097127660 -0.0738890130
C 0.0583378377 0.2218628648 0.0083090578
C 0.9709135439 1.3007542688 0.0847935712
C 2.3274768538 1.0503480764 0.0799552707
H 2.2672666546 -2.3533380032 -0.1409662860
H -0.1706762283 -1.9288334670 -0.1311643326
C -1.3136278081 0.5272471770 0.0179471487
H 0.6006619138 2.3168786740 0.1465299887
H 3.0338050570 1.8669180505 0.1383905652
O -2.2140910363 -0.3745756667 -0.0437726855
C -3.6331337544 -0.0265157869 -0.0343378334
H -4.0445656001 -0.3792486697 -0.9762273804
H -4.0737516709 -0.5624460926 0.8016751986
H -3.7524154698 1.0496699448 0.0754685219
H -1.6385772038 1.5666782649 0.0806152314

4-Methylbenzaldehyde methyl oxonium

C	1.8310222817	0.5083777722	0.0073214073
C	0.4522441476	0.2681232889	0.0044991897
C	-0.0956275971	-1.0404036983	-0.0107879948
C	-1.4555116297	-1.2046284685	-0.0135677026
C	-2.3261073890	-0.0922027761	-0.0010746910
C	-1.7790536054	1.2002071209	0.0142777968
C	-0.4159383654	1.3860421298	0.0168617298
H	0.5638661470	-1.8975382480	-0.0202543523
H	-1.8754597224	-2.2024181202	-0.0254989111
C	-3.8036662874	-0.3042538719	-0.0041050960
H	-2.4392383825	2.0572605459	0.0239329343
H	-0.0039378295	2.3878556529	0.0282323229
O	2.6929325808	-0.4383215068	-0.0024235948
H	-4.3538346297	0.6341914261	0.0034163738
H	-4.1039117455	-0.8779470132	-0.8852406783
H	-4.1050639406	-0.8924429805	0.8670795259
C	4.1224254674	-0.1512980791	-0.0001476688
H	4.2897871574	0.9242317193	0.0159065621
H	4.5311672879	-0.6011644223	-0.9009199317
H	4.5335046019	-0.6280955544	0.8855636947
H	2.2034033216	1.5331802952	0.0178653887

10. REFERENCES

1. B. J. Dennis-Smither, Z. Yang, C. Buda, X. Liu, N. Sainty, X. Tan and G. J. Sunley, *Chem. Commun.*, 2019, **55**, 13804-13807.
2. J. W. Harris, A. A. Verma, J. W. Arvay, A. J. Shih, W. N. Delgass and F. H. Ribeiro, *J. Catal.*, 2020, **389**, 468-475.
3. G. B. Tolstorozhev, I. V. Skornyakov, M. V. Bel'kov, O. I. Shadyro, S. D. Brinkevich and S. N. Samovich, *Opt. Spectrosc.*, 2012, **113**, 179-183.
4. B. Chiavarino, M. E. Crestoni, S. Fornarini, O. Dopfer, J. Lemaire and P. Maître, *The Journal of Physical Chemistry A*, 2006, **110**, 9352-9360.
5. I. Ahmad, J. A. Anderson, C. H. Rochester and T. J. Dines, *J. Mol. Catal. A: Chem.*, 1998, **135**, 63-73.
6. I. Ahmad, J. A. Anderson, T. J. Dines and C. H. Rochester, *J. Colloid Interface Sci.*, 1998, **207**, 371-378.
7. G. Kresse and J. Furthmüller, *Computational Materials Science*, 1996, **6**, 15-50.
8. G. Kresse and J. Furthmüller, *Physical Review B*, 1996, **54**, 11169-11186.
9. G. Kresse and J. Hafner, *Physical Review B*, 1993, **47**, 558-561.
10. G. Kresse and D. Joubert, *Physical Review B*, 1999, **59**, 1758-1775.
11. J. Klimeš, D. R. Bowler and A. Michaelides, *Physical Review B*, 2011, **83**, 195131.
12. J. Klimeš, D. R. Bowler and A. Michaelides, *J. Phys.: Condens. Matter*, 2009, **22**, 022201.
13. H. Jónsson, G. Mills and K. W. Jacobsen, in *Classical and Quantum Dynamics in Condensed Phase Simulations*, WORLD SCIENTIFIC, 1998, pp. 385-404.
14. G. Mills, H. Jónsson and G. K. Schenter, *Surf. Sci.*, 1995, **324**, 305-337.
15. G. Henkelman and H. Jónsson, *The Journal of Chemical Physics*, 1999, **111**, 7010-7022.
16. https://america.iza-structure.org/IZA-SC/framework.php?STC=MFI.
17. R. A. Angnes, mechaSVG, GitHub repository, 2020, https://github.com/ricalmang/mechaSVG.
18. *MAPS Platform, Scienomics*, www.scienomics.com.
19. Y. Shao, Z. Gan, E. Epifanovsky, A. T. B. Gilbert, M. Wormit, J. Kussmann, A. W. Lange, A. Behn, J. Deng, X. Feng, D. Ghosh, M. Goldey, P. R. Horn, L. D. Jacobson, I. Kaliman, R. Z. Khaliullin, T. Kuś, A. Landau, J. Liu, E. I. Proynov, Y. M. Rhee, R. M. Richard, M. A. Rohrdanz, R. P. Steele, E. J. Sundstrom, H. L. Woodcock, P. M. Zimmerman, D. Zuev, B. Albrecht, E. Alguire, B. Austin, G. J. O. Beran, Y. A. Bernard, E.

Berquist, K. Brandhorst, K. B. Bravaya, S. T. Brown, D. Casanova, C.-M. Chang, Y. Chen, S. H. Chien, K. D. Closser, D. L. Crittenden, M. Diedenhofen, R. A. DiStasio, H. Do, A. D. Dutoi, R. G. Edgar, S. Fatehi, L. Fusti-Molnar, A. Ghysels, A. Golubeva-Zadorozhnaya, J. Gomes, M. W. D. Hanson-Heine, P. H. P. Harbach, A. W. Hauser, E. G. Hohenstein, Z. C. Holden, T.-C. Jagau, H. Ji, B. Kaduk, K. Khistyaev, J. Kim, J. Kim, R. A. King, P. Klunzinger, D. Kosenkov, T. Kowalczyk, C. M. Krauter, K. U. Lao, A. D. Laurent, K. V. Lawler, S. V. Levchenko, C. Y. Lin, F. Liu, E. Livshits, R. C. Lochan, A. Luenser, P. Manohar, S. F. Manzer, S.-P. Mao, N. Mardirossian, A. V. Marenich, S. A. Maurer, N. J. Mayhall, E. Neuscamman, C. M. Oana, R. Olivares-Amaya, D. P. O'Neill, J. A. Parkhill, T. M. Perrine, R. Peverati, A. Prociuk, D. R. Rehn, E. Rosta, N. J. Russ, S. M. Sharada, S. Sharma, D. W. Small, A. Sodt, T. Stein, D. Stück, Y.-C. Su, A. J. W. Thom, T. Tsuchimochi, V. Vanovschi, L. Vogt, O. Vydrov, T. Wang, M. A. Watson, J. Wenzel, A. White, C. F. Williams, J. Yang, S. Yeganeh, S. R. Yost, Z.-Q. You, I. Y. Zhang, X. Zhang, Y. Zhao, B. R. Brooks, G. K. L. Chan, D. M. Chipman, C. J. Cramer, W. A. Goddard, M. S. Gordon, W. J. Hehre, A. Klamt, H. F. Schaefer, M. W. Schmidt, C. D. Sherrill, D. G. Truhlar, A. Warshel, X. Xu, A. Aspuru-Guzik, R. Baer, A. T. Bell, N. A. Besley, J.-D. Chai, A. Dreuw, B. D. Dunietz, T. R. Furlani, S. R. Gwaltney, C.-P. Hsu, Y. Jung, J. Kong, D. S. Lambrecht, W. Liang, C. Ochsenfeld, V. A. Rassolov, L. V. Slipchenko, J. E. Subotnik, T. Van Voorhis, J. M. Herbert, A. I. Krylov, P. M. W. Gill and M. Head-Gordon, *Mol. Phys.*, 2015, **113**, 184-215.

20. A. D. Becke, *The Journal of Chemical Physics*, 1993, **98**, 5648-5652.
21. P. J. Stephens, F. J. Devlin, C. F. Chabalowski and M. J. Frisch, *The Journal of Physical Chemistry*, 1994, **98**, 11623-11627.
22. F. Weigend and R. Ahlrichs, *PCCP*, 2005, **7**, 3297-3305.
23. E. Glendening, J. Badenhoop, A. Reed, J. Carpenter, J. Bohmann, C. Morales and F. Weinhold, *NBO 5.0. Natural Bond Orbital Analysis Program*, 2001.
24. A. Verloop, in *Pesticide Chemistry: Human Welfare and Environment*, eds. P. Doyle and T. Fujita, Pergamon, 1983, pp. 339-344.
25. A. Verloop, W. Hoogenstraaten and J. Tipker, in *Drug Design*, ed. E. J. Ariëns, (Academic Press), 1976, vol. 11, pp. 165-207.
26. K. Jorner, MORFEUS, https://github.com/kjelljorner/morfeus).
27. C. Hansch, A. Leo and R. W. Taft, *Chem. Rev.*, 1991, **91**, 165-195.
28. C. B. Santiago, A. Milo and M. S. Sigman, *J. Am. Chem. Soc.*, 2016, **138**, 13424-13430.
29. S. Chakraborty, A. Patzer and O. Dopfer, *The Journal of Chemical Physics*, 2010, **133**, 044307.
30. M. K. Kesharwani, B. Brauer and J. M. Martin, *J. Phys. Chem. A*, 2015, **119**, 1701-1714.
31. M. R. Berthold, N. Cebron, F. Dill, T. R. Gabriel, T. Kötter, T. Meinl, P. Ohl, C. Sieb, K. Thiel and B. Wiswedel, in *KNIME: The Konstanz Information Miner in Data Analysis, Machine Learning and Applications. Studies in Classification, Data Analysis, and Knowledge Organization.*, eds. C. Preisach, H. Burkhardt, L. Schmidt-Thieme and R. Decker, Springer Berlin Heidelberg, Berlin, Heidelberg, 2008, pp. 319-326.
32. L. S. Crocker, G. L. Gould and D. M. Heinekey, *J. Organomet. Chem.*, 1988, **342**, 243-244.
33. A. Sylvain and C. Alain, *Statistics Surveys*, 2010, **4**, 40-79.